

THYLAKOID MEMBRANE ARCHITECTURE IN CYANOBACTERIA



Dissertation

zur Erlangung des Grades eines Doktors der Naturwissenschaften
an der Fakultät für Biologie
der Ludwig-Maximilians-Universität München

vorgelegt von

Anna Margareta Rast

München, 03. Mai 2018

1. Gutachter: Prof. Dr. Jörg Nickelsen

2. Gutachter: Prof. Dr. Andreas Klingl

Tag der Abgabe: 03.05.2018

Tag der mündlichen Prüfung: 22.06.2018

TABLE OF CONTENT

SUMMARY	5
ZUSAMMENFASSUNG	7
1 INTRODUCTION	9
1.1 Evolution of oxygenic photosynthesis	9
1.2 Thylakoid structure	10
1.2.1 Thylakoid structure in plastids	10
1.2.2 Thylakoid structure in cyanobacteria	11
1.3 Thylakoid membrane shaping factors	13
1.4 Photosynthesis in cyanobacteria	17
1.4.1 Electron transport chain	17
1.4.2 Light harvesting	19
1.4.3 Lateral heterogeneity	20
1.5 PSII biogenesis and repair in cyanobacteria	21
1.6 Cryo-electron tomography	23
2 AIMS OF THIS WORK	27
3 RESULTS	28
3.1 The role of Slr0151, a tetratricopeptide repeat protein from <i>Synechocystis</i> sp. PCC 6803, during photosystem II assembly and repair	28
3.2 Thylakoid membrane architecture in <i>Synechocystis</i> depends on CurT, a homolog of the granal CURVATURE THYLAKOID1 proteins	41
3.3 <i>In situ</i> cryo-electron tomography of cyanobacterial thylakoid convergence zones reveals a biogenic membrane connecting thylakoids to the plasma membrane.	65
4 DISCUSSION	86
4.1 Structural and photosystem II specific role of Slr0151 and CurT	86
4.1.1 The role of Slr0151	86
4.1.2 The role of CurT	88
4.1.3 Connection between Slr0151 and CurT via phosphorylation?	90
4.2 The thylapse – a contact area between thylakoids and plasma membrane	91
4.2.1 Factors possibly involved in thylapse formation	93
4.2.2 Membrane contact – a common feature	94
4.3 Lateral heterogeneity in cyanobacteria	95
4.4 Conclusions and future perspectives	97

5	REFERENCES	99
6	APPENDIX	112
6.1	Biogenesis of thylakoid membranes	112
6.2	Supplementary Material - The role of Slr0151, a tetratricopeptide repeat protein from <i>Synechocystis</i> sp. PCC 6803, during photosystem II assembly and repair	123
6.3	Supplemental data - Thylakoid membrane architecture in <i>Synechocystis</i> depends on CurT, a homolog of the granal CURVATURE THYLAKOID1 proteins	125
6.4	Supporting material - <i>In situ</i> cryo-electron tomography of cyanobacterial thylakoid convergence zones reveals a biogenic membrane connecting thylakoids to the plasma membrane.	143
	LIST OF PUBLICATIONS	147
	LIST OF ABBREVIATIONS	148
	DANKSAGUNG	150
	PERMISSIONS AND COPYRIGHTS	152
	EIDESSTATTLICHE VERSICHERUNG UND ERKLÄRUNG	160

SUMMARY

Oxygenic photosynthesis takes place at a specialized membrane system called the thylakoids. The evolutionary origin of thylakoid membranes present in algae and plants are the ancestors of present-day cyanobacteria. In the cyanobacterium *Synechocystis* sp. PCC 6803, the thylakoid membranes are sheets oriented parallel to the plasma membrane, toward which the thylakoids occasionally converge. These regions are therefore termed convergence zones. The biogenesis of the thylakoid-embedded photosystem II (PSII) complex starts at the convergence zones, which are hence also named biogenesis centers. The PSII biogenesis is a complex stepwise mechanism, which is highly ordered and relies on several assembly factors. These are required to place the 20 protein subunits, many cofactors such as pigments or iron-sulfur clusters, and metal ions in the correct manner. Further research is needed for a comprehensive understanding of the architecture and function of the biogenesis centers, which continue to be controversially debated.

This study focusses on two assembly factors, which have been investigated and characterized: the tetratricopeptide repeat protein Slr0151, and CurT, the cyanobacterial homologue of the grana-shaping CURVATURE THYLAKOID1 protein family from *Arabidopsis thaliana*. The Slr0151 protein plays a role during the attachment of the inner core antenna proteins to the PSII reaction center assembly intermediate. Furthermore, in the *slr0151*⁻ mutant, the thylakoid lumina are increased, which implies an additional structural function. The CurT protein possesses a thylakoid shaping function as well. In the *curT*⁻ knockout, the biogenesis centers are completely absent, which results in a less efficient PSII assembly and thus a reduction in PSII accumulation, activity, and repair. CFP-tagged CurT forms a network-like pattern at the cell periphery in regions of reduced chlorophyll autofluorescence, which resemble the biogenesis centers.

Moreover, the architecture of the convergence zones is analyzed with high resolution cryo-electron tomography. It was found that converging thylakoids are interconnected in those regions and form a convergence membrane, which is oriented perpendicularly to the thylakoid sheets. Occasionally, in some areas the convergence membrane is in very close proximity to the plasma membrane, separated only by a ~2.5 nm gap. This contact area was termed the thylapse as it is reminiscent of a synapse. The resolution of the recorded tomograms enabled structural studies of large macromolecular complexes, i.e. the phycobilisomes and ribosomes. Noticeably, the convergence membrane and the thylapse were devoid of phycobilisomes but

SUMMARY

ribosomes were present, which substantiates the hypothesis that convergence membranes are indeed biogenic regions.

The data presented in this thesis characterize proteins involved in defining the thylakoid architecture and show comprehensively, for the first time, the ultrastructure of the convergence zones.

ZUSAMMENFASSUNG

Oxygene Photosynthese findet in einem hochspezialisierten Membransystem, den Thylakoiden, statt. Der evolutionäre Ursprung der Thylakoide in Algen und Pflanzen sind die Vorläufer heutiger Cyanobakterien. Im Cyanobakterium *Synechocystis* sp. PCC 6803 verlaufen die Thylakoide zwiebelschalenartig parallel zur Plasmamembran. An einigen Stellen innerhalb der Zelle scheinen sich die Thylakoide zur Zellhülle hin zu krümmen und auf einen Punkt an der Plasmamembran zu fokussieren, weshalb diese Stellen als Konvergierungszonen bezeichnet werden. Diese Regionen stellen den Ort der ersten Assemblierungsschritte des Photosystems II (PSII) dar und werden daher auch als Biogenesezentren beschrieben. PSII ist ein Multienzymkomplex und besteht aus 20 Proteinuntereinheiten, vielen Kofaktoren sowie einigen Metallionen. Der Zusammenbau dieses Komplexes beinhaltet klar strukturierte Assemblierungsschritte, unterstützt durch zahlreiche akzessorische Proteine, den Assemblierungsfaktoren, um alle Bestandteile in der richtigen Art und Weise zusammenzusetzen. Da die genaue Architektur und Wirkungsweise der Biogenesezentren seit langem jedoch sehr umstritten sind, sind weitere Untersuchungen notwendig.

In der vorliegenden Dissertationsschrift wurden zwei Assemblierungsfaktoren näher untersucht und charakterisiert: das Tetratrikopeptid-Wiederholungsprotein Slr0151 und CurT, das cyanobakterielle Homolog der granaformenden CURVATURE THYLAKOID1 Proteinfamilie aus *Arabidopsis thaliana*. Das Protein Slr0151 spielt eine Rolle bei der Anlagerung der inneren Antennenproteine an das wachsende Reaktionszentrumsmodul. Zudem weist die *slr0151* Mutante ein vergrößertes Thylakoidlumen auf. Ein Befund, der auf eine strukturgebende Rolle des Proteins hindeutet. Das CurT Protein besitzt ebenfalls eine strukturgebende Funktion bei der Ausbildung und Erhaltung der Thylakoidmorphologie. In seiner Abwesenheit in der *curT* Mutante fehlen die Biogenesezentren vollständig und infolgedessen ist die PSII Akkumulation, Aktivität, Reparatur und insbesondere die *de novo* Assemblierung gestört und reduziert.

Des Weiteren wurde die Struktur der Konvergierungszonen mit hochauflösender Kryo-Elektronentomographie untersucht, da der exakte Verlauf der Thylakoidmembranen an diesen Stellen seit langem Gegenstand von Diskussionen ist. Die Thylakoide verbinden sich dort und bilden eine sogenannte Konvergierungsmembran, die senkrecht zu den zwiebelschalenartigen Thylakoiden verläuft. An einigen Stellen kommt die Konvergierungsmembran der Plasmamembran sehr nahe, sodass nur noch ein kleiner ~2,5 nm breiter Spalt die beiden

Membranen trennt. Diese enge Kontaktstelle zwischen Thylakoid- und Plasmamembran wurde aufgrund ihrer Ähnlichkeit zum synaptischen Spalt Thylapse genannt. Zudem erlaubte die gute Auflösung der Tomogramme strukturelle Analysen von großen Komplexen wie der Phycobilisomen und Ribosomen. Die Verteilung beider makromolekularer Komplexe wurde angesichts der Thylapse und der Konvergierungsmembran untersucht, da sie jeweils als Indikator für aktive Photosynthese und biogene Regionen angesehen werden können. Auffallend ist, dass die Konvergierungsmembran und die Thylapse frei von Phycobilisomen, aber nicht von Ribosomen sind. Diese Beobachtung untermauert die Annahme, dass die Konvergierungszonen tatsächlich biogene Regionen sind.

Diese Dissertationsschrift charakterisiert Faktoren, welche an der Ausbildung der Thylakoidmembranen beteiligt sind und zeigt erstmals eindeutig die Architektur der Konvergierungszonen.

1 INTRODUCTION

1.1 Evolution of oxygenic photosynthesis

Around 2.4 billion years ago, a massive diversification in photosynthetic cyanobacteria-like prokaryotes transformed the world's biosphere into an oxygenic environment (Tomitani *et al.*, 2006; Hohmann-Marriott and Blankenship, 2011). Photosynthesis is a process, which utilizes sunlight for biochemical reactions (Nelson and Junge, 2015). This process is called oxygenic photosynthesis since water serves as the electron donor, and thus oxygen is produced as by-product (Gould *et al.*, 2008; Hohmann-Marriott and Blankenship, 2011). Oxygenic photosynthesis occurs in cyanobacteria and in specialized organelles, called plastids, within algae and plants (Nelson and Junge, 2015). Photosynthetic eukaryotes gained the ability to perform oxygenic photosynthesis through an endosymbiotic event (Schimper, 1883; Mereschkowsky, 1905; Sagan, 1967). A eukaryotic host cell already containing organelles as nucleus, mitochondria, endoplasmatic reticulum and Golgi apparatus engulfed an ancient cyanobacteria-like cell and, over time, the endosymbiont was transformed into present-day primary plastids. This event gave rise to the three eukaryotic primary photosynthetic lineages, the rhodophytes (red algae), the glaucophytes and the chloroplastida (green algae and land plants). Analogous to their cyanobacterial relatives, primary plastids have an internal membrane system, termed the thylakoids, which is surrounded by two envelope membranes that resemble the plasma and outer membrane of the Gram-negative endosymbiont (Archibald, 2015). Secondary endosymbiosis, describing the uptake of a red or a green alga by a eukaryotic host cell and, thus, resulting in the formation of complex secondary plastids, further increased the complexity of eukaryotic photosynthetic life. Secondary plastids derived from red algae are surrounded by four envelope membranes, while descendants from green algae usually have three envelope membranes (Archibald, 2012). Significantly, even tertiary endosymbiotic events, consisting of the uptake of a secondary plastid-bearing organism, as well as serial endosymbiosis, whereby an organism loses its plastid and takes up another organism with a photosynthetic capability, have been observed (Archibald, 2009; McFadden, 2014). The compartmentalization resulting from plastid evolution constituted a gain of function, as the specialization and separation of different biochemical pathways made possible multicellular eukaryotic photosynthetic life.

1.2 Thylakoid structure

Photosynthesis takes place at the specialized internal thylakoid membrane system. This system is surrounded by the cytoplasm of cyanobacteria and the stroma of plants' and algae's plastids (Nelson and Junge, 2015). The appearance of plastids and their thylakoid membrane architecture differs significantly between lineages and species (Figure I; section 6.1, Rast *et al.*, 2015).

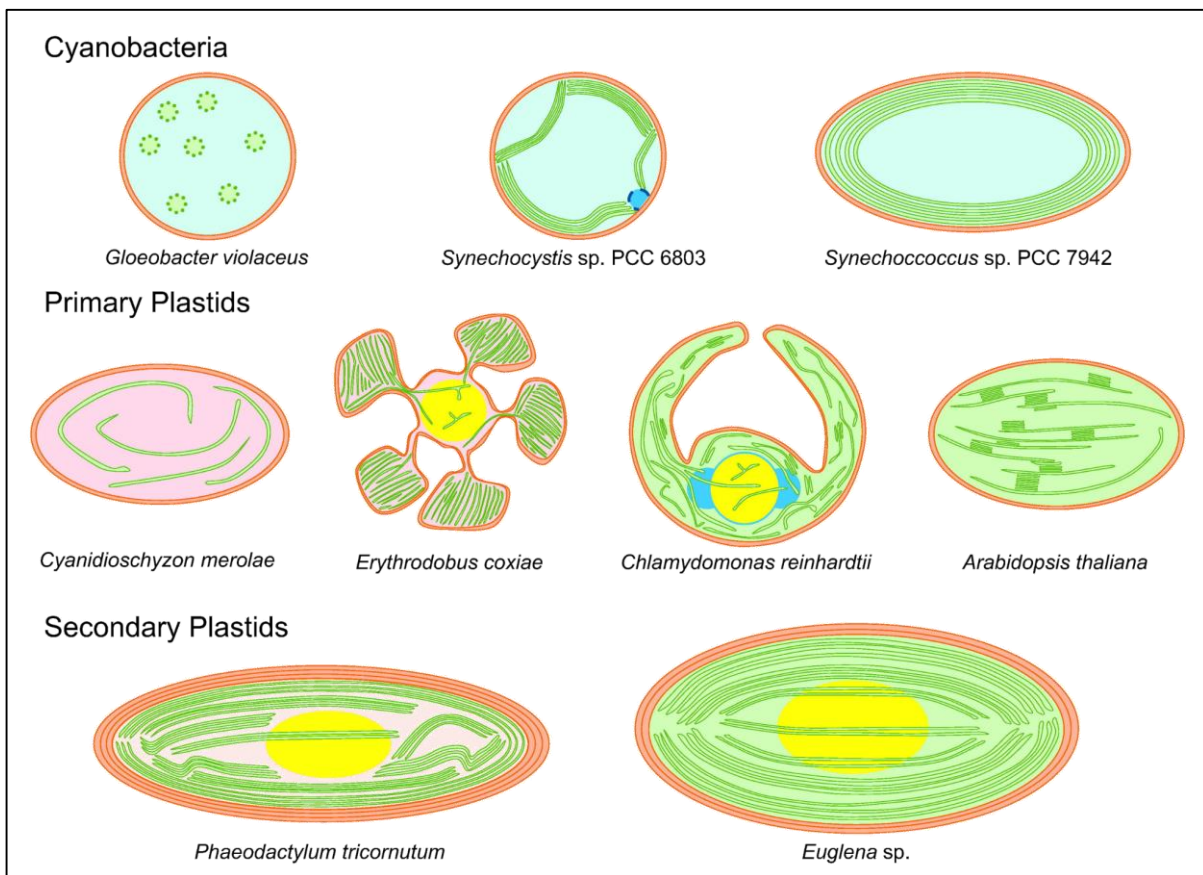


Figure I. Different architecture of thylakoid membranes in oxygenic photosynthetic organisms. The diversity of thylakoids (green) is significant in cyanobacteria, primary as well as secondary plastids. PSII biogenetic areas are highlighted in blue, pyrenoids in yellow, envelope, plasma and outer membranes in brown. Adapted from Rast *et al.* (2015) with permission from Elsevier.

1.2.1 Thylakoid structure in plastids

While the diversity of the thylakoid morphology in primary plastids is high and varies between different organisms, all primary plastids are surrounded by two envelope membranes (Figure I; Archibald, 2012; section 6.1, Rast *et al.*, 2015). The thylakoid membrane architecture of green algae is arranged in appressed thylakoid regions and loose stroma thylakoids (Kim and Archibald, 2008). In plants, an even higher level of separation exists, which divides the

thylakoids into grana stacks and stroma lamellae (Kirchhoff, 2013). Red algae thylakoid membrane architecture is more diverse and it is often impossible to distinguish differentially stacked regions (Figure I; Kim and Archibald, 2008; section 6.1, Rast *et al.*, 2015). For a long time, several mechanisms have been discussed regarding the formation of thylakoids. However, only one single study reported membrane fusions between the inner envelope and mature thylakoids to date. Recently, it was shown in the green algae *Chlamydomonas reinhardtii* by cryo-electron tomography that the chloroplast inner envelope forms invaginations. Those invaginations fuse in some rare examples with the thylakoid membrane tips, perhaps for lipid and protein exchange (Engel *et al.*, 2015). Furthermore, the thylakoid membrane system in plants forms a sophisticated and entirely interconnected network (Dekker and Boekema, 2005).

As mentioned above, secondary plastids are typically surrounded by three to four envelope membranes (Archibald, 2012). The thylakoid architecture in secondary plastids is less diverse than in primary plastids. Usually the thylakoid membranes in secondary plastids are arranged in stacks of three (Figure I; Kim and Archibald, 2008; section 6.1, Rast *et al.*, 2015). However, thylakoids traversing the pyrenoid, the area of carbon dioxide fixation in algae, are always paired thylakoid sheets (Figure I; Kim and Archibald, 2008; section 6.1, Rast *et al.*, 2015). Comparable to red algal plastids, the thylakoids of secondary plastids are also not clearly distinguishable into grana and stroma lamellae. Nevertheless, interconnections between thylakoids have recently been reported in diatoms, suggesting that thylakoid membranes in secondary plastids form a network as well (Flori *et al.*, 2017).

1.2.2 *Thylakoid structure in cyanobacteria*

The thylakoid structure in cyanobacteria is organized differently when compared to plastids in general, as it is onion shaped and runs parallel to the plasma membrane (Figure I). In contrast to plant chloroplasts, no grana stacking can be observed here. In some species, such as *Synechocystis* sp. PCC 6803 (hereafter *Synechocystis*), the model organism used in this thesis, the thylakoid membranes occasionally converge toward the plasma membrane, thereby forming convergence zones (Kunkel, 1982; van de Meene *et al.*, 2006). The only known exception of an oxygenic organism without internal thylakoids is *Gloeobacter violaceus*, a cyanobacterium that harbors its photosynthetic complexes in the plasma membrane in thylakoid-like “green patches”, which are distinct from areas of the respiratory chain (Rexroth *et al.*, 2011).

In the early 1980s, one of the earliest studies on the cyanobacterial ultrastructure was carried out with electron microscopy. In this study, the cells of four different cyanobacterial

species were used, which had the presence of convergence zones in common (Kunkel, 1982). Moreover, in the middle of the convergence zone a cylindrical, electron dense material was observed, from which thylakoid membranes appeared to emerge. Subsequently, this electron dense structure was described as “the thylakoid center” (Figure II A, B; Kunkel, 1982). The first attempt to investigate the three-dimensional (3D) structure of thylakoid membranes was carried out in the cyanobacterium *Synechococcus* sp. PCC 7002 (formerly known as *Agmenellum quadruplicatum*), which equally exhibits convergence zones (Figure II C, D;

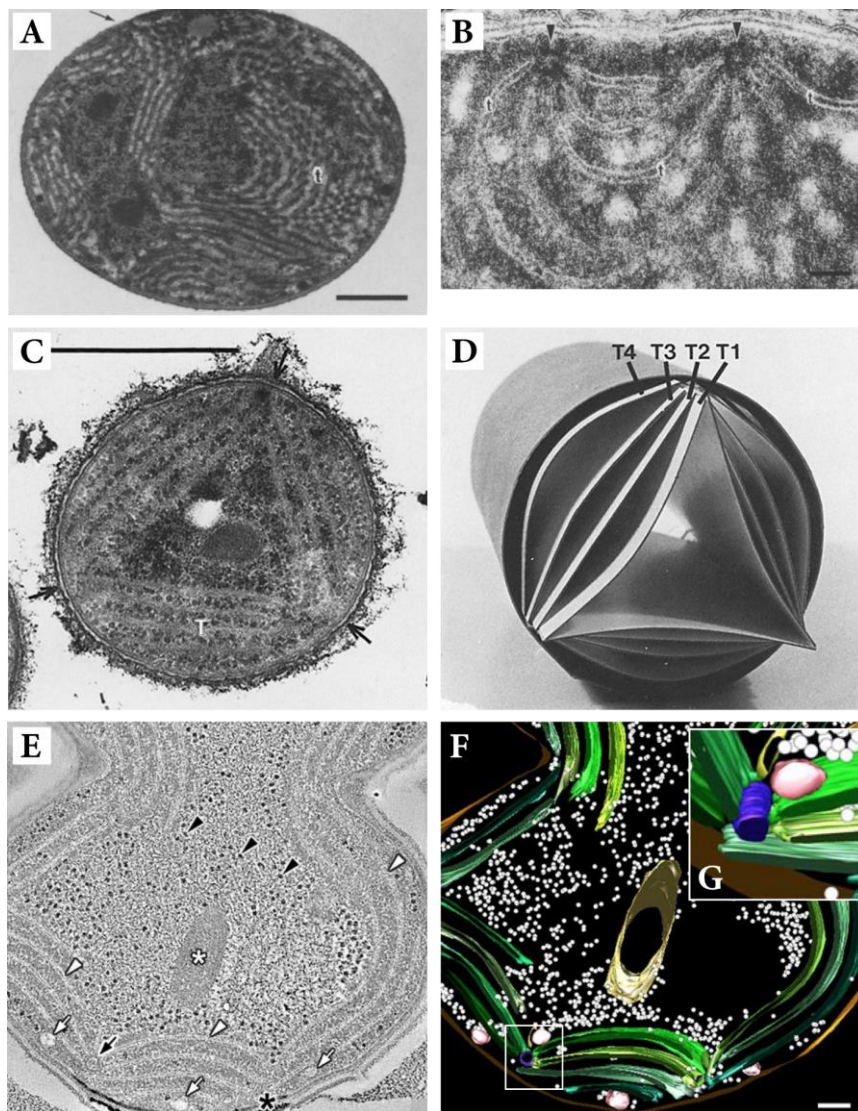


Figure II. Cyanobacterial ultrastructure. A) Overview and B) close-up of *Pleurocapsa minor* ultrastructure with thylakoids (t), convergence zones (arrow) and thylakoid center (arrowhead). Scale bars A) 5 μm and B) 50 nm. Adapted from Kunkel (1982) with permission from Springer Nature. C) Ultrastructure of *Synechococcus* sp. PCC 7002 with convergence zones (arrow) and D) 3D representation of thylakoids (T). Scale bar 1 μm . Adapted from Nierzwicki-Bauer *et al.* (1983b) with permission from Rockefeller University Press. E) Ultrastructure and F) 3D representation with G) close-up of convergence zones (E, black arrow; F-G, white box) with thylakoid center (F-G; purple) of a *Synechocystis* cell. Thylakoids are highlighted with white arrowheads (E) and displayed in green (F-G). Ribosomes are indicated by black arrowheads (E) and displayed in white (F-G). Scale bar 20 nm. Adapted from van de Meene *et al.* (2006) with permission from Springer Nature.

Nierzwicki-Bauer *et al.*, 1983a). Serial sections of resin embedded *Synechococcus* sp. PCC 7002 cells were produced, analyzed and then used to build a 3D model employing a program called “computer aided reconstruction of serial thin sections”. Based on this computer generated model, a paper model was built to gain a better understanding of the thylakoid system (Figure II C, D; Nierzwicki-Bauer *et al.*, 1983a,b). Unfortunately, neither the thylakoid structure in the convergence zone itself nor the thylakoid center could be resolved clearly in this study.

The next attempts to analyze a 3D structure of convergence zones and thylakoid centers in more detail were performed 26 years later by two different research groups independently (Liberton *et al.*, 2006; van de Meene *et al.*, 2006). Both used resin embedded cells followed by electron tomography and were able to show that the thylakoids come in very close proximity to the plasma membrane at convergence zones. Van de Meene *et al.* (2006) described the thylakoid center as a rod-like structure, which might be continuous with the thylakoid membrane (Figure II E-G). Furthermore, a “semicircular structure” around the thylakoid center has been noticed which appears to interconnect the thylakoids in the convergence zone and thus assuming that indeed the thylakoid center might be continuous with the thylakoid lumen (Stengel *et al.*, 2012). On the other hand, these studies were unable to find evidence for continuity with the periplasm in cyanobacteria. Given that a continuous system of thylakoid lumen and periplasm is widely spread amongst anoxygenic photosynthetic purple bacteria, such as *Rhodospseudomonas palustris*, it has been discussed for years whether this holds for cyanobacteria as well (Tauschel and Drews, 1967; Oelze and Drews, 1972; Drews, 2013). In addition, the thylakoid system was analyzed in two cyanobacteria without convergence zones (*Synechococcus elongatus* sp. PCC 7942 and *Microcoleus* sp.). It was found to be entirely interconnected, comparable to the observations made in diatoms and plants (Nevo *et al.*, 2007).

1.3 Thylakoid membrane shaping factors

In recent years, a growing number of factors have been identified and described to be involved in shaping the thylakoid membrane in plants, algae as well as in cyanobacteria.

Amongst the first described proteins effecting thylakoid architecture was the vesicle-inducing protein in plastids 1 (VIPP1; Kroll *et al.*, 2001; Westphal *et al.*, 2001). Upon depletion and knockdown of this protein in the land plant *Arabidopsis thaliana* as well as in *Synechocystis*, respectively, the thylakoid membrane system is massively disordered and almost absent. Hence, *vipp1* mutants from both species are not able to grow photoautotrophically (Kroll *et al.*, 2001; Westphal *et al.*, 2001). By the use of fluorescence light microscopy, it has

further been shown that VIPP1 localizes to the convergence zones of *Synechocystis* and to the inner envelope membrane of *A. thaliana* chloroplasts in a punctuated manner (Bryan *et al.*, 2014; Zhang and Sakamoto, 2015; Gutu *et al.*, 2018). Moreover, Rütgers and Schroda (2013) hypothesized that VIPP1 oligomers resemble the cyanobacterial cylindrical thylakoid centers described by Kunkel (1982). Additionally, VIPP1 may induce membrane connections between the thylakoids and the inner envelope or plasma membrane via vesicle transport or direct contact (Kroll *et al.*, 2001; Fuhrmann *et al.*, 2009; Junglas and Schneider, 2018). Indeed, *in vitro* studies have revealed that VIPP1 is able to tubulate membranes, which might result in membrane connections between thylakoids and their enclosing membranes (plasma membrane or inner envelope membrane; Hennig *et al.*, 2015; Heidrich *et al.*, 2017). However, no proof for membrane fusion *in vivo* between those membranes induced by VIPP1 has been found to date. Despite having been heavily researched and discussed for years, the working mode of the VIPP1 protein thus remains an enigma.

There are several proteins, which have been identified to be involved in defining grana and stroma lamellae. First, the dynamin-like protein FZL localizes to the thylakoids and the inner envelope in *A. thaliana*. In a *fzl* knockout mutant, thylakoids are no longer arranged in clearly separated grana and stroma lamellae (Gao *et al.*, 2006). In the cyanobacterium *Nostoc punctiforme*, a protein, which shares sequence similarities with FZL from *A. thaliana*, was found and described as the bacterial dynamin-like protein (BDLP; Low and Lowe, 2006; Low *et al.*, 2009). This protein localizes in a punctuated manner to the cell periphery, the septum during cell division, and to the cell's interior, which suggests that BDLP is present at the plasma and thylakoid membranes. Nevertheless, how this protein is involved in thylakoid membrane dynamics *in vivo* remains unknown and requires further research (Jilly *et al.*, 2018). In general, dynamin-like proteins in non-photosynthetic bacteria are reportedly involved in membrane fusion, fission, and stability mechanisms, which in turn also increases the probability of a thylakoid membrane-dynamic function in cyanobacteria (Bramkamp, 2012; Sawant *et al.*, 2016). FZL and BDLP proteins belong to the superfamily of large GTPases, which possess a GTPase domain. Characteristic for dynamins and dynamin-like proteins is the formation of homodimers when GDP is bound. Upon GTP binding, they self-assemble around liposomes, which leads to membrane tubulation *in vitro* (see reviews: Praefcke and McMahon, 2004; Jilly *et al.*, 2018).

In addition, a novel protein family in *A. thaliana* has been identified, which strongly affects the formation of grana and stroma lamellae. The CURVATURE THYLAKOID1 (CURT1) protein family contains four members CURT1A-D that all possess two

transmembrane domains and a N-terminal amphipathic helix (Armbruster *et al.*, 2013). CURT1 proteins define and localize to the grana margins and, upon loss of all four members in the quadruple mutant *curt1abcd*, the thylakoids do not differentiate into grana and stroma lamellae anymore. This observation is comparable to the *fzl* mutant phenotype mentioned above. Although thylakoids are affected, photosynthetic complexes can normally form and accumulate. Only cyclic electron flow and non-photochemical quenching were slightly diminished. CURT1A-D proteins form homo and hetero oligomers of different sizes, possibly regulated by phosphorylation. In addition, it has been demonstrated that these proteins are able to tubulate liposomes *in vitro* (Armbruster *et al.*, 2013). Nevertheless, the mode of action of the CURT1 proteins on a molecular level still needs clarification. However, homologs of the CURT1 family are present throughout photosynthetic life and, although cyanobacterial thylakoids do not differentiate into grana stacks and stroma lamellae, a homologue is present in *Synechocystis* (Armbruster *et al.*, 2013).

Taken together, VIPP1, FZL/BDLP and CURT1 proteins have in common that they form oligomers and they are able to tubulate liposomes *in vitro*. Thereby, they play important roles in thylakoid structure formation in plant chloroplasts, algal plastids as well as in cyanobacteria.

Furthermore as summarized by Karim and Aronsson (2014), some proteins, which are involved in the chloroplast vesicle transport pathway, show defects in thylakoid formation in plants as well: i.e. the two small GTPases CPRapA5e (chloroplast localized Rap GTPase) and CPSAR1 (homologue of the cytosolic coat protein complex II), as well as the THYLAKOID FORMATION1 (THF1) protein (Wang *et al.*, 2004; Garcia *et al.*, 2010; Bang *et al.*, 2012; Karim *et al.*, 2014; Zhan *et al.*, 2016). In this context it is notable, that the CPRapA5e protein was shown to interact with the CURT1A protein from *A. thaliana* in a yeast two-hybrid screen (Karim *et al.*, 2014). Nevertheless, no homologue the CPRapA5e protein is present in cyanobacteria. However, homologues of CPSAR1 and THF1 are found throughout photosynthetic life including cyanobacteria, but to this point, only the THF1 has been studied in *Synechococcus* sp. PCC 7942 (Garcia *et al.*, 2010; Zhan *et al.*, 2016). The *thf1* mutant exhibits only slight effects on thylakoid architecture under high-light conditions as less thylakoid layers are present (Zhan *et al.*, 2016).

Another factor, termed RIQ1 and RIQ2 (reduced induction of non-photochemical quenching), was identified in *A. thaliana* and was found to be solely present in land plants and some green algae. In *riq* mutants, the grana stacks were increased which contrasts with the phenotype observed in the *curt1abcd* mutant, in which grana were less defined (Armbruster *et al.*, 2013; Yokoyama *et al.*, 2016).

To put it in a nutshell, only VIPP1, FZL/BDLP, CURT1, CPSAR1, and THF1 proteins are present in plants as well as in cyanobacteria. Membrane shaping capacities were only reported for VIPP1, FZL/BDLP and CURT1 proteins. In *A. thaliana*, however, all above mentioned proteins are present and show effects on the thylakoid ultrastructure suggesting that these proteins belong to a large network of factors regulating the thylakoid membrane architecture in plants. This network of factors might vary in different photosynthetic lineages.

Table 1. Diameter of thylakoid lumina and interthylakoid spaces in cyanobacteria, green algae, and plants. D dark, NL normal light. NL for cyanobacteria 30-40 $\mu\text{mol photons m}^{-2}\text{s}^{-1}$, for plants 500 $\mu\text{mol photons m}^{-2}\text{s}^{-1}$ and for green algae 90 $\mu\text{mol photons m}^{-2}\text{s}^{-1}$.

	Thylakoid lumen diameter		Interthylakoid space (= stromal gap)		References
	D	NL	D	NL	
Cyanobacteria	10-300 nm*	5-8 nm [#]	30-120 nm*	30-50 nm [#]	[#] van de Meene <i>et al.</i> (2006) [*] van de Meene <i>et al.</i> (2012)
Green algae	n. d.	9.0±1.4 nm	n. d.	3.6±0.5 nm	Engel <i>et al.</i> (2015)
Higher plants	4.7±0.8 nm [§]	9.2±0.6 nm [§]	4.2±1.3 nm [§]	3.2±0.7 nm [§]	[§] Kirchhoff <i>et al.</i> (2011) [§] Kirchhoff <i>et al.</i> (2017)

Finally, light itself influences thylakoid morphology. In plants, thylakoids undergo several changes according to the light intensity (Table 1). Under dark adapted conditions, the thylakoid lumen in grana stacks is 4.7 nm, which increases upon illumination to 9.2 nm (Daum *et al.*, 2010; Kirchhoff *et al.*, 2011). The width of the stromal gap (distance between adjacent thylakoids), however, decreases under illumination from 4.2 to 3.2 nm. It has been postulated that the swelling of the thylakoid lumen in the light results from an increased influx of calcium and chloride ions (Kirchhoff *et al.*, 2011). As a reason for the luminal expansion, it has been proposed that the diffusion of the soluble electron carrier plastocyanin, requires the increase of the thylakoid lumen's diameter (Kirchhoff *et al.*, 2011). It can reasonably be assumed that the same holds for green algae, but thus far data has only been collected under normal continuous light (Engel *et al.*, 2015).

In contrast, the situation in cyanobacteria is different as 1) the respiratory chain and photosynthesis are neither separated by space nor time and occur simultaneously (reviewed by Liu, 2016), 2) the thylakoids are arranged differently, and 3) they possess large soluble light harvesting antennas. Hence, the interthylakoid space in cyanobacteria (30-50 nm; Table 1) is determined by the presence of their light harvesting complexes, the phycobilisomes (Olive *et al.*, 1997; van de Meene *et al.*, 2006; Mullineaux, 2008). In the light, photosynthesis and

respiration takes place and the proton gradient across the thylakoid membrane is generated. Therefore, the thylakoid membrane is stiffer compared to the situation in the dark, where photosynthesis stops and only respiration contributes to the formation of the proton gradient (Stingaciu *et al.*, 2016). In this context, Stingaciu *et al.* (2016) claim that the proton gradient becomes equilibrated over time due to the generation of adenosine triphosphate (ATP). The gradient itself induces membrane charging, resulting in the luminal side being positively charged and the cytosolic side of the membrane being negatively charged. This might repel adjacent membranes from each other. Due to the release of protons from the lumen, the membrane is more flexible in dark conditions and allows an increase in the luminal and interthylakoid distances (Stingaciu *et al.*, 2016).

1.4 Photosynthesis in cyanobacteria

Photosynthesis consists of two parts: First, light-driven transformation of sunlight into chemical energy results in the formation of ATP and nicotinamide adenine dinucleotide hydrogenphosphate (NADPH). Second, the Calvin-Benson cycle uses the generated chemical energy for carbon dioxide fixation, which leads to the generation of sugars. The light driven reactions use four major macromolecular complexes that are embedded in the thylakoid membranes, i.e. photosystem II (PSII), cytochrome *b₆f*, photosystem I (PSI), and ATP synthase.

1.4.1 *Electron transport chain*

Photosynthesis starts with the excitation of the PSII dimer. Thereby, light energy excites the chlorophylls of the special pair P680 in the PSII reaction center at the D1/D2 interface (Figure III). The excited P680 releases an electron that travels through the PSII reaction center until it reduces plastoquinone. Once plastoquinone is loaded with two electrons, it detaches from PSII into the thylakoid membrane and enters the plastoquinone pool (PQ-pool; see Figure III). The resulting electron gap at P680 is filled with electrons from the oxidation of water at the manganese cluster on the luminal side. The manganese cluster functions as a catalyzer for the oxidation of water, which requires a high energy potential (Hohmann-Marriott and Blankenship, 2011). In cyanobacteria, the manganese cluster is stabilized by the subunits of the water oxidizing complex PsbO, PsbU, PsbV and likely CyanoQ (Figure III). The splitting of water leads to the release of oxygen and protons into the thylakoid lumen, which contribute to the formation of a proton gradient across the thylakoid membrane. The electrons from the PQ-pool are further transferred into the cytochrome *b₆f* complex, where one electron cycles within

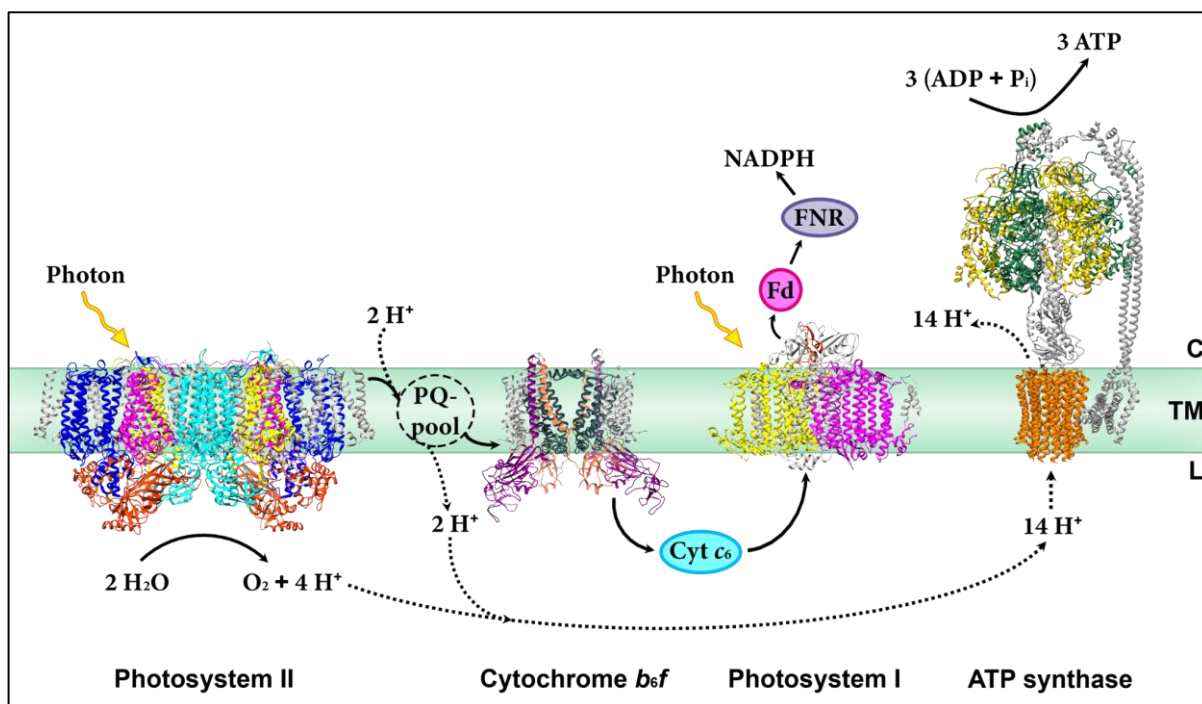


Figure III. Scheme of photosynthetic light reactions in cyanobacteria. Initial charge separation and oxidation of water is occurring at PSII (PsbO, U and V, red; D1, pink; D2, yellow; CP47, cyan; CP43, blue). Electron flow further proceeds via the plastoquinone pool (PQ-pool) to cytochrome *b₆f* (cytochrome *f*, violet; cytochrome *b₆*, dark grey; Rieske iron sulfur protein, orange). Via the soluble electron carrier cytochrome *c₆*, one electron is transferred to PSI (PsaA, pink; PsaB, yellow; PsaC, red). Sunlight leads to the oxidation of ferredoxin (Fd). Finally, Fd transfers its electron to NADPH via ferredoxin-NADPH reductase (FNR). The generated proton gradient is used to generate ATP. Per one 360° turn of the ATP synthase's c-ring (orange) 3 ATPs are generated in the cytosol at each α/β subunits interface (yellow/green). For Figure generation the crystal structures of PSII (Umeha *et al.* (2011), protein data bank entry: 3WU2), cytochrome *b₆f* (Hasan *et al.* (2013), PDB entry: 4H44) and PSI (Jordan *et al.* (2001), PDB entry: 1JB0) and the cryo-EM structure of ATP Synthase (Sobti *et al.* (2016), PDB entry: 5T4O) were used and only the backbones were displayed with UCSF Chimera software (Pettersen *et al.*, 2004). Proton flow is indicated with black dashed arrows and electron flow with black arrows. Cytosol, C; thylakoid lumen, L; thylakoid membrane, TM.

the cytochrome *b₆* subunit and reenters the PQ-pool. The other electron is transferred to the soluble electron carrier cytochrome *c₆* or plastocyanin via the Rieske iron-sulfur protein and the cytochrome *f* subunit (Figure III). The activity of the PQ-pool and the cytochrome *b₆f* complex results in further proton release into the thylakoid lumen. Cytochrome *c₆* as well as plastocyanin have the ability to transport one single electron to PSI (Hohmann-Marriott and Blankenship, 2011; Bialek *et al.*, 2014). The PSI reaction center special pair P700 (at the PsaA/PsaB interface) is excited with light energy. The released electron then travels through the reaction center and is finally used to reduce ferredoxin at the PsaC subunit (Figure III). The cyanobacterial PSI complex differs from the plant PSI complex in two main aspects: 1) in cyanobacteria the electron gap at P700 is usually filled with the electron from cytochrome *c₆*

(reviewed by Liu, 2016). 2) Cyanobacterial PSI forms a trimer whereas in other organisms it is usually present as monomers (Boekema *et al.*, 1987).

Subsequently, ferredoxin is oxidized by the ferredoxin-NADP-reductase, which in turn reduces the redox equivalent NADP that is released into the cytosol as NADPH. Finally, the generated proton gradient across the thylakoid membrane fuels the ATP synthase to generate ATP at its head in the cytosol. The ATP synthase's head consists of three α/β heterodimers and at each α/β interface one ATP can be produced per one 360° turn of the c-ring (Figure III). Hence, the number of protons used to perform one turn is equivalent to the number of c subunits forming the integral membrane c-ring which varies between species (Ferguson, 2000). In the case of the cyanobacterium *Synechocystis* and land plants the c-ring harbors 14 c subunits and thus the costs for 1 ATP are 4.67 protons (Pogoryelov *et al.*, 2007).

1.4.2 Light harvesting

In plants, green algae and most secondary plastid bearing organisms, the light harvesting antennas are integral membrane complexes. They collect light energy via bound chlorophylls and shuffle it to the photosystems. In cyanobacteria however, the light harvesting antennas are soluble and not integrated into the membrane. These antennas, which are called phycobilisomes, are huge and can reach molecular weights of several megadaltons (Adir, 2005; Zhang *et al.*, 2017). Phycobilisomes are only present in cyanobacteria, glaucophytes and red algae. As already outlined above, phycobilisomes are the main factor that determines the interthylakoid distance in cyanobacteria (section 1.3; Olive *et al.*, 1997).

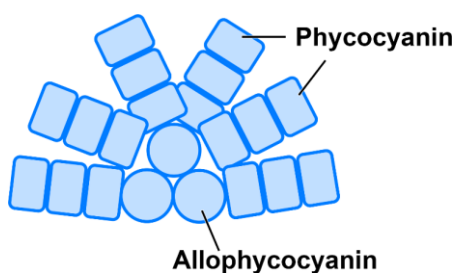


Figure IV. Model of a *Synechocystis* phycobilisome. The phycobilisome core is made of three allophycocyanin cylinders. The six lateral phycocyanin rods, that radiate from the core, consist of three phycocyanin cylinders each. Linker proteins interconnect the core components with each other, with the membrane and with the rods. The rod components are interconnected by linker proteins as well.

In the cyanobacterium *Synechocystis*, the main players in phycobilisome function and architecture are allophycocyanin, phycocyanin, several linker proteins and the terminal emitter protein ApcE (Figure IV; Arteni *et al.*, 2009; Chang *et al.*, 2015; Tang *et al.*, 2015). Allophycocyanin and phycocyanin are both multimers whose smallest building blocks are α - and β -phycobiliproteins which covalently bind via cysteine residues up to three bilin chromophores, which are linear tetrapyrroles. The α and β units dimerize and subsequent form

α/β heterotrimeric rings. Those rings stack into cylinders, which consist in *Synechocystis* of four stacked allophycocyanin rings and two stacked phycocyanin rings. The phycocyanin cylinders stack further into rods that consist of three cylinders (Figure IV). The fully assembled phycobilisome has a allophycocyanin core which consists of three allophycocyanin cylinders and six phycocyanin rods (Figure IV).

Under normal growth conditions, light harvesting occurs in state I and thus phycobilisomes are coupled to PSII and light energy is transferred to the closest chlorophyll in CP43 (Mullineaux, 2008; Chang *et al.*, 2015; Zhang *et al.*, 2017). The change in phycobilisome coupling to PSI is occurring under excess light conditions (reviewed by Harris *et al.*, 2018). To this point, it is not completely understood how state transition to PSI (state II) is achieved. However, two main theories have been proposed since the late 1990s. First, the phycobilisomes bind directly to PSI via the allophycocyanin core or the lateral phycocyanin rods (Su *et al.*, 1992; Mullineaux, 1994). Second, energy transfer between the photosystems' reaction center chlorophylls was proposed and termed spillover (van Thor *et al.*, 1998). Furthermore, the discovery of large megacomplexes harboring PSII, PSI and phycobilisomes hints towards the spillover theory and is additionally believed to be part of photo-protecting mechanisms (Liu *et al.*, 2013).

1.4.3 Lateral heterogeneity

The photosynthetic complexes, that are embedded in the thylakoids, are not evenly distributed along the thylakoid membrane network. This phenomenon is called lateral heterogeneity (Andersson and Anderson, 1980). In plant's chloroplasts, the PSII dimer is solely present in appressed grana stacks, whereas the PSI and ATP synthase complexes can only be found at stroma-facing thylakoids (stroma lamellae and outermost grana thylakoid; Pribil *et al.*, 2014). Cytochrome *b₆f* seems to be ubiquitously distributed and thus can be identified in stroma lamellae and grana stacks (Dekker and Boekema, 2005). Very recently, comparable results were obtained in the green algae *Chlamydomonas reinhardtii* (personal communication with Benjamin D. Engel). In the early 1990s, proof was found for lateral heterogeneity in diatoms, and recently, this was further analyzed and confirmed in the diatom *Phaeodactylum tricornutum* (Pyszniak and Gibbs, 1992; Lepetit *et al.*, 2012; Flori *et al.*, 2017). PSI and cytochrome *b₆f* were localized at stroma-facing thylakoid membranes, whereas PSII was mainly found in stacked areas on thylakoids facing other thylakoids.

In cyanobacteria, separation of PSI and PSII complexes was observed in the 1990s as well. Nevertheless, this separation has often been discussed but never really accepted as lateral

heterogeneity since the thylakoids are not distinguishable into stroma lamellae and grana thylakoids (Mullineaux, 2014; Liu, 2016). For years, several groups have analyzed the composition and distribution of the photosynthetic complexes in cyanobacteria by various techniques, i.e. fluorescence microscopy, immunogold-labeling transmission electron microscopy, atomic force microscopy and freeze fracture (Sherman *et al.*, 1994; Olive *et al.*, 1997; Westermann *et al.*, 1999; Vermaas *et al.*, 2008; Collins *et al.*, 2012; Tóth *et al.*, 2015; Casella *et al.*, 2017). The overall emerging picture is that all four photosynthetic protein complexes are differently distributed in distinct patches throughout the cellular membranes (Casella *et al.*, 2017). The PSII dimer, for example, forms rows and the PSI trimer seems to be crowded between those rows (Olive *et al.*, 1997; Westermann *et al.*, 1999). Moreover, several studies, using freeze fractures and atomic force microscopy, revealed thylakoid regions, which were almost completely filled with PSI trimers suggesting the presence of clearly separated PSI areas (Westermann *et al.*, 1999; MacGregor-Chatwin *et al.*, 2017). It is believed that those patches are located at the innermost thylakoid membranes (facing the cytoplasm) and the thylakoids adjacent to the plasma membrane (Sherman *et al.*, 1994; Vermaas *et al.*, 2008; Collins *et al.*, 2012). Immunogold-labeling of the ATP synthase located it to the outermost thylakoid sheet (adjacent to the plasma membrane) whereas cytochrome *b₆f* seems to locate to all types of membranes (Sherman *et al.*, 1994).

Additionally, membrane fractionations via sucrose density gradients of the thylakoids revealed, that early PSII assembly intermediates and the active monomer and dimer are laterally separated from each other (reviewed by Heinz *et al.*, 2016a). Interestingly, the D1 precursor (pD1) is found in lighter fractions together with the PSII assembly factor PrtA (processing associated tetratricopeptide repeat protein; Rengstl *et al.*, 2011). Therefore, these fractions were termed PrtA-defined membranes (PDM) presenting a distinct area dedicated to PSII assembly (see section 1.5).

1.5 PSII biogenesis and repair in cyanobacteria

The convergence zones in cyanobacteria, described above in subsection 1.2.2, have also been termed PSII biogenesis centers due to their role during PSII assembly (Schottkowski *et al.*, 2009a; Stengel *et al.*, 2012; Heinz *et al.*, 2016a). The biogenesis centers harbor the above mentioned PDMs where early assembly steps take place. As already indicated in subsection 1.4.1, the PSII monomer consists of 20 different subunits and various cofactors which have to be properly assembled in the right manner (Umena *et al.*, 2011). Therefore, a multitude of

specific assembly factors is involved in facilitating and assisting the step-wise biogenesis of the PSII complex (Komenda *et al.*, 2012b; Nickelsen and Rengstl, 2013; Heinz *et al.*, 2016a). The initial steps of the PSII assembly take place at the PDMs, which harbor the tetratricopeptide repeat (TPR) protein PratA. The PratA protein preloads pD1 with manganese, which is later required for the formation of the oxygen evolving complex (Schottkowski *et al.*, 2009a; Stengel *et al.*, 2012). Thereafter, the C-terminal extension of pD1 is cleaved in two steps by the protease CtpA (c-terminal processing protease) giving rise to mature D1 (Anbudurai *et al.*, 1994; Zak *et al.*, 2001; Komenda *et al.*, 2007). Meanwhile, the assembly factor Ycf48 assists in the D1/D2 dimerization and thus the reaction center complex is formed (Komenda *et al.*, 2004; 2008). In this course, the assembly factor CyanoP is associated with the luminal side of the D2 protein and, it is assumed that it escorts PSII during maturation until the attachment of the luminal subunits shielding the manganese cluster (Knoppová *et al.*, 2016). Thereafter, the PSII assembly leaves the biogenesis center and further proceeds in the thylakoid membranes (Rengstl *et al.*, 2011; Heinz *et al.*, 2016a). The inner core antenna proteins CP47 and CP43 are recruited successively to the reaction center complex. First, CP47 is attached with the assistance of Psb28 and Sll0933 and hence the reaction center complex RC47 is built. Subsequent to the RC47 formation, CP43 binding follows with the help of the assembly factor Sll0933 resulting in a PSII monomer lacking the oxygen evolving complex (Komenda *et al.*, 2004; Rengstl *et al.*, 2013). Thereafter, the water oxidizing complex is formed at the luminal side, assisted by the assembly proteins CyanoP and Psb27 (Nowaczyk *et al.*, 2006; Becker *et al.*, 2011; Komenda *et al.*, 2012a; Cormann *et al.*, 2014; Knoppová *et al.*, 2016). The oxygen evolving complex consists of the manganese cluster and its protective proteins PsbO, PsbV, PsbU and likely CyanoQ (Roose *et al.*, 2007; reviewed by Shen, 2015). As soon as the water oxidizing complex is attached, the fully functional PSII monomer is present. The dimerization of PSII monomers creates the attachment site for phycobilisome binding.

The phycobilisome binds to the PSII dimer but whether it assembles before PSII binding or on top of PSII is not entirely clear. However, some studies like van de Meene *et al.* (2012) favor phycobilisome assembly prior to PSII binding, since in the PSI/PSII double knockouts, phycobilisomes are still present and fully assembled. Moreover, fully assembled phycobilisomes were shown to float on thylakoid membranes until they connect to PSII dimers (Sarcina *et al.*, 2001). Nevertheless, not much is known about the assembly of the phycobilisomes themselves, but at least the assembly of the allophycocyanin and phycocyanin cylinders do not require assembly factors since they are able to self-assemble *in vitro* (Zhang

et al., 2002). Furthermore, it is generally believed that also *in vivo* the formation of phycobilisomes is a self-assembled process (reviewed by Harris *et al.*, 2018).

Once all components are in place and photosynthesis occurs, PSII has to be repaired every 20 - 30 minutes due to the rapid photodamage of the D1 protein. The D1 subunit is damaged in consequence of the toxicity of the water oxidation (Barber and Andersson, 1992; Tyystjärvi *et al.*, 1994). During PSII repair, the complex is partially disassembled, starting with the water oxidizing complex and followed by the inner antenna protein CP43 (Mabbitt *et al.*, 2014). The FtsH2/3 protease complex is the main player for the degradation machinery of the damaged D1 protein (Silva *et al.*, 2003; Boehm *et al.*, 2012; Yoshioka-Nishimura and Yamamoto, 2014). Subsequently, a new D1 copy is co-translationally inserted, followed by CtpA-mediated processing. Finally, the reattachment of the core antenna protein CP43 occurs with the assistance of Psb27 and Slr0933 or the TPR protein Slr0151 (Zhang *et al.*, 1999; Mabbitt *et al.*, 2014; Yang *et al.*, 2014).

As described above, PrtA and Slr0151 are TPR proteins and those are generally involved protein-protein interactions which facilitate processes as assembly of large protein complexes, gene expression, cell cycle, and protein transport (Blatch and Lässle, 1999). They consist of a 34 amino acids long TPR motif that can be repeated up to 16 times (reviewed by Bohne *et al.*, 2016). In total, 29 TPR proteins are encoded in the *Synechocystis* genome, five have a known function during assembly or repair of the photosystems (Bohne *et al.*, 2016). Amongst them, PrtA plays a role in early PSII biogenesis and Slr0151 is reported to be involved in PSII repair (Klinkert *et al.*, 2004; Yang *et al.*, 2015). Moreover, the Pitt (POR interacting TPR) protein regulates the chlorophyll synthesis by interacting with the light-dependent POR protein (protochlorophyllide oxidoreductase; Schottkowski *et al.*, 2009b; Rengstl *et al.*, 2011). Last but not least, the PSI assembly requires two TPR proteins as well, i.e. Ycf3 and Ycf37 (Boudreau *et al.*, 1997; Wilde *et al.*, 2001).

1.6 Cryo-electron tomography

Electron microscopy (EM) exploits the wave nature of moving electrons, as defined by de Broglie (1924). An electron with the momentum p can be described as a wave with the wavelength λ (1). Due to the much smaller wavelength of electrons, EM overcomes Abbé's diffraction limit of light microscopy (Abbé, 1873). This limit defines resolution as the distance d of two objects that still can be displayed as two (2) and is written as the quotient of the wavelength λ of the illuminating light and the numerical aperture (NA) of the objective.

$$(1) \quad \lambda = \frac{h}{p} \quad \text{where:} \quad \begin{array}{l} h: \text{Planck's constant} \\ p: \text{momentum of particle wave} \end{array}$$

$$(2) \quad d = \frac{\lambda}{2 \cdot n \cdot \sin\alpha} \quad \text{where:} \quad \begin{array}{l} n: \text{refractive index} \\ \alpha: (\text{aperture angle of objective})/2 \\ \text{NA} = n \sin\alpha \end{array}$$

Hence, Ernst Ruska used electrons as imaging source and built the first EM, which was awarded with the Nobel Prize in Physics in 1986. In principle, he used the construction of a light microscope as archetype for the structural design of the EM (Ruska and Knoll, 1931). The electrons are emitted from the electron source – a field emission gun – and bundled by a system of magnetic field lenses that function as condenser. Subsequently, the electron beam illuminates the specimen and the image is enlarged by two additional sets of magnetic field lenses that work as objective and projection lenses. For image generation, mostly non- or elastically scattered electrons are used, which pass the specimen and therefore, the technique is called transmission electron microscopy (TEM; Frank, 2006).

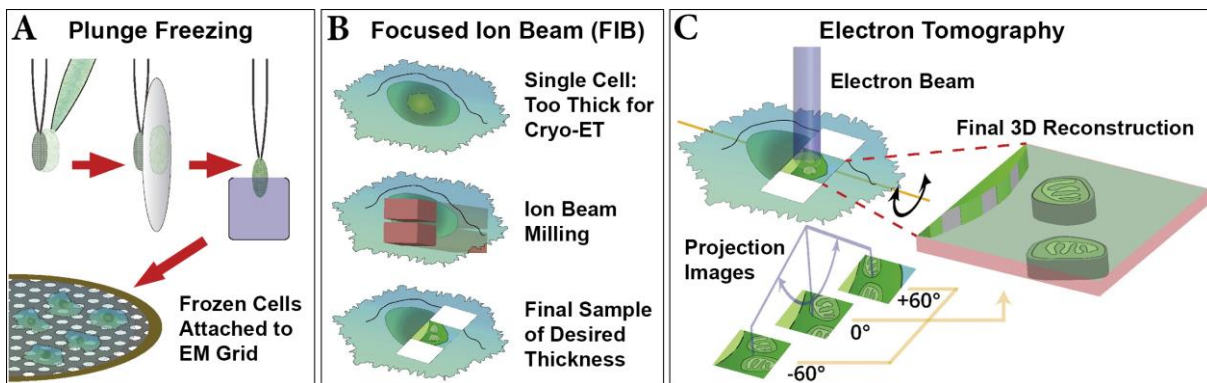


Figure V. Workflow of the sample preparation and data acquisition for cryo-ET. **A)** Plunge freezing for vitrification of the specimen directly on the EM grid. **B)** FIB milling to thin the sample and to generate an optimal lamella thickness of 100 nm. **C)** Electron tomography of the lamella by tilting the sample along a fixed axis (orange line) from -60° to $+60^\circ$ with 2° increments. Images of each tilt angle are back projected into the 3D volume of the tomogram. Adapted from Asano *et al.* (2016) with permission from Elsevier.

The image can be detected either photographically or digitally. Recently, the development of direct electron detectors revolutionized data acquisition and replaced charge coupled devices (CCD), especially for high resolution TEM. In contrast to CCD detectors, which can only detect electrons that are converted into photons by a scintillator, direct electron detectors register electrons directly via a semiconductor membrane (McMullan *et al.*, 2014).

To avoid interactions of the electrons with air or dust, all components mentioned above reside in a vacuum column. Since the sample is therefore exposed to vacuum throughout the imaging process, biological specimens have to be fixed and prepared for that purpose. For high resolution data acquisition, the sample is cryo-fixed to reduce and avoid artefacts that typically occur due to chemical fixation, dehydration, and resin infiltration (Dubochet *et al.*, 1988). For the investigation of single or isolated cells' architecture *in situ*, plunge freezing is the method of choice (Figure V A). Here, the sample is rapidly frozen, which leads to vitrification without ice crystal formation. The plunge freezing technique is not suited for studying tissue since the maximum freezing depth is 10 μm . To study thicker specimens (up to 200 nm), high pressure freezing should be used. In order to prepare a thin sample, which is required for TEM, the specimen is either thinned with a diamond knife or by the use of focused ion beam (FIB) milling (Figure V B; Rigort *et al.*, 2012).

For conventional TEM techniques, the contrast in biological samples is enhanced with heavy metals like lead or uranium, as the sample provides only low contrast by itself. Thanks to direct electron detectors and phase contrast using the Volta phase plate, however, heavy metal contrasting is not needed for high resolution TEM devices (Danev *et al.*, 2014; McMullan *et al.*, 2014).

In order to analyze cellular volumes in three dimensions, tomography is typically performed. During tomogram acquisition for cryo-electron tomography (cryo-ET), the sample is tilted from -60° to $+60^\circ$ with 2° increments (Figure V C). At each tilt angle, several frames are recorded and later aligned to one image stack. Each tilt image is then projected back into the 3D volume by weighted back projection, thereby generating the tomogram volume (Figure V C; Asano *et al.*, 2016). Those tomograms are 3D representations of the interior of the cell and hence, they are used for further data procession and analysis. Due to the high resolution data in tomograms, not only large recognizable protein complexes (i.e. ribosomes or proteasomes) but also previously unknown densities can be structurally analyzed by subtomogram averaging (Asano *et al.*, 2016). The big advantage of cryo-ET is that *in situ* protein structures can be characterized and investigated with respect to their native cellular environment.

Cryo-electron microscopy, including single particle analysis and cryo-ET has been knighted as "the resolution revolution" (Kühlbrandt, 2014). Indeed, the Nobel Prize for Chemistry 2017 was granted to Jacques Dubochet, Joachim Frank and Richard Henderson for "developing cryo-electron microscopy for the high-resolution structure determination of biomolecules in solution" (Press release of the Nobel Committee for Chemistry, 2017). It

appreciates the cryo fixation techniques without crystal formation (Jacques Dubochet), computer aided particle alignment, using cross-correlation functions (Joachim Frank), and the first published single particle structure (Richard Henderson).

2 AIMS OF THIS WORK

Since recording the first EM micrographs of cyanobacteria, researchers tried to understand how the thylakoid membranes are arranged at convergence zones and which factors are taking part in forming these regions. Over the years, a multitude of factors were described which are influencing the thylakoid membrane architecture but thus far, no factor could clearly be connected to the formation of the convergence zones. Moreover, extensive work to illuminate the biological function of the convergence zones revealed that they are implicated in PSII biogenesis. Henceforth, the convergence zones have been described as PSII-related biogenesis centers. PSII assembly is a complex process which requires the correct order and timing of the subunit attachment. Several specific assembly factors are involved in the assembly of various PSII subunits thereby shedding light on the complex interacting network of proteins that are required for the biogenesis of the active PSII complex.

Here, the function of the Slr0151 protein in PSII *de novo* assembly is presented, which was initially found to be part of the PSII repair machinery (section 3.1, Rast *et al.*, 2016). Moreover, the cyanobacterial CurT protein is an important player in convergence zone formation and hence, it creates the environment for efficient PSII assembly (section 3.2, Heinz *et al.*, 2016b). However, how membranes are really arranged at the convergence zones/ biogenesis centers have been debated for years. The study in section 3.3 describes for the first time the native molecular thylakoid membrane architecture of cyanobacterial thylakoid convergence zones determined by cryo-ET (Rast *et al.*, in preparation).

Hence, the data presented in this thesis enhances the understanding of the complex thylakoid membrane architecture and the sophisticated PSII assembly network. Alteration of the thylakoid convergence zones and the thylakoids in general seem to effect PSII biogenesis. Moreover, the ultrastructure of the membranes within the convergence zones was analyzed and comprehensively revealed membrane regions thus far unknown.

3 RESULTS

The following chapter contains two peer-reviewed studies published in international journals and in addition, one study in manuscript form, which will be submitted soon. The main findings and conclusions are shortly summarized in the beginning of each section. Supplemental data of each section are shown in chapter 6.

3.1 The role of Slr0151, a tetratricopeptide repeat protein from *Synechocystis* sp. PCC 6803, during photosystem II assembly and repair

Rast, A., Rengstl, B., Heinz, S., Klingl, A. and Nickelsen, J. (2016). Front. Plant Sci. 7: 605.

The assembly of the PSII complex depends on a huge amount of different assembly proteins. Previously, the TPR protein Slr0151 was reported to be a PSII repair factor under photodamaging conditions in *Synechocystis* (Yang *et al.*, 2014). Under normal light conditions however, structural changes on the thylakoids were observed. Several mutants with affected PSII assembly or accumulation exhibit changes in Slr0151 localization and protein level. It seems that Slr0151 and Sll0933 share similar functions since both proteins seem to be involved in the attachment of the inner core antennas to the PSII reaction center complex. Furthermore, Slr0151 is a membrane protein with locally increased levels at the thylakoids as well as the plasma membrane as shown by immunofluorescence.

<https://doi.org/10.3389/fpls.2016.00605>

3.2 Thylakoid membrane architecture in *Synechocystis* depends on CurT, a homolog of the granal CURVATURE THYLAKOID1 proteins

Heinz, S., **Rast, A.**, Shao, L., Gutu, A., Gügel, I.L., Heyno, E., Labs, M., Rengstl, B., Viola, S., Nowaczyk, M.M., Leister, D. and Nickelsen, J. (2016). *Plant Cell* 28: 2238-2260

The thylakoid membranes in the wild-type are oriented parallel to the plasma membrane and occasionally they converge toward it and form convergence zones. The cyanobacterial homolog of the *A. thaliana* CURVATURE THYLAKOID1 family, CurT, plays a fundamental role in the formation of these biogenesis centers which are dedicated to initial PSII assembly. Upon loss of the CurT protein convergence zones cannot be formed any longer, which in turn leads to a less efficient PSII assembly. Moreover, CurT localizes to the thylakoids with increased amounts at the biogenesis centers in fluorescence microscopy-based experiments and additionally, it possesses membrane tubulating capacities *in vitro*. Furthermore, CurT re-localizes in the wild-type to the plasma membrane if osmotic stress conditions are applied. Thus, the CurT protein influences the PSII biogenesis process as well as osmotic stress response via its structural role.

<https://doi.org/10.1105/tpc.16.00491>

3.3 *In situ* cryo-electron tomography of cyanobacterial thylakoid convergence zones reveals a biogenic membrane connecting thylakoids to the plasma membrane.

Rast, A., Albert, S., Schaffer, M., Beck, F., Pfeffer, S., Nickelsen, J. and Engel, B.D.

Thylakoid convergence zones are defined and maintained by the CurT protein as described in section 3.2 (Heinz *et al.*, 2016b). Here, the ultrastructure of the thylakoid membrane is described in detail regarding the arrangement of the thylakoid convergence zones. Thylakoid membranes are interconnected at the convergence zones and thus, form a convergence membrane. The convergence membrane comes in close contact to the plasma membrane and this contact area was termed the thylapse. Two large protein complexes were chosen as markers to distinguish between photosynthetically active regions and biogenic areas: the cyanobacterial light harvesting complexes, the phycobilisomes and the 70S ribosomes, respectively. Hence, areas dedicated to either function could clearly be identified, i.e the convergence membrane is free of phycobilisomes but covered with ribosomes and thylakoids in loosely stacked regions are covered with phycobilisomes.

***In situ* cryo-electron tomography of cyanobacterial thylakoid convergence zones reveals a biogenic membrane connecting thylakoids to the plasma membrane.**

Anna Rast^a, Sahradha Albert^{b*}, Miroslava Schaffer^{b*}, Florian Beck^b, Stefan Pfeffer^b, Jörg Nickelsen^{a#} and Benjamin D. Engel^{b#}

* contributed equally

corresponding authors

^a Department of Molecular Plant Sciences, LMU Munich, Großhaderner Str. 2-4, 82152 Planegg-Martinsried, Germany

^b Department of Molecular Structural Biology, Max Planck Institute of Biochemistry, 82152 Planegg-Martinsried, Germany

Abstract

In the cyanobacterium *Synechocystis* sp. PCC 6803, thylakoid membranes form sheet-like layers that are oriented parallel to the plasma membrane. The spacing between thylakoids is determined by the phycobilisomes, large light-harvesting antenna complexes that decorate the thylakoid surface. Convergence zones, regions where the tips of multiple thylakoids point to a specific spot on the plasma membrane, have been implicated in thylakoid biogenesis and the assembly of photosystem II. We analyzed the native membrane architecture and molecular organization of thylakoid convergence zones by focused ion beam (FIB) milling of frozen cells followed by *in situ* cryo-electron tomography. We observed that the tips of several thylakoids merge to form a novel membrane substructure, which we term the convergence membrane. At a structure that we name the thylapse, the convergence membrane and plasma membrane become closely appressed, separated by a ~2.5 nm gap. Using subtomogram averaging, we generated native structures of phycobilisomes and 70S ribosomes from within the cell. Phycobilisomes are found as single units, but often stack together into long arrays that are interconnected via specific linking densities between the phycocyanin rods. We mapped each phycobilisome and membrane-associated ribosome back into the cellular tomograms as markers for photosynthesis and protein biosynthesis, respectively. This identified two distinct biogenic regions in the thylakoid network: thylakoids that face the cell's cytosolic interior and the convergence membrane, which makes the thylapse connection to the plasma membrane.

Introduction

In almost all oxygenic phototrophs, the light driven reactions of photosynthesis are performed in a specialized network of internal membranes called the thylakoids. The thylakoids harbor four major protein complexes: photosystem II (PSII), cytochrome *b₆f*, photosystem I (PSI), and ATP synthase (reviewed by Nelson and Junge, 2015). In the cyanobacterium *Synechocystis* sp. PCC 6803 (hereafter *Synechocystis*), the thylakoid membranes are organized in non-appressed stacks of parallel sheets, which run parallel to the plasma membrane. Each cell contains a few convergence zones, where two or more of these sheets converge and point their thylakoid tips toward a specific spot on the plasma membrane (Nierzwicki-Bauer *et al.*, 1983; Liberton *et al.*, 2006; van de Meene *et al.*, 2006). Classical electron microscopy studies have reported an electron dense structure at the center of the convergence zones, which was termed the “thylakoid center” (Kunkel, 1982; van de Meene *et al.*, 2006; Stengel *et al.*, 2012). Thylakoid centers, which have a cylindrical appearance and seem to be associated with the thylakoid network, have been described as the origin point for the thylakoids at the cell’s periphery, positioned 50-200 nm from the plasma membrane (Kunkel, 1982; van de Meene *et al.*, 2006). In addition, a semicircular structure has been observed around the thylakoid center, which was proposed to be a membrane that connects to the converging thylakoid tips (Stengel *et al.*, 2012).

The convergence zones have also been termed “biogenesis centers” due to their special role during the early steps of PSII assembly (Stengel *et al.*, 2012; Heinz *et al.*, 2016b). In contrast to our very detailed knowledge about the structure and function of PSII, our understanding of PSII assembly and the biogenesis of thylakoid membranes is just starting to emerge (Umena *et al.*, 2011; Nelson and Junge, 2015; Heinz *et al.*, 2016a). The *curT* mutant, which is devoid of the cyanobacterial homolog of the CURTVATURE THYLAKOIDS1 family, has no convergence zones. The absence of convergence zones indicates an important role of the CurT protein in shaping the membrane architecture of these regions. Furthermore, the loss of convergence zones results in reduced PSII levels due to a deficiency in PSII assembly (Heinz *et al.*, 2016b). PratA, which is required for manganese preloading of the D1 protein during PSII assembly, has been localized by immunogold-labeling transmission electron microscopy to a punctate spot at the convergence zone that likely contains the thylakoid center and semicircular structure (Stengel *et al.*, 2012). Distinct PratA-defined membranes (PDMs) can be biochemically isolated, indicating that there may be a specialized membrane in this region (Schottkowski *et al.*, 2009; Rengstl *et al.*, 2011).

Thylakoids are decorated by two large cytosolic complexes: ribosomes, which perform biosynthesis of photosynthetic proteins such as the D1 subunit, and phycobilisomes which are the light-harvesting antennas that transfer their excitation energy to the photosystems. Whereas the convergence zones coordinate the early steps of PSII assembly, the presence of phycobilisomes decorating the parallel thylakoid sheets, in such high abundance that they determine the spacing between the sheets, indicates that these membranes contain fully functional photosystems (Olive *et al.*, 1997, Mullineaux, 2008; Watanabe and Ikeuchi, 2013). In *Synechocystis*, phycobilisomes are composed of allophycocyanin, phycocyanin, several linker proteins and the terminal emitter protein ApcE, which transfers excitation energy to the closest chlorophyll of CP43 in PSII (Arteni *et al.*, 2009; Chang *et al.*, 2015; Tang *et al.*, 2015). Under normal growth conditions, phycobilisomes transfer energy to PSII, which is called state I (Mullineaux, 2008; Chang *et al.*, 2015; Zhang *et al.*, 2017). High-light conditions induce a transition to state II, where phycobilisomes instead funnel energy to PSI (reviewed by Harris *et al.*, 2018).

Since the first report of cyanobacterial membrane ultrastructure in the 1980s (Nierzwicki-Bauer *et al.*, 1983), the existence of a direct connection between the thylakoids and the plasma membrane has been widely discussed. A comparable rare membrane fusion between thylakoid tips and the chloroplast inner envelope was recently reported in the eukaryotic green alga *Chlamydomonas reinhardtii* (Engel *et al.*, 2015). Moreover, in anoxygenic photosynthetic bacteria such as *Rhodospirillum* and *Rhodospseudomonas*, connections between the thylakoids and the plasma membrane are common throughout the cell and have been reported numerous times (Drews and Giesbrecht, 1965; Holt and Marr, 1965; Giesbrecht and Drews, 1966; Eimhjellen *et al.*, 1967; Tauschel and Drews, 1967; Remsen *et al.*, 1968; Oelze and Drews, 1972; Drews, 2013).

To analyze the native membrane architecture of *Synechocystis*, with special regard to the thylakoid convergence zones, we thinned frozen cells by focused ion beam milling and then used *in situ* cryo-electron tomography to visualize the 3D native cellular environment at molecular resolution.

Results

Wild-type *Synechocystis* cells were grown under normal conditions, vitrified by plunge-freezing, thinned with a focused ion beam, and then imaged by cryo-electron tomography. The final dataset consisted of 49 tomograms, within which we observed 61 thylakoid convergence

zones. Twenty-nine of these convergence zones contained distinct features at the focal point of the converging thylakoid tips, the area that was previously observed by classical electron microscopy to contain a cylindrical thylakoid center surrounded by a semicircular structure (Kunkel, 1982; van de Meene *et al.*, 2006; Stengel *et al.*, 2012). Our tomograms of the native cellular environment revealed that these convergence zone structures are unmistakably a membrane that connects to multiple thylakoid tips (Figure 1 and Figure 2 A-H). This

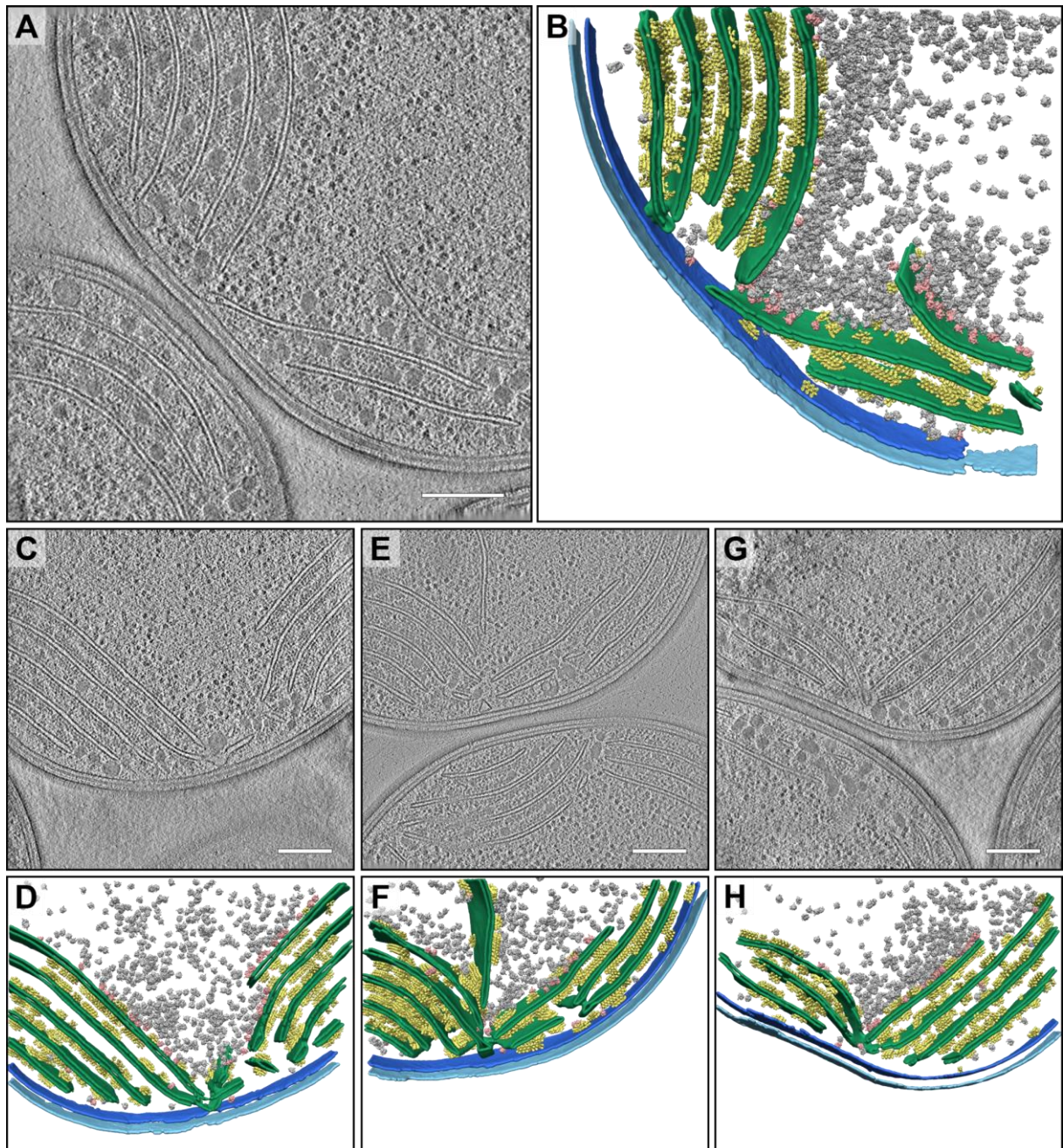


Figure 1. *In situ* cryo-ET of *Synechocystis* wild-type cells. Variety of membrane architecture at thylakoid convergence zones. Slices through tomogram volumes (A, C, E, G) and corresponding 3D segmentations (B, D, F, H) of the cellular membranes (OM in light blue, PM in dark blue, TM in green), with mapped in subtomogram averages of membrane-associated ribosomes (red), free cytosolic ribosomes (grey) and phycobilisomes (yellow). Scale bars: 200 nm.

“convergence membrane” varies in morphology and in some regions appears tubular and runs roughly perpendicular to the thylakoid sheets. In 14 cases, the convergence membrane made a close contact with the plasma membrane (Figure 1 E, F and Figure 2 A-C). As this tight connection between the thylakoid network and the plasma membrane has a shape that is reminiscent of a synapse, we have termed this connection “the thylapse”.

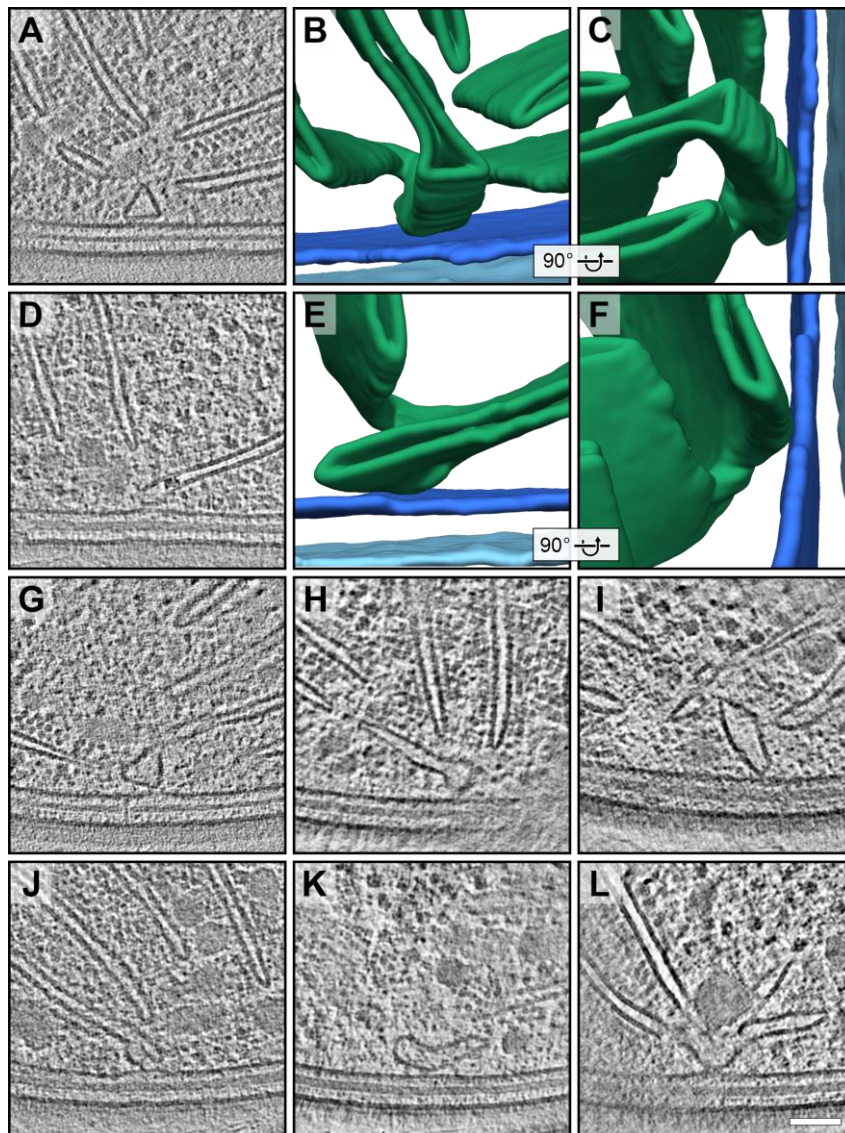


Figure 2. Thylapse gallery. Convergence membranes (CM) exhibit a large variety of morphology and make a close contact with the plasma membrane (PM) to form the thylapse. A, D) Tomographic slices containing a thylapse and (B, C, E, F) corresponding 3D segmentations of the CM (green), PM (dark blue) and OM (light blue) shown in (B, E) top view and (C, F) side view. (G-H) Tomographic slices showing different examples of thylapses. The mean distance between the CM and PM at the thylapse is $2.63 \text{ nm} \pm 0.68$ (N= 13). Scale bar: 50 nm.

To investigate the architecture of convergence membranes and the thylapse, four tomograms with convergence zones were analyzed in more detail. Figure 1 shows overviews

of the tomograms with their respective segmented 3D models of the membranes (outer membrane, plasma membrane and thylakoid membranes). While the architecture of the convergence zone varies widely, each region has at least two interconnecting thylakoids that

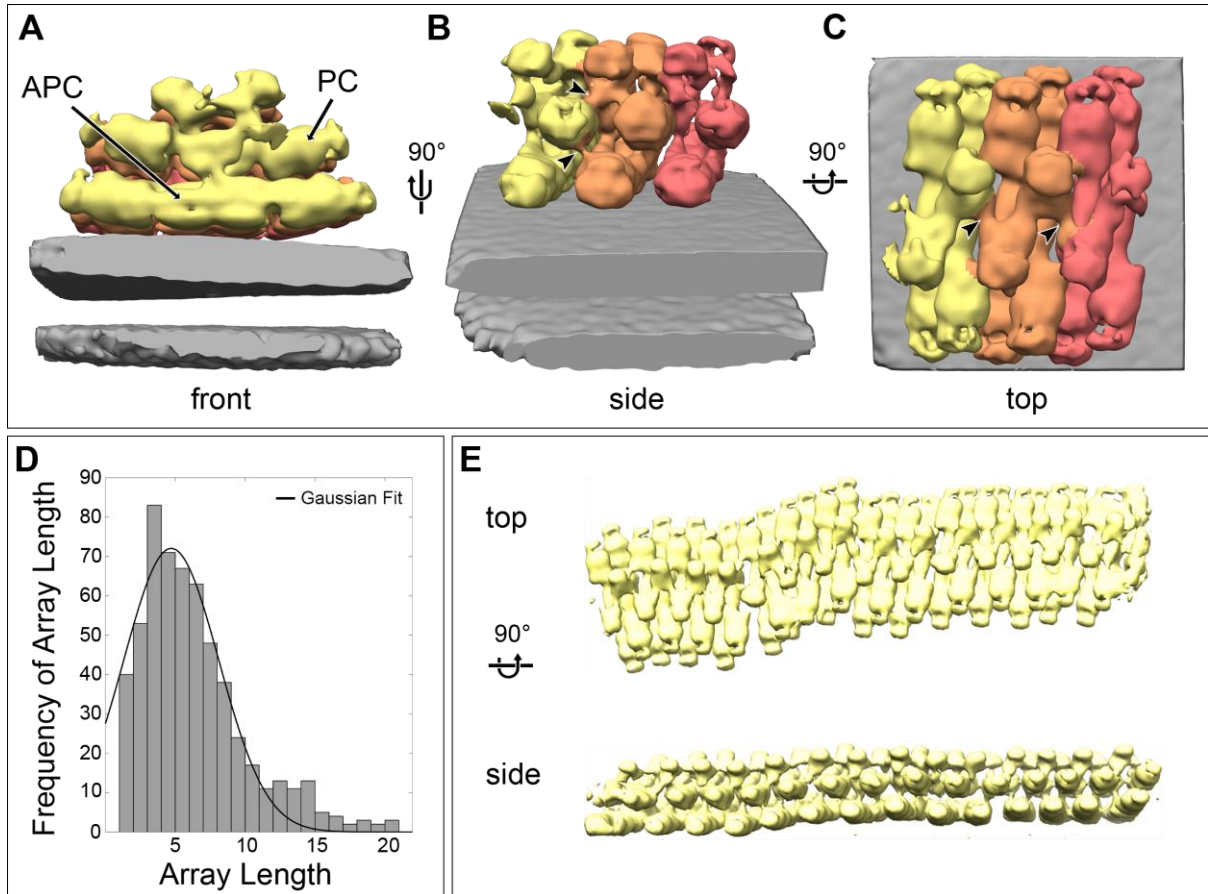


Figure 3. Phycobilisome structure. A-C) Three different views (front (A), side (B) and top (C)) of the phycobilisome array subtomogram average. The average contains three phycobilisome units, each displayed in a different shade of blue. Allophycocyanin (APC) and phycocyanin (PC) subunits are labeled with black arrows. Connections between phycobilisome units are indicated with black arrowheads. D) Histogram showing the distribution of phycobilisome array length. The Gaussian fit peaks at an array length of 5 phycobilisome units with a standard deviation of ± 3 . The histogram contains phycobilisome arrays from the four tomograms shown in Figure 1. E) Phycobilisome array from the tomogram in Figure 1B.

form the convergence membrane (Figure 2 A-F). At discrete points, the convergence membrane comes into very close proximity of the plasma membrane, thereby forming the thylapse contact between the thylakoids and plasma membrane (Figures 1 and 2). Following the diversity of the convergence zone architecture, thylapse shape is also quite variable (Figure 2). Figure 2A-F additionally emphasizes the 3D shape of the convergence membrane and the thylapse. The mean distance between the convergence membrane and the plasma membrane at the thylapse is $2.63 \text{ nm} \pm 0.68$, which is about half the diameter of a membrane bilayer (4 nm thick,

Kirchhoff *et al.*, 2011). The closely appressed thylapse contact appears to be bridged by small protein densities of unknown identity that might probably facilitate it (Figure 2 and Figure S1).

We performed *in situ* subtomogram averaging of two different membrane-associated macromolecular complexes to gain further insights into the biological function of the thylapse. Phycobilisomes, the light harvesting antennas of cyanobacteria, were used as markers for fully functional photosystems, while 70S ribosomes were used as markers for protein biosynthesis. The phycobilisome subtomogram average is shown in Figure 3 A-C. In total, 4207 particles were averaged from 21 tomograms to produce a 29 Å resolution structure. We found that the phycobilisomes form linear arrays, ranging from one single phycobilisome to 20 phycobilisome units in a row. The frequency distribution of array lengths follows a Gaussian function (Figure 3 D). An array length of three shows the highest incidence, which was also the array length we used for template matching and subtomogram averaging. The Gaussian fit shows that the mean phycobilisome array length is 5 units with a standard deviation of ± 3 , which means that 68 % of all arrays range from two to eight phycobilisome units in a row. Connections between adjacent phycobilisome single units in an array could be resolved in the average, showing that phycobilisomes are physically interconnected via the lateral phycocyanin rods (Figure 3 B, C, E).

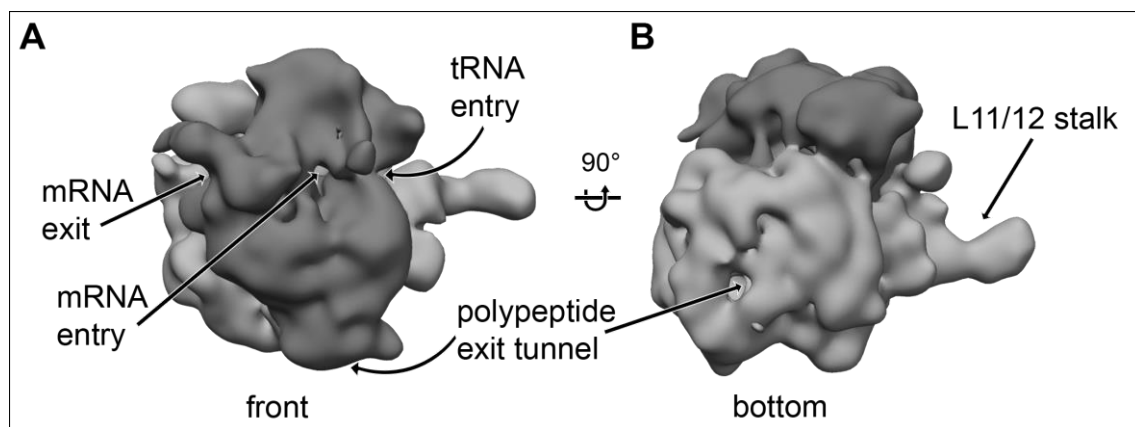


Figure 4. 70S ribosome structure. A) Front view and B) bottom view of the *Synechocystis* 70S ribosome subtomogram average. Highlighted are the tRNA entry site, mRNA entry and exit sites, as well as the polypeptide exit tunnel. 30S small subunit and 50S large subunit are depicted in dark and light grey, respectively.

The ribosome subtomogram average is shown in Figure 4. In total, 5707 ribosomes from six tomograms were averaged to generate a 22 Å resolution structure. The structure clearly reveals mRNA entrance and exit sites, as well as the tRNA entry and polypeptide exit tunnels

(Figure 4). Free cytosolic ribosomes were distinguished from membrane-associated ribosomes using a distance constraint of 27.4 nm from the ribosome center to the membrane.

To comprehensively identify all phycobilisome single units, we combined the template matching approach with membranograms, a visualization technique that provides a view of the membrane surface. Membranograms project densities from the tomographic volume onto a segmented membrane surface, thus visualizing integral and membrane-associated molecular complexes that protrude from the membrane (<https://github.com/dtegunov/membranorama>). All phycobilisome units were hand picked in the four tomograms shown in Figure 1. Five 3D segmented membrane surfaces decorated with phycobilisomes and ribosomes are shown in Figure 5D. The membranogram representation of these membrane surfaces with a projection width of ~ 5.5 nm are depicted in Figure S2. As already observed during template matching and subtomogram averaging of the phycobilisomes, the membranogram analysis also revealed that phycobilisomes form arrays. Close-ups from the top and the side of a phycobilisome array are presented in Figure 3 E. The arrays themselves are not always perfectly straight and can change their direction (Figures 3 E, 5 D and Figure S2). Moreover, some of the arrays are parallel to each other, while others are more randomly oriented (see Figure 5 D and Figure S2).

Finally, the subtomogram averages of phycobilisomes and ribosomes were pasted back into the tomogram volumes at their respective positions (Figure 1). To quantify the distribution of these complexes throughout the thylakoid network, we divided the thylakoid membranes into four categories according to their architecture (Figure 5 A): 1) thylakoid membranes that face the plasma membrane, 2) thylakoid membranes within a stack that therefore face other thylakoids, 3) thylakoid membranes that face the internal cytosol of the cell, and 4) thylakoids that interconnect with each other to form a convergence membrane. Already by qualitative visual inspection, one can see that the distributions of phycobilisomes and membrane-associated ribosomes vary between the different membrane regions (Figure 1). Hence, we quantified these observations, using the positions picked from the membranograms.

For the quantification of phycobilisome and ribosomes distributions, we calculated the concentration of both complexes as the number of particles per square micron of the different membrane regions. In all recorded and analyzed tomograms, the convergence membrane and the thylapse were free of phycobilisomes (Figures 1 and 5 B). Surprisingly, some phycobilisomes were detected at the plasma membrane (52.6 particles/ μm^2). Phycobilisomes were found at plasma membrane-facing, thylakoid-facing, and cytosol-facing thylakoid membranes with differing concentrations of 465.0 particles/ μm^2 , 612.0 particles/ μm^2 and 315.9 particles/ μm^2 , respectively.

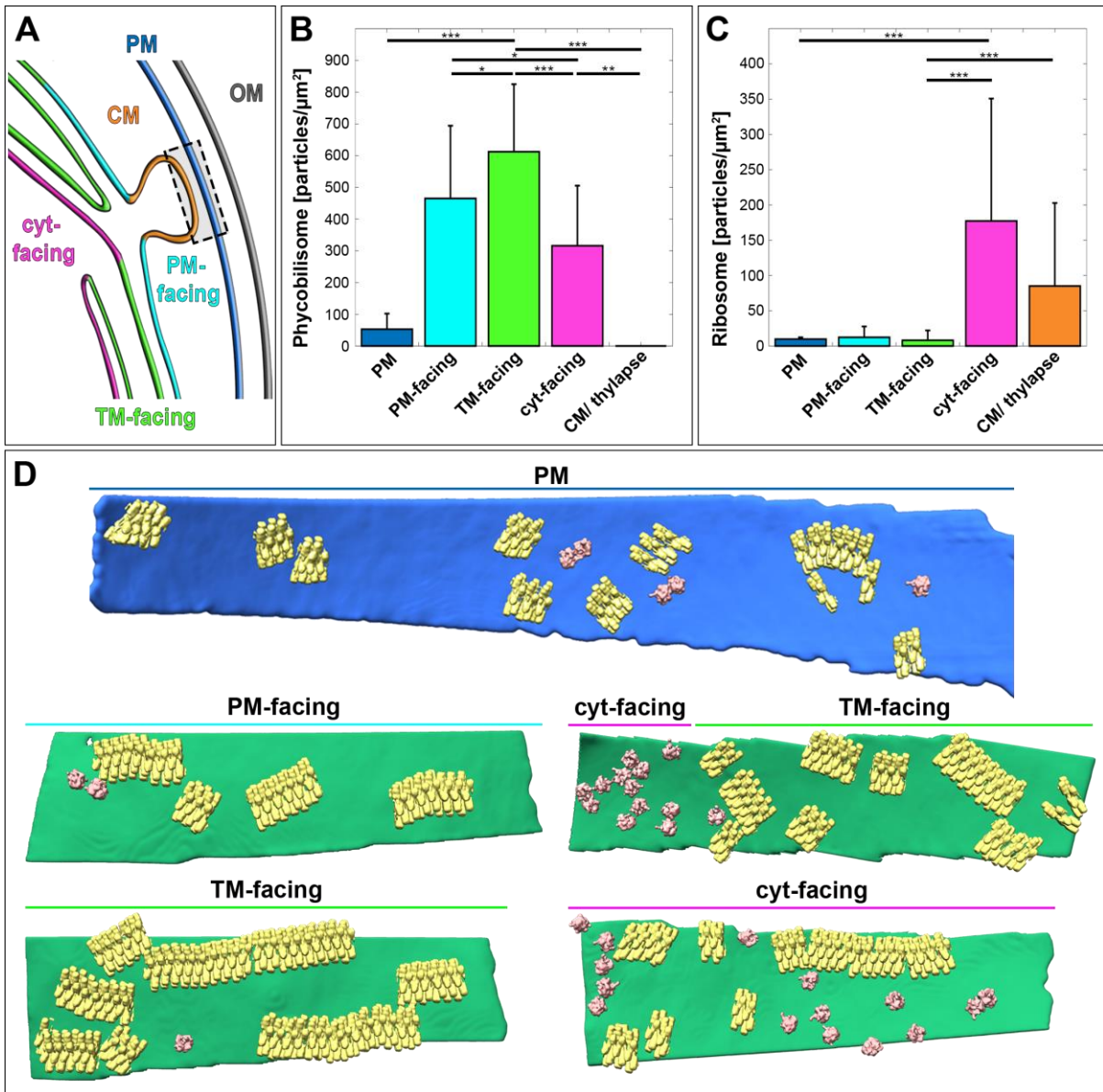


Figure 5. Concentrations of phycobilisomes and membrane-associated ribosomes at different membrane regions. A) Diagram of membrane regions at a convergence zone of a *Synechocystis* cell. Outer membrane (OM; grey), plasma membrane (PM; blue), thylakoid membranes that face the PM (PM-facing TM; light blue), thylakoid membranes that face other thylakoids (TM-facing TM; green), thylakoid membranes that face the cytosol (cyt-facing TM; pink), convergence membranes (CM, orange), and thylapse region (boxed). B) Phycobilisome concentrations at different membrane regions: PM (52.6 particles/μm²), PM-facing TM (465.0 particles/μm²), TM-facing TM (612.0 particles/μm²), and cyt-facing TM (315.9 particles/μm²). The CM and its thylapse are free of phycobilisomes. C) Concentrations of membrane-associated ribosomes at different membrane regions: PM (9.7 particles/μm²), PM-facing TM (12.3 particles/μm²), TM-facing TM (8.1 particles/μm²), cyt-facing TMs (177.2 particles/μm²), and CM (85.0 particles/μm²). The plotted values are mean concentration ± SD, measured from the four tomograms shown in Figure 1. Significant differences between the concentrations in different regions were determined by the Student's t test, with significance levels of 0.1, 0.01 and 0.001 indicated by one, two and three asterisks, respectively. The relatively high standard deviation of the ribosome concentrations at convergence membranes and cytosol-facing thylakoids indicates a high variance of membrane-associated ribosomes at those membranes. D) Segmented surfaces of different membrane regions decorated with back mapped phycobilisomes (yellow) and membrane-associated ribosomes (red). For membranogram representation see also Figure S2.

The majority of the ribosomes were free in the cytosol, but they clustered close to the innermost thylakoid sheet (Figure 1). Consistent with this, membrane-associated ribosomes were mainly found at the cytosol-facing thylakoid membranes (177.2 particles/ μm^2) and only very few were present at the plasma membrane (9.7 particles/ μm^2), at the thylakoids facing the plasma membrane (12.3 particles/ μm^2) or between thylakoid sheets (8.1 particles/ μm^2 , Figures 1 and 5 E). As a single thylakoid membrane transitioned from thylakoid-facing to cytosol-facing, lateral segregation could be observed between phycobilisomes and ribosomes in the two respective regions (Figure 5 D and Figure S2). A parallel can also be drawn to the lateral heterogeneity between PSI and PSII in the grana and stroma lamellae of higher plants' chloroplasts (Andersson and Anderson, 1980; Pribil *et al.*, 2014). In contrast to the phycobilisomes, membrane-associated ribosomes were present at the convergence membrane and thylapse (85.0 particles/ μm^2 , Figures 1 and 5 B, C).

To summarize, we found that thylakoid membranes interconnect with each other at convergence zones, forming convergence membranes at the cell's periphery (Figure 1). These convergence membranes make a specialized contact with the plasma membrane called the thylapse, where the two membranes are held closer together than the diameter of a single membrane bilayer (Figure 2). Whereas the thylakoids are covered with phycobilisome light-harvesting antennas, interestingly, the convergence membrane and thylapse are not (Figure 1 and 5). Membrane-associated ribosomes are abundant at both the innermost cytosol-facing thylakoid membrane and the convergence membrane (Figures 1, 4 and 5). Thus, the continuous network of thylakoid membranes has distinct photosynthetic and biogenic regions. The high concentration of ribosomes and the lack of phycobilisomes at the convergence membrane and thylapse suggests that these regions are specialized for biogenesis.

Discussion

This study describes the native membrane architecture at thylakoid convergence zones and the distribution of phycobilisomes and ribosomes in respect to these membranes. The cylindrical thylakoid center (Kunkel, 1982; van de Meene *et al.* 2006) and surrounding semicircular structure (Stengel *et al.*, 2012) previously observed by classical electron microscopy were clearly identified in our tomograms as membranes. Thus, we describe both of these structures as the convergence membrane to avoid misunderstanding. The convergence membrane was found to be continuous with the thylakoid membrane system, but not with the plasma membrane (Figures 1 and 2). The geometry of the convergence membrane is highly

diverse. Although it does form tubular structures, which likely resulted in the previous description of a cylindrical thylakoid center, the convergence membrane does not resemble a geometrical cylinder (Figures 1 and 2). Our elucidation of the convergence zone's native architecture demonstrates how *in situ* cryo-electron tomography with a direct electron detector is better suited for analyzing detailed membrane structures due to the higher resolution and the absence of artefacts that result from the preparation of plastic-embedded samples.

Out of the 61 thylakoid convergence zones observed in our study, 29 formed a convergence membrane and 14 possessed a thylapse that mediates the contact with the plasma membrane. Our tomograms each contain only about 4-8 % the total cell volume, depending on the lamella thickness (100-200 nm) and the chosen tomogram position (Figure S3). Moreover, we identified convergence zones in low magnification overviews and choose those positions for data acquisition, which resulted in tomogram volumes that often showed parts of more than one cell. This biased selection of the tomogram positions does not permit estimations about the number of thylapses within the whole cell. Van de Meene *et al.* (2006), however, previously reported that there are 3-10 convergence zones per cell, with a maximum of four thylakoid centers.

Our dataset allows us to answer a long standing question that researchers have been pursuing since the first attempts to analyze cyanobacterial convergence zones in the 1980s (Nierzwicki-Bauer *et al.*, 1983): Is there a connection between the thylakoids and the plasma membrane (Hinterstoisser *et al.*, 1993; Liberton *et al.*, 2006; van de Meene *et al.*, 2006)? Van de Meene *et al.* (2012) partially addressed this question when they showed that thylakoids fuse with the plasma membrane in wild-type cells grown in the dark. This seems logical since the photochemical proton gradient across the thylakoid membrane is not generated in the dark, fusion would not result in a massive leakage of protons from the thylakoid lumen to the periplasm. Our study helps to complete the picture by showing that under normal cultivation conditions (30 °C and 40 $\mu\text{mol photons m}^{-2}\text{s}^{-1}$) the thylakoid network's convergence membrane does *not* fuse with the plasma membrane, and thus the periplasm is not continuous with the thylakoid lumen.

In recent years, there has been debate about the involvement of the VIPP1 protein in thylakoid biogenesis and turnover. Cyanobacterial VIPP1 self-assembles into ring structures *in vitro* (Hennig *et al.*, 2015; Saur *et al.*, 2017). However, this structure could not be found in our cellular tomograms by either visual inspection or template matching. Moreover, the ring structure is too big to mediate the connection between the thylakoids and plasma membrane, as recently proposed by Junglas and Schneider (2018). The mean distance between the

convergence membrane and plasma membrane at the thylapse connection is 2.63 nm, whereas the VIPP1 ring is between 13.1 and 15.4 nm tall (Saur *et al.*, 2017). Thus, it is impossible for a fully assembled VIPP1 ring to mediate thylapse formation. However, 30 kDa VIPP1 monomers are too small to be identified in the tomograms by template matching. It is possible, therefore, that VIPP1 monomers or small oligomers are involved in the formation of the convergence membrane and thylapse.

Our study provides the first *in situ* structure of phycobilisomes within their native cellular environment. To the best of our knowledge, all attempts to determine the structure of the fully-assembled *Synechocystis* phycobilisome have failed thus far, with crystal structures only available for single subunits (allophycocyanin, phycocyanin and linkers; Marx and Adir, 2013; Tang *et al.*, 2015). The first attempts to visualize the whole structure of isolated phycobilisomes with negative stain electron microscopy were made by Glazer (1985) and Arteni *et al.* (2009). In 2015, the first cryo-EM single particle structure of an intact phycobilisome in association with PSII was published at 21 Å resolution from the cyanobacterium *Anabaena* sp. PCC 7120 (Chang *et al.*, 2015). Very recently, a high-resolution (3.5 Å) cryo-EM single particle structure was determined from the red alga *Griffithsia pacifica* (Zhang *et al.*, 2017). Unlike our *in situ* subtomogram average, none of these structures show the interplay with the thylakoid membrane, the interconnections between adjacent phycobilisome units, or the arrangement and distribution of the phycobilisomes in their native environment. Moreover, our study is the first to clearly show connections between adjacent phycobilisome units and array formation within the cell. This has already been hypothesized by Mullineaux (2008), based on the freeze-fracture observation that PSII forms rows while PSI seems to be randomly distributed between the rows (Olive *et al.*, 1997; Westermann *et al.*, 1999), and the atomic force microscopy observation that PSI forms large patches that are devoid of PSII (MacGregor-Chatwin *et al.*, 2017). Currently, it is not entirely clear how phycobilisomes transfer energy to PSI. There are two main theories of state transition mechanisms that have been discussed since the late 1990s: 1) direct binding of phycobilisomes to PSI via the allophycocyanin core or lateral phycocyanin rods might excite the PSI complex (Su *et al.*, 1992; Mullineaux, 1994) and 2) spillover of energy between the photosystems' reaction center chlorophylls might transfer excitation energy to PSI (van Thor *et al.*, 1998). Interestingly, in mutants lacking PSI and PSII, the phycobilisomes are still assembled and attached to the thylakoid membrane, and moreover, it has been shown that fully assembled phycobilisomes float on thylakoids until they connect to PSII (Sarcina *et al.*, 2001; Sarcina *et al.*, 2003; van de Meene *et al.*, 2012). In addition, a PSI/PSII/phycobilisome supercomplex was identified via crosslinking mass spectrometry, which favors the idea of the

spillover theory (Liu *et al.*, 2013). Taken together, these findings might explain why the phycobilisome arrays we observed are not perfectly straight. Perhaps some phycobilisomes in an array are attached to PSI instead of PSII, while other phycobilisomes might be detached from the photosystems, which could introduce flexibility into the arrays. It should be noted, however, that the cells used in this study were grown under normal conditions and dark adapted for several minutes before plunge freezing, which should favor PSII coupling of the phycobilisomes (state I).

The distinct distributions we measured for phycobilisomes and membrane-associated ribosomes lead to the conclusion that intracellular thylakoid membranes can be assigned to two different functions: First, biogenic membranes, including the convergence membrane and cytosol-facing thylakoids, are defined by a high concentration of ribosomes. Future research may reveal where PSII subunits are synthesized, which might clarify whether there are distinct membrane regions for *de novo* assembly and repair. Second, photosynthetically active regions are indicated by phycobilisomes, especially in stacked regions where thylakoid membranes face other thylakoids or the plasma membrane. In these regions, phycobilisomes mark fully functional PSII dimers, as cells were grown under normal conditions (30 °C and 40 $\mu\text{mol photons m}^{-2}\text{s}^{-1}$). Why occasional phycobilisomes are also present at the plasma membrane is not yet clear and awaits further research.

Recently, it was shown that the formation of convergence zones (biogenesis centers) is dependent on the CurT protein (Heinz *et al.*, 2016b). It seems likely that CurT is involved in shaping of the convergence membrane and thylapase, as it bends membranes and is located in thylakoid regions of high curvature. Moreover, when CurT-CFP expression was analyzed by fluorescence microscopy, a tubular network rich in CurT was observed traversing the cell periphery. It is plausible that this tubular network corresponds to the convergence membrane described here. Additionally, the convergence membrane and thylapase seems to functionally resemble the biochemically-described PratA-defined membranes (Stengel *et al.*, 2012). PratA has been localized with immunogold-labeling transmission electron microscopy to the biogenesis centers and is involved in manganese preloading of the D1 protein (Schottkowski *et al.*, 2009; Stengel *et al.*, 2012).

We propose the following molecular model of convergence zone architecture and function. The thylakoid membranes have defined molecular organization, with clear lateral separation of biogenic and photosynthetic regions. The biogenic convergence membrane and thylapase are shaped by the CurT protein, a hypothesis supported by the loss of convergence zones in the *curT* mutant and the tubule network-like appearance of CFP-tagged CurT.

Additional factors such as VIPP1 might also play a role in thylapse formation. Moreover, it seems reasonable that the thylapse orchestrates PrtA-dependent manganese uptake for PSII assembly, since immunogold EM places PrtA close to the plasma membrane at the focal point of the convergence zone, the same location as the thylapse. Currently, direct proof for the localization of these three proteins to the convergence membrane and thylapse is not possible by *in situ* cryo-ET due to the small molecular weights of CurT (14 kDa), VIPP1 (30 kDa) and PrtA (35 kDa).

Supporting Material

The material shown in section 6.4 is additional and supportive to the data depicted in this manuscript.

Methods

Cell Culture and Growth Conditions

Wild-type *Synechocystis* sp. PCC 6803 cells were cultivated in liquid BG 11 medium (Rippka *et al.*, 1979), supplemented with 5 mM glucose at 30°C under continuous white light at a photon irradiance of 40 $\mu\text{mol photons m}^{-2} \text{s}^{-1}$. Cell cultures were adapted 30 min to the dark and kept at constant 30°C temperature followed by plunge freezing at a cell density of $\text{OD}_{750\text{nm}} = 0.6$.

Cell Vitrification and Cryo-FIB Milling

Suspended cells in culture medium (3.3 μL) were blotted onto R1.2/1.3 carbon-coated copper grids (Quantifoil Micro Tools) and plunge frozen in a mixture of liquid ethane/propane using a Vitrobot Mark 4 (FEI). Subsequently, grids were loaded into Autogrid supports (FEI) followed by transfer into a focused ion beam-equipped (FIB) dual-beam scanning electron microscope (FEI Scios or FEI Quanta). To avoid charging and aid milling, the grids were coated with platinum. Thinning of the cells was achieved with a gallium FIB to a final thickness of about 100-200 nm.

Cryo-ET

We used a 300kV Titan Krios microscope (FEI) to acquire tilt series of cells. A tilt series in 2 degrees increments was recorded from about -60° to $+60^\circ$ in SerialEM software (Mastrorarde, 2005). Each tilt image was recorded by a direct electron detector camera (K2 summit, Gatan),

which was operated in movie mode at 12 frames per second. For high resolution, we chose an object pixel size of 3.42 Å, a maximal total accumulated dose of $<100 \text{ e}^- / \text{Å}$ and equipped the microscope with a Gatan postcolumn energy filter (968 Quantum). Contrast was ensured by recording the tilt series were either at defocus (-4 to -6 μm) using an objective aperture or in-focus using the Volta phase plate.

Tomogram Reconstruction

The recorded frames (K2 direct detector) were drift corrected using the MontionCor2 software with 3x3 patches (Zheng *et al.*, 2017). Frames of bad quality were omitted from the alignment. The tilt series were aligned with patch tracking and tomograms were reconstructed with weighted back projection using IMOD software (Kremer *et al.*, 1996). For template matching and averaging of phycobilisomes, only tomograms with high-quality alignments and power spectra were used, reducing our initial dataset from 49 to 21 tomograms. Many tomograms contain multiple cells due to the targeting of convergence zones that sit next to the plasma membrane. The tom_deconv deconvolution filter (https://github.com/dtegunov/tom_deconv) was used to enhance the contrast of defocus tomograms in Figures 1 and 2.

Phycobilisome Template Matching

Phycobilisome positions were determined with a combination of template matching (Frangakis *et al.*, 2002) with PyTom software (Hrabe *et al.*, 2012) and manual particle picking along membrane surfaces using membranograms (<https://github.com/dtegunov/membranorama>) of twice-binned tomograms (13.68 Å pixel size). The initial template was generated *de novo* from 10 handpicked particles that were aligned and averaged. This template was further optimized in subsequent rounds of template matching and averaging. The final template produced strong hits for phycobilisomes within our tomograms. High cross-correlation peaks were extracted from within the cellular volumes, and the corresponding subtomograms were visually screened for the presence of phycobilisomes at proper orientation.

Phycobilisome Subtomogram Averaging and Classification

Subtomogram averages were determined in Realspace with PyTom (Chen *et al.*, 2014) from 4207 unbinned particles from 21 tomograms, which were CTF-corrected in IMOD. The resolution was then calculated with Fourier shell correlation (FSC). Classification of the final dataset was achieved by iterative rounds of auto-focused 3D classification (AC3D) in PyTom with an oversampled class number and subsequent hierarchical clustering.

Ribosome Template Matching

The 70S ribosomes were initially matched with a high-resolved *E. coli* structure (PDB 4V69, Villa *et al.*, 2009) and the first hundred particles handpicked in CHIMERA. Initial alignment with FRM in PyTom resulted in a new template. Additionally, to enable automatic picking, we partially masked the small subunit before template matching. The first dataset was identified by CC values and then classified for the recovery of the missing density with CPCA in PyTom. Membrane-bound ribosomes were determined by a distance threshold of 20 pixels (membrane-associated ribosomes) and subsequent classification. As bacterial membrane-bound ribosomes easily dissociate from the membrane, we chose all membrane-associated ribosomes for the statistical analysis.

Phycobilisome and Ribosome Concentration Measurements

For the determination of the particle concentrations, the particles were counted in each membrane region using the positions determined by template matching and membranograms. Concentrations are displayed as the number of particles per square micron of membrane surface (see equation).

$$c_{particle} [particles * \mu m^{-2}] = \frac{\text{number of particles}}{\text{number of voxels in membrane} * \text{pixel size}^2 [nm^2]};$$

$$= \frac{\text{number of particles}}{\text{number of voxels in membrane}} * \frac{10^6}{1.368^2} * \mu m^{-2}$$

Visualization of Phycobilisomes and Ribosomes within the Cell

The positions and the angles after subtomogram averaging were used for pasting the phycobilisome and ribosome particles back into the 3D segmented cellular volumes. These volumes depicting the molecular environment of the cell were visualized in 3D using Chimera software (Pettersen *et al.*, 2004).

References

- Andersson, B. and Anderson, J. M.** (1980). Lateral heterogeneity in the distribution of chlorophyll-protein complexes of the thylakoid membranes of spinach chloroplasts. *Biochim. Biophys. Acta* 593(2): 427-440.
- Arteni, A. A., Ajlani, G. and Boekema, E. J.** (2009). Structural organisation of phycobilisomes from *Synechocystis* sp. strain PCC6803 and their interaction with the membrane. *Biochim. Biophys. Acta* 1787(4): 272-279.

- Chen, Y., Pfeffer, S., Fernandez, J. J., Sorzano, C. O. and Förster, F.** (2014). Autofocused 3D classification of cryoelectron subtomograms. *Structure* 22(10): 1528-1537.
- Chang, L., Liu, X., Li, Y., Liu, C. C., Yang, F., Zhao, J. and Sui, S. F.** (2015). Structural organization of an intact phycobilisome and its association with photosystem II. *Cell Res.* 25(6): 726-737.
- Drews, G.** (2013). The intracytoplasmic membranes of purple bacteria - Assembly of energy-transducing complexes. *J. Mol. Microbiol.* 23(1-2): 35-47.
- Drews, G. and Giesbrecht, P.** (1965). Die Thylakoidstrukturen von *Rhodospseudomonas spec.* *Arch. Mikrobiol.* 52(3): 242-250.
- Eimhjellen, K. E., Steensland, H. and Traetteberg, J.** (1967). A *Thiococcus* sp. nov. gen., its pigments and internal membrane system. *Arch. Mikrobiol.* 59(1): 82-92.
- Engel, B. D., Schaffer, M., Cuellar, L. K., Villa, E., Plitzko, J. M. and Baumeister, W.** (2015). Native architecture of the Chlamydomonas chloroplast revealed by *in situ* cryo-electron tomography. *eLife* 4: e04889.
- Frangakis, A. S., Bohm, J., Förster, F., Nickell, S., Nicastro, D., Typke, D., Hegerl, R. and Baumeister, W.** (2002). Identification of macromolecular complexes in cryoelectron tomograms of phantom cells. *Proc. Natl. Acad. Sci. USA* 99(22): 14153-14158.
- Giesbrecht, P. and Drews, G.** (1966). Über die Organisation und die makromolekulare Architektur der Thylakoide "lebender" Bakterien. *Arch. Mikrobiol.* 54(4): 297-330.
- Glazer, A. N.** (1985). Light harvesting by phycobilisomes. *Annu. Rev. Biophys. Biophys. Chem.* 14: 47-77.
- Harris, D., Bar-Zvi, S., Lahav, A., Goldshmid, I. and Adir, N.** (2018). Membrane Protein Complexes: Structure and Function. The structural basis for the extraordinary energy-transfer capabilities of the phycobilisome. *Springer Singapore. Subcellular Biochemistry* 87: 57-82. ISSN: 978-981-10-7757-9.
- Heinz, S., Liauw, P., Nickelsen, J. and Nowaczyk, M.** (2016a). Analysis of photosystem II biogenesis in cyanobacteria. *Biochim. Biophys. Acta* 1857(3): 274-287.
- Heinz, S., Rast, A., Shao, L., Gutu, A., Gügel, I. L., Heyno, E., Labs, M., Rengstl, B., Viola, S., Nowaczyk, M. M., Leister, D. and Nickelsen, J.** (2016b). Thylakoid membrane architecture in *Synechocystis* depends on CurT, a homolog of the granal CURVATURE THYLAKOID1 proteins. *Plant Cell* 28: 2238-2260.
- Hennig, R., Heidrich, J., Saur, M., Schmäser, L., Roeters, S. J., Hellmann, N., Woutersen, S., Bonn, M., Weidner, T., Markl, J. and Schneider, D.** (2015). IM30 triggers membrane fusion in cyanobacteria and chloroplasts. *Nat. Commun.* 6: 7018.
- Hinterstoisser, B., Cichna, M., Kuntner, O. and Peschek, G. A.** (1993). Cooperation of plasma and thylakoid membranes for the biosynthesis of chlorophyll in cyanobacteria: the role of the thylakoid centers. *J. Plant Physiol.* 142(4): 407-413.

- Holt, S. C. and Marr, A. G.** (1965). Location of chlorophyll in *Rhodospirillum rubrum*. *J. Bacteriol.* 89: 1402-1412.
- Hrabe, T., Chen, Y., Pfeffer, S., Cuellar, L. K., Mangold, A. V. and Förster, F.** (2012). PyTom: a python-based toolbox for localization of macromolecules in cryo-electron tomograms and subtomogram analysis. *J. Struct. Biol.* 178(2): 177-188.
- Junglas, B. and Schneider, D.** (2018). What is Vipp1 good for? *Mol. Microbiol.* 108(1): 1–5.
- Kirchhoff, H., Hall, C., Wood, M., Herbstova, M., Tsabari, O., Nevo, R., Charuvi, D., Shimoni, E. and Reich, Z.** (2011). Dynamic control of protein diffusion within the granal thylakoid lumen. *Proc. Natl. Acad. Sci. USA* 108(50): 20248-20253.
- Kremer, J. R., Mastronarde, D. N. and McIntosh, J. R.** (1996). Computer visualization of three-dimensional image data using IMOD. *J. Struct. Biol.* 116(1): 71-76.
- Kunkel, D. D.** (1982). Thylakoid centers: Structures associated with the cyanobacterial photosynthetic membrane system. *Arch. Microbiol.* 133(2): 97-99.
- Liberton, M., Howard Berg, R., Heuser, J., Roth, R. and Pakrasi, H. B.** (2006). Ultrastructure of the membrane systems in the unicellular cyanobacterium *Synechocystis* sp. strain PCC 6803. *Protoplasma* 227(2-4): 129-138.
- Liu, H., Zhang, H., Niedzwiedzki, D. M., Prado, M., He, G., Gross, M. L. and Blankenship, R. E.** (2013). Phycobilisomes supply excitations to both photosystems in a megacomplex in cyanobacteria. *Science* 342: 1104-1107.
- MacGregor-Chatwin, C., Sener, M., Barnett, S. F. H., Hitchcock, A., Barnhart-Dailey, M. C., Maghlaoui, K., Barber, J., Timlin, J. A., Schulten, K. and Hunter, C. N.** (2017). Lateral segregation of photosystem I in cyanobacterial thylakoids. *Plant Cell* 29(5): 1119-1136.
- Marx, A. and Adir, N.** (2013). Allophycocyanin and phycocyanin crystal structures reveal facets of phycobilisome assembly. *Biochim. Biophys. Acta* 1827(3): 311-318.
- Mastronarde, D. N.** (2005). Automated electron microscope tomography using robust prediction of specimen movements. *J. Struct. Biol.* 152(1): 36-51.
- Mullineaux, C. W.** (1994). Excitation energy transfer from phycobilisomes to photosystem I in a cyanobacterial mutant lacking photosystem II. *Biochim. Biophys. Acta* 1184(1): 71-77.
- Mullineaux, C. W.** (2008). The cyanobacteria. Molecular biology, genomics and evolution. Chapter 11: Biogenesis and dynamics of thylakoid membranes and the photosynthetic apparatus. *Caister Academic Press*: 289-303. ISSN: 978-1-904455-15-8.
- Nelson, N. and Junge, W.** (2015). Structure and energy transfer in photosystems of oxygenic photosynthesis. *Annu. Rev. Biochem.* 84(1): 659-683.
- Nierzwicki-Bauer, S. A., Balkwill, D. L. and Stevens, S. E.** (1983). Three-dimensional ultrastructure of a unicellular cyanobacterium. *J. Cell Biol.* 97(3): 713-722.

- Oelze, J. and Drews, G.** (1972). Membranes of photosynthetic bacteria. *Biochim. Biophys. Acta* 265(2): 209-239.
- Olive, J., Ajlani, G., Astier, C., Recouvreur, M. and Vernotte, C.** (1997). Ultrastructure and light adaptation of phycobilisome mutants of *Synechocystis* PCC 6803. *Biochim. Biophys. Acta* 1319(2): 275-282.
- Pettersen, E. F., Goddard, T. D., Huang, C. C., Couch, G. S., Greenblatt, D. M., Meng, E. C. and Ferrin, T. E.** (2004). UCSF Chimera—A visualization system for exploratory research and analysis. *J. Comput. Chem.* 25(13): 1605-1612.
- Pribil, M., Labs, M. and Leister, D.** (2014). Structure and dynamics of thylakoids in land plants. *J. Exp. Bot.* 65(8): 1955-1972.
- Remsen, C. C., Watson, S. W., Waterbury, J. B. and Trüper, H. G.** (1968). Fine Structure of *Ectothiorhodospira mobilis* Pelsh. *J. Bacteriol.* 95(6): 2374-2392.
- Rengstl, B., Oster, U., Stengel, A. and Nickelsen, J.** (2011). An intermediate membrane subfraction in cyanobacteria is involved in an assembly network for photosystem II biogenesis. *J. Biol. Chem.* 286(24): 21944-21951.
- Rippka, R., Deruelles, J., Waterbury, J. B., Herdman, M. and Stanier, R. Y.** (1979). Generic assignments, strain histories and properties of pure cultures of cyanobacteria. *Mircobiol.* 111(1): 1-61.
- Sarcina, M., Murata, N., Tobin, M. J. and Mullineaux, C. W.** (2003). Lipid diffusion in the thylakoid membranes of the cyanobacterium *Synechococcus* sp.: effect of fatty acid desaturation. *FEBS Lett.* 553(3): 295-298.
- Sarcina, M., Tobin, M. J. and Mullineaux, C. W.** (2001). Diffusion of phycobilisomes on the thylakoid membranes of the cyanobacterium *Synechococcus* 7942. Effects of phycobilisome size, temperature, and membrane lipid composition. *J. Biol. Chem.* 276(50): 46830-46834.
- Saur, M., Hennig, R., Young, P., Rusitzka, K., Hellmann, N., Heidrich, J., Morgner, N., Markl, J. and Schneider, D.** (2017). A janus-faced IM30 ring involved in thylakoid membrane fusion is assembled from IM30 tetramers. *Structure* 25(9): 1380-1390.e1385.
- Schotchkowski, M., Gkalypoudis, S., Tzekova, N., Stelljes, C., Schünemann, D., Ankele, E. and Nickelsen, J.** (2009). Interaction of the periplasmic PratA factor and the PsbA (D1) protein during biogenesis of photosystem II in *Synechocystis* sp. PCC 6803. *J. Biol. Chem.* 284(3): 1813-1819.
- Stengel, A., Gügel, I. L., Hilger, D., Rengstl, B., Jung, H. and Nickelsen, J.** (2012). Initial steps of photosystem II *de novo* assembly and preloading with manganese take place in biogenesis centers in *Synechocystis*. *Plant Cell* 24(2): 660-675.
- Su, X., Fraenkel, P. G. and Bogorad, L.** (1992). Excitation energy transfer from phycocyanin to chlorophyll in an *apcA*-defective mutant of *Synechocystis* sp. PCC 6803. *J. Biol. Chem.* 267(32): 22944-22950.

- Tang, K., Ding, W.-L., Höppner, A., Zhao, C., Zhang, L., Hontani, Y., Kennis, J. T. M., Gärtner, W., Scheer, H., Zhou, M. and Zhao, K.-H.** (2015). The terminal phycobilisome emitter, LCM: A light-harvesting pigment with a phytochrome chromophore. *Proc. Natl. Acad. Sci. USA* 112(52): 15880-15885.
- Tauschel, H. D. and Drews, G.** (1967). Thylakoidmorphogenese bei *Rhodospseudomonas palustris*. *Arch. Mikrobiol.* 59(4): 381-404.
- Umena, Y., Kawakami, K., Shen, J. R. and Kamiya, N.** (2011). Crystal structure of oxygen-evolving photosystem II at a resolution of 1.9 Å. *Nature* 473(7345): 55-60.
- van de Meene, A. M., Hohmann-Marriott, M. F., Vermaas, W. F. and Roberson, R. W.** (2006). The three-dimensional structure of the cyanobacterium *Synechocystis* sp. PCC 6803. *Arch. Microbiol.* 184(5): 259-270.
- van de Meene, A. M., Sharp, W. P., McDaniel, J. H., Friedrich, H., Vermaas, W. F. and Roberson, R. W.** (2012). Gross morphological changes in thylakoid membrane structure are associated with photosystem I deletion in *Synechocystis* sp. PCC 6803. *Biochim. Biophys. Acta* 1818(5): 1427-1434.
- van Thor, J. J., Mullineaux, C. W., Matthijs, H. C. P. and Hellingwerf, K. J.** (1998). Light harvesting and state transitions in cyanobacteria. *Bot. Acta* 111(6): 430-443.
- Villa, E., Sengupta, J., Trabuco, L. G., LeBarron, J., Baxter, W. T., Shaikh, T. R., Grassucci, R. A., Nissen, P., Ehrenberg, M., Schulten, K. and Frank, J.** (2009). Ribosome-induced changes in elongation factor Tu conformation control GTP hydrolysis. *Proc. Natl. Acad. Sci. USA* 106(4): 1063-1068.
- Watanabe, M. and Ikeuchi, M.** (2013). Phycobilisome: architecture of a light-harvesting supercomplex. *Photosynth. Res.* 116(2-3): 265-276.
- Westermann, M., Neuschaefter-Rube, O., Morschel, E. and Wehrmeyer, W.** (1999). Trimeric photosystem I complexes exist *in vivo* in thylakoid membranes of the *Synechocystis* strain B09201 and differ in absorption characteristics from monomeric photosystem I complexes. *J. Plant Physiol.* 155(1): 24-33.
- Zhang, J., Ma, J., Liu, D., Qin, S., Sun, S., Zhao, J. and Sui, S. F.** (2017). Structure of phycobilisome from the red alga *Griffithsia pacifica*. *Nature* 551(7678): 57-63.
- Zheng, S. Q., Palovcak, E., Armache, J. P., Verba, K. A., Cheng, Y. and Agard, D. A.** (2017). MotionCor2: anisotropic correction of beam-induced motion for improved cryo-electron microscopy. *Nat. Meth.* 14(4): 331-332.

4 DISCUSSION

4.1 Structural and photosystem II specific role of Slr0151 and CurT

The data presented in this thesis showed that Slr0151 as well as CurT influence the thylakoid membrane architecture and PSII biogenesis. While Slr0151 seems to be directly involved in PSII assembly, CurT's role is more indirect and seems to be a consequence of its structural function by forming PSII-related biogenic membranes. In the following subsections their respective function is separately discussed in more detail.

4.1.1 The role of Slr0151

The TPR protein Slr0151 is a membrane protein, which possesses two TPR motifs (Yang *et al.*, 2014; Rast *et al.*, 2016). It is part of the gene cluster *slr0144 – slr0152* that was described as operon with PSII related functions (Wegener *et al.*, 2008). Initial studies indicated an association of the Slr0151 protein with PSI assembly but recent studies revealed an involvement in the PSII biogenesis process (Wegener *et al.*, 2008; Kubota *et al.*, 2010; Yang *et al.*, 2014; section 3.1, Rast *et al.*, 2016). The *slr0151*⁻ knockout was first described by Yang *et al.* (2014), and an effect on the PSII turnover at high-light was demonstrated. Additionally, it was found by a split-ubiquitin assay that Slr0151 directly interacts with the D1 and CP43 subunits of PSII. These findings are in line with the research carried out under normal growth conditions, where *slr0151*⁻ exhibits a milder PSII phenotype than at high-light (section 3.1, Rast *et al.*, 2016). The PSII-related function of Slr0151 is underlined by the changes in Slr0151 accumulation in several different PSII-affected mutants. The most striking effect is the over-accumulation of the Slr0151 protein in the *slr0933*⁻ mutant, suggesting a functional relationship between both proteins. The Slr0933 protein is an assembly factor involved in the attachment of the inner antenna proteins CP47 and CP43 to the reaction center complex, resulting in the PSII monomer lacking the water oxidizing complex (see section 1.5; Rengstl *et al.*, 2013). Membrane fractionation experiments of wild-type membranes revealed that the Slr0151 protein is localized in all types of membranes, i.e. plasma membrane, PDMs, and mature thylakoids (Figures 3 and 4 in section 3.1, Rast *et al.*, 2016). This distribution in membrane fractionation experiments has already been reported for one other assembly factor that is involved in PSII assembly as well as repair, i.e. Ycf48, thereby further substantiating that Slr0151 is involved in both processes (Komenda *et al.*, 2008; Rengstl *et al.*, 2011). Interestingly, in the *pratA*⁻ and

slr0151 mutants, Slr0151 containing fractions shifted more toward the PDMs as compared to the wild-type fractions, which further underlines a functional relationship between Slr0151 and Sll0933 (Figures 3 and 4 in section 3.1, Rast *et al.*, 2016).

On the other hand, in the *slr0151* mutant, the membrane distribution of most analyzed PSII subunits and assembly factors remained unaltered except for the inner core antenna protein CP47 (Figure 4 in section 3.1, Rast *et al.*, 2016). In the wild-type, CP47 is exclusively present in mature thylakoid membrane fractions, since the PSII reaction center pre-complex leaves the PDMs before the attachment of the antenna proteins (reviewed by Heinz *et al.*, 2016a; Figure 4 in section 3.1, Rast *et al.*, 2016). The misslocalization of CP47 to the PDMs further implies that Slr0151 might guide the antenna proteins to the reaction center complex and, this functionally resembles the role of the assembly factor Sll0933 (Rengstl *et al.*, 2013). Moreover, the shift of CP47 toward the PDMs was observed in *ctpA* and *curT* mutants as well, substantiating Slr0151's dual role in PSII *de novo* biogenesis and repair. This is in agreement with the previous study at high-light, in which reduced levels of the assembly intermediate RC47 were detected (Yang *et al.*, 2014).

To further prove the ubiquitous membrane distribution, the localization of Slr0151 was analyzed under normal light and high-light conditions using immunofluorescence light microscopy. In fact, a punctuated pattern of the Slr0151 signals at the plasma and thylakoid membranes could be shown for both conditions. Moreover, in regions at the cell periphery with no or less chlorophyll autofluorescence, increased levels of Slr0151 were observed thereby emphasizing a localization to the PSII biogenesis centers. Comparable localization results were reported for the PSII repair factor FtsH2 underlining Slr0151's involvement in PSII repair under high-light (Yang *et al.*, 2014; Sacharz *et al.*, 2015).

Additionally, the ultrastructure of *slr0151* showed an increased thylakoid lumen, which is an observation already made in wild-type cells and carotenoid mutants grown at very low light intensities ($0.5 \mu\text{mol photons m}^{-2}\text{s}^{-1}$) as well as in the dark with 10 min light per day, respectively (van de Meene *et al.*, 2012; Tóth *et al.*, 2015). As mentioned in section 1.3, the proton gradient is less pronounced in the dark as compared to light conditions and thus, the thylakoid membranes are more flexible in cyanobacteria (Stingaciu *et al.*, 2016). Therefore, the Slr0151 protein may probably take part in regulating the flexibility of the thylakoid membranes by adding a structural effect to the PSII biogenesis process, maintenance and turnover. How Slr0151 achieves the structural effect on a molecular level remains elusive and has to be investigated further.

Taken together it could be shown that Slr0151 is involved in the formation of larger reaction center complexes during *de novo* and repair assembly of PSII, and that the disordered thylakoid architecture in the *slr0151*⁻ mutant seem to affect the PSII assembly.

Furthermore, it was recently shown that the Slr0151 protein is additionally involved in the phosphorylation network of another gene of the operon *slr0144 – slr0152* described above. The gene *slr0148* encodes the ferredoxin 5 protein which is an unusual ferredoxin due to possessing a C-terminal extension (Angeleri *et al.*, 2018). Ferredoxin 5 has two threonine residues (T18 and T72) that can be phosphorylated by the serine/threonine protein kinase G (SpkG). SpkG is encoded by the operon as well, and is the gene product of the *slr0152* open reading frame. Moreover, ferredoxin 5 is over-phosphorylated by SpkG in the *slr0151*⁻ knockout. In the *spkG*⁻ mutant however, the Slr0151 expression is reduced to about half of the wild-type level (Angeleri *et al.*, 2018). It is noteworthy, that SpkG has been shown to sense salt stress and, thus influences the expression of various genes (Liang *et al.*, 2011). Another study demonstrated that Slr0151 is present in the plasma membrane under mild salt conditions as well (Huang *et al.*, 2006). Therefore, it seems likely that Slr0151 may take part in high-light and salt stress response possibly by sensing and indirectly regulating the phosphorylation of different proteins. Besides the involvement of Slr0151 in PSII biogenesis and repair, Slr0151 is also part of the phosphorylation system of ferredoxin 5. Further research on the whole operon with “PSII related function” might reveal if and how this phosphorylation network might be connected to photosynthesis.

4.1.2 The role of CurT

The cyanobacterial homologue of the plant CURT1 protein family, CurT, shapes the thylakoid architecture in *Synechocystis* as well. CurT is a membrane protein with two transmembrane domains and a N-terminal extension harboring an amphipathic helix. *In vitro*, it tubulates artificial liposomes, a feature observed for many thylakoid membrane shaping proteins as outlined in section 1.3, i.e. VIPP1, FZL/BDLP as well as *A. thaliana* CURT1A-D (Figure 1 in section 3.2; Heinz *et al.*, 2016b). The cyanobacterial CurT protein localizes to the thylakoid membranes and forms a tubular network at the cell periphery in regions of low chlorophyll autofluorescence, which likely represents the thylakoid convergence zones containing the PDMs (Figures 7-9 in section 3.2; Heinz *et al.*, 2016b). The investigation of the CurT deficient strain revealed that the thylakoid membranes do not converge toward the plasma membrane and hence, convergence zones can no longer be formed (Figure 2 in section 3.2; Heinz *et al.*, 2016b).

Intriguingly, the *curT* knockout – unlike its plant counterpart *curt1abcd* – exhibits multiple effects on the PSII complex. The major subunits of PSII (D1, D2, CP43 and CP47) are all reduced to 50 % of the wild-type level, and several PSII assembly factors are affected in the mutant whereas subunits of other photosynthetic complexes (cytochrome *f* and PsaA) remained unaltered (Figure 3 in section 3.2; Heinz *et al.*, 2016b). Accordingly, photosynthetic activity expressed by the oxygen evolution rate is reduced to 50 % as well (Table 1 in section 3.2; Heinz *et al.*, 2016b). As consequence of the altered ultrastructure and the changes in assembly factor amounts, the PSII biogenesis process is less efficient. On the one hand, the assembly in general is slowed down, whereas on the other hand, PSII biogenesis is stuck in smaller precomplexes. Indeed, fully functional PSII dimers could almost not be detected, which in turn has effects on electron release from PSII, and on phycobilisome coupling (Figures 5 and 6 in section 3.2; Heinz *et al.*, 2016b). The PSII dependent reduction of P700 is reduced in *curT* due to the above mentioned effects on PSII. Since the loss of CurT does not concern PSI and cytochrome *b₆f* complexes, it is not surprising that the relative electron transport rate downstream of PSII remains unaltered compared to the wild-type (Figure 4 in section 3.2; Heinz *et al.*, 2016b).

As observed for the *slr0151* knockout, the inner antenna protein CP47 shifts to PDMs which is an indicator for defects in the formation of larger reaction center complexes. Moreover, PratA and pD1 are no longer co-localized in the same membrane fractions, as pD1 is solely present in the thylakoids and no longer in the PDMs (Figure 7 in section 3.2; Heinz *et al.*, 2016b). Furthermore, this observation might explain the delay of the larger PSII subunits' assembly since PratA-mediated manganese preloading of pD1 seems to be difficult. Thus, alternate manganese uptake systems and delivery sources, as 1) the periplasmic manganese binding protein MncA (Tottey *et al.*, 2008), 2) the plasma membrane-located manganese transporter MntABC (Bartsevich and Pakrasi, 1995; Bartsevich and Pakrasi, 1996; Bartsevich and Pakrasi, 1999), 3) the plasma and thylakoid membrane-located manganese transporter SynPAM71 (Gandini *et al.*, 2017), or 4) type IV pili-dependent manganese uptake (Lamb and Hohmann-Marriott, 2017), might be able to partially complement the PratA-dependent manganese delivery to PSII in the *curT* mutant.

Taken together, these findings demonstrated that the cyanobacterial thylakoid convergence zones are required for efficient PSII assembly but not for the biogenesis of the other photosynthetic complexes. However, since the *curT* knockout is viable and able to perform photosynthesis, as well as the fact that several cyanobacteria do not possess convergence zones, it can reasonably be assumed that these structures are an evolutionary benefit for a more efficient PSII biogenesis. It seems likely that the convergence zones are the

structural basis for a PSII specific and very efficient manganese uptake system since PrtA-mediated manganese preloading is localized to the PDMs.

As observed and extensively studied for VIPP1 and FZL/BDLP proteins the membrane shaping function of those proteins *in vitro* is related to their capability to form oligomers, which was observed for *A. thaliana* CURT1 proteins as well (section 1.3). Oligomerization of *A. thaliana* CURT1 proteins and its cyanobacterial homolog occurs and may be triggered by phosphorylation (Armbruster *et al.*, 2013; Pribil *et al.*, 2014; Heinz *et al.*, 2016b). Indeed, two studies reported that the CurT protein in *Synechocystis* can be phosphorylated at its N-terminus at two specific threonine residues (T21 and T34), which might explain the four identified CurT isoforms found by isoelectric focusing (Spät *et al.*, 2015; Angeleri *et al.*, 2016; Figure 11 in section 3.2; Heinz *et al.*, 2016b).

Moreover, as suggested by an increased IsiA (iron stress induced) protein level, indicating stress in general, the *curT* mutant is exposed to stress which might be directly connected to the loss of the biogenesis centers (Figures 6 and 12 in section 3.2; Heinz *et al.*, 2016b). Therefore, the response to high-light was analyzed and, it had only minor effects on growth and photosynthesis. Henceforth, the D1 protein degradation under high-light intensities was delayed which suggests that the FtsH complex has problems finding its target in *curT* mutant cells. Another tested stressor was osmotic stress due to the already mentioned study by Huang *et al.* (2006), showing that Slr0151 is present in the plasma membrane under mild salt conditions as well. The accumulation of CurT and VIPP1 proteins, however, was increasing in the plasma membrane under high salt stress. Therefore, the induction of osmotic stress by the addition of salt or maltose revealed an accumulation of CurT-CFP signals at the plasma membrane (Figure 12 in section 3.2; Heinz *et al.*, 2016b).

4.1.3 Connection between Slr0151 and CurT via phosphorylation?

Taken together, it seems that Slr0151 as well as CurT have structural properties on the thylakoid membrane ultrastructure thereby affecting PSII biogenesis and/ or repair. Slr0151 was additionally shown to be part of the complex phosphorylation system of the unusual ferredoxin 5 by the kinase SpkG (Angeleri *et al.*, 2018). CurT however, has itself two sites that can be phosphorylated and moreover, Slr0151 protein levels are reduced to 50 % in the *curT* mutant (Spät *et al.*, 2015; Angeleri *et al.*, 2016). Furthermore, both proteins are co-migrating in density gradient experiments suggesting that a direct or indirect interaction is possible (section 3.2, Heinz *et al.*, 2016b; section 3.1, Rast *et al.*, 2016). Moreover, phosphorylation of photosynthetic proteins in general seems to play an important role in the responses during state

transitions and photodamage in plants and cyanobacteria (Fristedt *et al.*, 2009; Pesaresi *et al.*, 2011; Chen *et al.*, 2015; Angeleri *et al.*, 2016). Hence, it can reasonably be assumed that Slr0151 may somehow be indirectly involved in the phosphorylation of the CurT protein, which in turn might probably affect its oligomerization as well.

Furthermore, both proteins seem to play a role during salt stress response: CurT re-localizes to the plasma membrane under high-salt stress and Slr0151 seems to be present in the plasma membrane under milder salt conditions (Huang *et al.*, 2006; Heinz *et al.*, 2016b). Nevertheless, a direct interaction between Slr0151 and CurT could not be shown by co-immunoprecipitation (unpublished data) suggesting that these findings are either coincidental or that pieces are missing. Therefore, further research on CurT's phosphorylation sites and Slr0151's possible role during phosphorylation via the SpkG kinase is required.

4.2 The thylapse – a contact area between thylakoids and plasma membrane

As outlined in section 3.2, the thylakoid convergence zones in the cyanobacterium *Synechocystis* depend on the presence of the CurT protein. Hence, the membrane architecture at the convergence zones was analyzed in the wild-type by *in situ* cryo-ET, revealing membrane regions continuous with the thylakoid network (section 3.3, Rast *et al.*, in preparation). This area resides in the middle of the convergence zone and was described as convergence membrane (Figures 1 and 2 in section 3.3, Rast *et al.*, in preparation). It interconnects incoming thylakoids and unlike assumed for many years it has not a cylinder-like shape. The geometry of the convergence membrane presents a high diversity in its appearance, which depends on the incoming and interconnecting thylakoids. Henceforth, the convergence membrane cannot be described with conventional geometric bodies (Figures 1 and 2 in section 3.3, Rast *et al.*, in preparation). Moreover, the reported “semicircular structure” is most likely the result of the superposition of signals in thin-sections (Stengel *et al.*, 2012). When standard TEM micrograph acquisition is performed, the whole thickness of the thin-sections is imaged and thus, as long as the convergence zone was not sectioned in a perfect perpendicular angle to all present membranes, the thylakoid tips might “smear” and appear as a “semicircular structure” around the “thylakoid center”.

In addition to the convergence membrane, certain sites within were identified where the convergence membrane comes in very close proximity to the plasma membrane. This region was termed “the thylapse” due to its synapse-like appearance (Figures 1 and 2 in section 3.3, Rast *et al.*, in preparation). The spacing between the convergence and plasma membrane at the

thylapse is ~2.5 nm which is less than the diameter of a lipid bilayer (4 nm, Kirchhoff *et al.*, 2011; Figure 2 in section 3.3, Rast *et al.*, in preparation). This space is filled with electron dense material which very likely arose from proteins of unknown identity and might be responsible for the closely appressed convergence and plasma membranes (Figure 2 in section 3.3 and Figure S1 in section 6.4, Rast *et al.*, in preparation). Nevertheless, the examples recorded to this point are too heterogeneous and some are not of the required quality and thus, subtomogram averaging of this electron dense material is not possible, yet. For a comprehensive investigation of the densities in the 2.5-nm-gap, tomograms of higher quality are necessary showing thylapses in the tomograms' center.

Although cryo-ET is an outstanding tool regarding *in situ* membrane structure studies and structural analysis of large proteins in respect to the native cellular environment, only 4-8 % of the total *Synechocystis* cellular volume can be displayed (Figure S3 in section 6.4, Rast *et al.*, in preparation). The issue at hand is that the thicker the lamella, the worse the tomogram quality becomes, leading for instance to blurry membranes and preventing structural analysis of membranes and protein complexes. In turn, this results in favoring thin lamellas, which reduce the probability of acquiring thylapses and convergence membranes in the tomogram's center. To overcome this problem, convergence zones were identified in low magnification overviews for tomogram acquisition. Therefore, one cannot unbiasedly extrapolate the number of convergence zones, convergence membranes and thylapses for the total cellular volume.

To analyze the total number of these sites other methods should be used that allow imaging of the whole cell as e.g. fluorescence microscopic approaches or FIB-based tomography. In recent years, progress was made in imaging protein distributions in cyanobacteria in high quality by fluorescence microscopy, such as the localization of the CurT and VIPP1 proteins (Heinz *et al.*, 2016b; Gutu *et al.*, 2018). FIB-based tomography however, is another possibility: the focused gallium ion beam is used to remove material slice by slice from resin embedded cells followed by the detection of the backscattered electrons which results in "TEM-like" images (Inkson *et al.*, 2001; Flori *et al.*, 2017). The resolution of this approach in x, y and z dimension is about 4 nm which is enough for gaining a complete overview of the whole cell. This approach was recently used to analyze the 3D architecture of the unicellular diatom *P. tricornutum* (Flori *et al.*, 2017). Unfortunately, FIB-based tomography is as cryo-ET not really suited for high throughput analyzes and extensive mutant research.

4.2.1 Factors possibly involved in thylapse formation

It seems likely that the proper formation of the convergence membrane and thylapse *in vivo* requires a large number of proteins. Other factors additional to CurT might be involved in convergence zone, convergence membrane and thylapse formation. As already mentioned, VIPP1 and BDLP are promising candidates in cyanobacteria (section 1.3). In the *Synechocystis vipp1* knockdown, the thylakoid membranes are severely disordered and less abundant compared to the wild-type (Westphal *et al.*, 2001). Moreover, fluorescence microscopy of a *Synechocystis* line expressing GFP-tagged VIPP1 and CFP-tagged CurT, revealed that VIPP1 localizes within the tubular CurT-network as puncta especially in regions of low chlorophyll autofluorescence next to the plasma membrane (Gutu *et al.*, 2018). This emphasizes that VIPP1 is located at the convergence zone and may induce thylapse formation as recently suggested by Junglas and Schneider (2018). Schneider and co-workers showed *in vitro* that cyanobacterial VIPP1 forms ring structures that connect liposomes (Hennig *et al.*, 2015; Saur *et al.*, 2017). These structures are rather big (13.1 to 15.4 nm tall) and thus, it seems unlikely that fully assembled VIPP1 rings mediate thylapse formation *in vivo* since the convergence and plasma membrane are just ~2.5 nm apart. However, it might be possible that smaller VIPP1 oligomers or monomers play a role in thylapse formation.

The BDLP protein might also play a role in convergence membrane and thylapse formation, since it was reported that this protein localizes to the thylakoid and plasma membranes and is able to tubulate liposomes *in vitro*. However, the deficiency of BDLP and thus possible effects on photosynthesis and the thylakoid membranes have not yet been studied in cyanobacteria (Low and Lowe, 2006).

The THF1 protein, which is involved in chloroplast vesicle transport in plants, shows no severe alterations in thylakoid membrane morphology in *Synechococcus* sp. PCC 7942. Nevertheless, a delay in the D1 turnover was observed in the *thf1*⁻ mutant as reported for *curT* in *Synechocystis* suggesting a direct or indirect effect on the D1 degrading protein FtsH (Heinz *et al.*, 2016b; Zhan *et al.*, 2016). FtsH protein levels are indeed significantly reduced in the *thf1*⁻ mutant, probably indicating that minor changes in thylakoid ultrastructure might occur that are not recognizable with conventional TEM techniques (Zhan *et al.*, 2016).

Taken together, in cyanobacteria several proteins are potentially involved in the formation and maintenance of the thylakoid ultrastructure and hence for the formation of the convergence zone and its substructures the convergence membrane and the thylapse. However, there is only one protein, which can directly be connected to the convergence zones and this is CurT. The *curT* mutant is the only mutant known that possesses “normal” thylakoids but lacks

the convergence zones. Furthermore, it can reasonably be assumed that the convergence membrane described in section 3.3 resembles the network-like pattern of the CurT-CFP signals and thus CurT might most likely be responsible for interconnecting thylakoid membranes and probably also for thylapse formation.

4.2.2 Membrane contact – a common feature

It has been debated for years whether thylakoids fuse with their enclosing membranes to exchange lipids, proteins and metal ions required for photosynthesis as iron and manganese. Thus far, in plant's chloroplasts, this phenomenon could only be observed for developing plastids (Carde *et al.*, 1982; Douce and Joyard, 1984; Pribil *et al.*, 2014). However, a fusion of mature thylakoid membranes and the inner envelope was found in a recent cryo-ET study of *C. reinhardtii* chloroplasts (Engel *et al.*, 2015). Nevertheless, these fusion events are rare and obviously not easy to analyze thus emphasizing that membrane fusions between thylakoids and the inner envelope are strongly regulated.

As mentioned in subsection 1.2.2, in anoxic photosynthetic purple bacteria connections between the intracellular membrane system and the plasma membrane are quite frequent and often observed. The intracellular membrane system in these prokaryotes seems to originate from plasma membrane invaginations and appears in many different shapes (Drews, 2013). As reviewed by Drews (2013) most anoxygenic bacteria either respire oxygen in the dark or utilize light energy for ATP generation (via cyclic electron flow) under anoxic conditions during the day. This time-resolved separation is very strict and tightly regulated by the oxygen partial pressure and the redox state of the ubiquinone pool (Gregor and Klug, 2002; Wu and Bauer, 2010). The development and differentiation of the intracellular membrane system of purple bacteria is also tied to these regulators. Cyanobacteria on the other side, run photosynthetic and respiration-dependent electron transport simultaneously in the light. In the night, as soon as photosynthesis stops, they solely respire (Liu, 2016). Intriguingly, a membrane fusion between the thylakoids and plasma membrane was overserved in dark grown cyanobacteria (van de Meene *et al.*, 2012). In the light, the thylakoids come in very close proximity (~2.5 nm) to the plasma membrane and hence form the thylapse contact but without membrane fusion (section 3.3, Rast *et al.*, in preparation).

Taken together, in eukaryotic phototrophs respiration and photosynthesis are spacially separated in chloroplasts and mitochondria. Fusion events of the thylakoids with the inner envelope have been reported in developing as well as in mature chloroplasts in plants and algae, respectively. In anoxygenic prokaryotes (as purple bacteria) respiration and photosynthesis are

separated by time. In cyanobacteria exposed to light both processes take place at the same space and time. Thus, this might possibly suggest that both processes occurring in the same compartment at the same time somehow prevent the internal membrane network to fuse with the plasma membrane.

In general, all studies regarding the contact of internal membrane systems with their enclosing membranes suggest that a membrane fusion is a rare event in oxygenic phototrophs and requires a strong regulation. It remains to be studied whether thylapse formation and membrane fusion of the convergence and plasma membrane really depend on separated respiration and photosynthesis in the dark.

4.3 Lateral heterogeneity in cyanobacteria

As outlined in subsection 1.4.3, the separation of PSI and PSII into stroma and grana thylakoids, respectively, in higher plants' chloroplasts is named lateral heterogeneity. Moreover, the chloroplast ATP synthase is unevenly distributed as well and, can be identified on thylakoid membranes facing the stroma as stroma lamellae and outermost thylakoid membranes of a grana stack. The only photosynthetic complex distributed evenly is cytochrome *b₆f* (Andersson and Anderson, 1980; Pribil *et al.*, 2014).

The situation in the cyanobacterium *Synechocystis* is different compared to plants, since the thylakoids are not differentiated into grana stacks and stroma lamellae and photosynthetic as well as respiratory complexes are distributed along the thylakoids (Liu, 2016). Several studies already reported lateral separations of photosynthetic complexes within the cyanobacterial thylakoid membrane network (Sherman *et al.*, 1994; Olive *et al.*, 1997; Westermann *et al.*, 1999; Vermaas *et al.*, 2008; Collins *et al.*, 2012; Casella *et al.*, 2017; MacGregor-Chatwin *et al.*, 2017). It is assumed the majority of PSI complexes is present at plasma membrane-facing and cytosol-facing thylakoids probably along with the ATP synthase, whereas PSII seems to be located to thylakoid-facing thylakoids. Cytochrome *b₆f* seems to locate to all types of membranes (Sherman *et al.*, 1994; Vermaas *et al.*, 2008; Collins *et al.*, 2012).

Furthermore, the PSII assembly intermediates are laterally separated as well, as reviewed by Heinz *et al.* (2016a), early PSII pre-complexes are located in the PDMs along with assembly proteins involved in these steps as PrtA and Ycf48 (Schottkowski *et al.*, 2009a; Rengstl *et al.*, 2011). However, components of larger PSII intermediates as the inner antenna proteins CP47 and CP43 are present in mature thylakoid fractions (Rengstl *et al.*, 2011). Thus, the PrtA

protein can be used as marker for PSII-specific biogenic areas (Figure VI). Moreover, as described in section 3.2, the CurT protein directs the thylakoids to the plasma membrane resulting in the formation of the convergence membrane (Figure VI; Heinz *et al.*, 2016b).

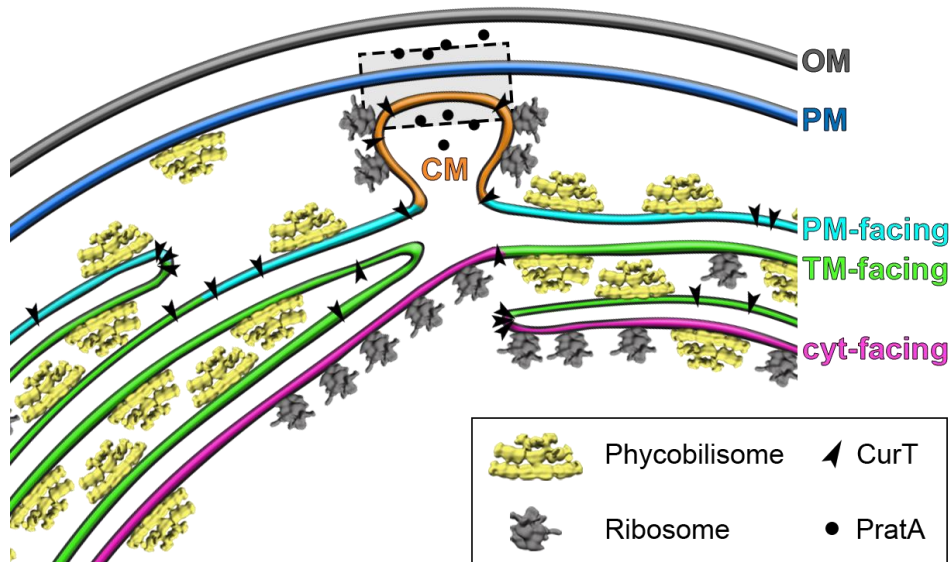


Figure VI. Model of different membrane regions at a convergence zone of a *Synechocystis* cell. As outlined in the text, a thylakoid membrane can locate next to the plasma membrane (PM-facing; cyan), can be adjacent to other thylakoids (TM-facing; green), face the cytosol (cyt-facing; pink), and form the convergence membrane (CM; orange), which gives rise to the thylakoid lumen (boxed). Distributions of phycobilisomes (yellow) and ribosomes (grey) are based on the data presented in section 3.3 and therefore serve as markers for photosynthetic and biogenic areas, respectively. CurT (black arrowheads) directs the TMs to the PM whereas PrtA (black circles) is a marker for early PSII biogenesis since it preloads the D1 protein with manganese.

The cryo-ET study presented in section 3.3, demonstrated that the thylakoids can be distinguished into different membrane regions according to their position within the thylakoid network (Figure VI; Figure 5 in section 3.3, Rast *et al.*, in preparation). Furthermore, within these regions the distribution of the phycobilisomes and the ribosomes was found to be laterally separated, especially at the convergence membrane and in regions transitioning from thylakoid-facing to cytosol-facing thylakoids (Figure VI; Figure 5 in section 3.3, Rast *et al.*, in preparation). Henceforth, the separation of phycobilisomes and ribosomes clearly indicated a functional lateral heterogeneity, as phycobilisomes mark photosynthetically active regions and ribosomes mark biogenic areas.

The localization of ribosomes at the convergence membrane is in line with previous studies about the early assembly factor PrtA, which was found to localize to the PDM fractions and to the cell periphery as shown by immunogold-labeling, thereby most likely resembling the convergence zones (Stengel *et al.*, 2012). In addition to PrtA's PDM localization, it was also

identified in the periplasmic space (area between plasma and outer membrane; Klinkert *et al.*, 2004; Schottkowski *et al.*, 2009a). Thus, the ribosome and the PrtA localization highlight the convergence membrane and the thylakoid as biogenic areas. Moreover, as indicated by the presence of ribosome on the cytosol-facing thylakoids, these membranes are biogenic regions as well. Nevertheless, to this point, it is not clear whether there are distinct regions for *de novo* biogenesis and repair assembly of PSII.

Furthermore, the observed phycobilisome distribution is in line with the previously identified PSI and PSII areas (Sherman *et al.*, 1994; Vermaas *et al.*, 2008; Collins *et al.*, 2012). As described in section 3.3, the phycobilisomes form arrays *in vivo*, which are interconnected via the phycocyanin rods (Rast *et al.*, in preparation). These arrays are not perfectly straight and slight changes of direction within some arrays were found, which possibly indicate phycobilisome coupling to both photosystems. Further detailed structural analysis of the interaction between the phycobilisomes and the thylakoid membrane might reveal whether all array-phycobilisomes are attached to the same photosystem. However, to identify different phycobilisome states on a structural level, high-light experiments are required that induce state II (phycobilisomes tunnel excitation energy to PSI). Thus, the phycobilisomes themselves might probably be suitable to distinguish between both photosystems in future studies.

In conclusion, “lateral heterogeneity” is a suitable term to describe laterally differently distributed protein complexes although cyanobacteria do not possess grana and stroma lamellae.

4.4 Conclusions and future perspectives

Although our understanding of the structure and function of photosynthetic complexes is very detailed and profound, the mechanisms of thylakoid membrane biogenesis and assembly of photosynthetic complexes are less well studied. Two proteins were investigated in the course of this thesis i.e. Slr0151 and CurT. Both are required for efficient PSII assembly but not essential for the survival of *Synechocystis* cells. Thus far, the precise molecular role of Slr0151 is not entirely clear, since in addition to its role in guiding the inner core antennas to the growing PSII reaction center complex during *de novo* assembly and repair, it seems to be involved in a complex phosphorylation network as well. However, it can reasonably be assumed that CurT is required for the formation of the convergence zones and thus for the convergence membrane as well. Nevertheless, it remains to be examined whether additional proteins are involved in convergence membrane formation, i.e. VIPP1, BDLP or THF1 in cyanobacteria. As a next step,

proof of function experiments should be performed as the introduction of the *Synechocystis curT* gene at a neutral site in the genome of a cyanobacterium without convergence zones. Hence, this mutant organism might form convergence zones or at least present effects on its thylakoid structure. Additionally, the ultrastructure of the *curT* mutant should be analyzed in the dark, which are conditions that facilitate a membrane fusion of the thylakoid and plasma membrane in the wild-type (van de Meene *et al.*, 2012). If continuity between the thylakoid lumen and periplasm is *not* established in the *curT* mutant in the dark as it can be seen in the wild-type, it might further substantiate CurT as the main player in establishing thylakoid membrane architecture. Furthermore, the search for interaction partners of Slr0151 as well as for CurT should be deepened, which might reveal additional known or unknown factors involved in the complex network of their working modes. It might also shed light on the hypothesis whether Slr0151 might possibly be involved in the phosphorylation of CurT and thus in regulating CurT's isoforms.

To further analyze the biological role of the thylapse and the convergence membrane, a comprehensive localization of the manganese-preloading factor PrataA is required. Thus far, it is impossible to localize PrataA to the convergence membrane with cryo-ET. PrataA, which has a molecular weight of 35 kDa, is too small to be identified by template matching in tomogram volumes. However, it is possible to localize manganese with TEM if manganese is present in high local amounts. This approach would require a microscope equipped with an energy dispersive x-ray (EDX) or an electron energy loss spectroscopy (EELS) detector, which both are suited to discriminate between different elements. This would clarify as well, whether or not the convergence membrane and the thylapse are PrataA's path for manganese uptake.

5 REFERENCES

- Abbé, E.** (1873). Beiträge zur Theorie des Mikroskops und der mikroskopischen Wahrnehmung. *Arch. mikroskop. Anat.* 9: 413-468.
- Adir, N.** (2005). Elucidation of the molecular structures of components of the phycobilisome: reconstructing a giant. *Photosynth. Res.* 85(1): 15-32.
- Anbudurai, P. R., Mor, T. S., Ohad, I., Shestakov, S. V. and Pakrasi, H. B.** (1994). The *ctpA* gene encodes the C-terminal processing protease for the D1 protein of the photosystem II reaction center complex. *Proc. Natl. Acad. Sci. USA* 91(17): 8082-8086.
- Andersson, B. and Anderson, J. M.** (1980). Lateral heterogeneity in the distribution of chlorophyll-protein complexes of the thylakoid membranes of spinach chloroplasts. *Biochim. Biophys. Acta* 593(2): 427-440.
- Angeleri, M., Muth-Pawlak, D., Aro, E. M. and Battchikova, N.** (2016). Study of O-phosphorylation sites in proteins involved in photosynthesis-related processes in *Synechocystis* sp. strain PCC 6803: Application of the SRM approach. *J. Proteome Res.* 15(12): 4638-4652.
- Angeleri, M., Zorina, A., Aro, E. M. and Battchikova, N.** (2018). Interplay of SpkG kinase and the Slr0151 protein in the phosphorylation of ferredoxin 5 in *Synechocystis* sp. strain PCC 6803. *FEBS Lett.* 592(3): 411-421.
- Archibald, J. M.** (2009). The puzzle of plastid evolution. *Curr. Biol.* 19(2): R81-R88.
- Archibald, J. M.** (2012). Genomic insights into the biology of algae. Chapter 3: The evolution of algae by secondary and tertiary endosymbiosis. *Elsevier Ltd.* 64: 87-118. ISSN: 9780123914996.
- Archibald, J. M.** (2015). Endosymbiosis and eukaryotic cell evolution. *Curr. Biol.* 25(19): R911-R921.
- Armbruster, U., Labs, M., Pribil, M., Viola, S., Xu, W., Scharfenberg, M., Hertle, A. P., Rojahn, U., Jensen, P. E., Rappaport, F., Joliot, P., Dörmann, P., Wanner, G. and Leister, D.** (2013). Arabidopsis CURVATURE THYLAKOID1 proteins modify thylakoid architecture by inducing membrane curvature. *Plant Cell* 25(7): 2661-2678.
- Arteni, A. A., Ajlani, G. and Boekema, E. J.** (2009). Structural organisation of phycobilisomes from *Synechocystis* sp. strain PCC6803 and their interaction with the membrane. *Biochim. Biophys. Acta* 1787(4): 272-279.
- Asano, S., Engel, B. D. and Baumeister, W.** (2016). *In situ* cryo-electron tomography: a post-reductionist approach to structural biology. *J. Mol. Biol.* 428(2 Pt A): 332-343.
- Bang, W. Y., Chen, J., Jeong, I. S., Kim, S. W., Kim, C. W., Jung, H. S., Lee, K. H., Kweon, H. S., Yoko, I., Shiina, T. and Bahk, J. D.** (2012). Functional characterization of ObgC in ribosome biogenesis during chloroplast development. *Plant J.* 71(1): 122-134.

- Barber, J. and Andersson, B.** (1992). Too much of a good thing: light can be bad for photosynthesis. *Trends Biochem. Sci.* 17(2): 61-66.
- Bartsevich, V. V. and Pakrasi, H. B.** (1995). Molecular identification of an ABC transporter complex for manganese: Analysis of a cyanobacterial mutant strain impaired in the photosynthetic oxygen evolution process. *EMBO J.* 14(9): 1845-1853.
- Bartsevich, V. V. and Pakrasi, H. B.** (1996). Manganese transport in the cyanobacterium *Synechocystis* sp. PCC 6803. *J. Biol. Chem.* 271(42): 26057-26061.
- Bartsevich, V. V. and Pakrasi, H. B.** (1999). Membrane topology of MntB, the transmembrane protein component of an ABC transporter system for manganese in the cyanobacterium *Synechocystis* sp. strain PCC 6803. *J. Bacteriol.* 181(11): 3591-3593.
- Becker, K., Cormann, K. U. and Nowaczyk, M. M.** (2011). Assembly of the water-oxidizing complex in photosystem II. *J. Photochem. Photobiol. B: Biol.* 104(1-2): 204-211.
- Bialek, W., Krzywda, S., Zatwarnicki, P., Jaskolski, M., Kolesinski, P. and Szczepaniak, A.** (2014). Insights into the relationship between the haem-binding pocket and the redox potential of *c6* cytochromes: four atomic resolution structures of *c6* and *c6*-like proteins from *Synechococcus* sp. PCC 7002. *Acta Cryst. D* 70(11): 2823-2832.
- Blatch, G. L. and Lässle, M.** (1999). The tetratricopeptide repeat: a structural motif mediating protein-protein interactions. *BioEssays* 21(11): 932-939.
- Boehm, M., Yu, J., Krynicka, V., Barker, M., Tichy, M., Komenda, J., Nixon, P. J. and Nield, J.** (2012). Subunit organization of a *Synechocystis* hetero-oligomeric thylakoid FtsH complex involved in photosystem II repair. *Plant Cell* 24(9): 3669-3683.
- Boekema, E. J., Dekker, J. P., van Heel, M. G., Rögner, M., Saenger, W., Witt, I. and Witt, H. T.** (1987). Evidence for a trimeric organization of the photosystem I complex from the thermophilic cyanobacterium *Synechococcus* sp. *FEBS Lett.* 217(2): 283-286.
- Bohne, A. V., Schwenkert, S., Grimm, B. and Nickelsen, J.** (2016). International Review of Cell and Molecular Biology. Chapter 5: Roles of tetratricopeptide repeat proteins in biogenesis of the photosynthetic apparatus. *Academic Press.* 324: 187-227. ISSN: 1937-6448.
- Boudreau, E., Takahashi, Y., Lemieux, C., Turmel, M. and Rochaix, J. D.** (1997). The chloroplast *ycf3* and *ycf4* open reading frames of *Chlamydomonas reinhardtii* are required for the accumulation of the photosystem I complex. *EMBO J.* 16(20): 6095-6104.
- Bramkamp, M.** (2012). Structure and function of bacterial dynamin-like proteins. *Biol. Chem.* 393(11): 1203-1214.
- Bryan, S. J., Burroughs, N. J., Shevela, D., Yu, J., Rupprecht, E., Liu, L.-N., Mastroianni, G., Xue, Q., Llorente-Garcia, I., Leake, M. C., Eichacker, L. A., Schneider, D., Nixon, P. J. and Mullineaux, C. W.** (2014). Localisation and interactions of the Vipp1 protein in cyanobacteria. *Mol. Microbiol.* 94(5): 1179-1195.

- Press Release: 04.10.2017. **Scientific background on the Nobel Prize in Chemistry 2017. The development of cryo-electron microscopy.** Brzezinski, P. The Royal Swedish Academy of Sciences.
https://www.nobelprize.org/nobel_prizes/chemistry/laureates/2017/press.html.
- Carde, J., Joyard, J. and Douce, R.** (1982). Electron microscopic studies of envelope membranes from spinach plastids. *Biologie cellulaire* 44: 315-324.
- Casella, S., Huang, F., Mason, D., Zhao, G.-Y., Johnson, G. N., Mullineaux, C. W. and Liu, L.-N.** (2017). Dissecting the native architecture and dynamics of cyanobacterial photosynthetic machinery. *Mol. Plant* 10(11): 1434-1448.
- Chang, L., Liu, X., Li, Y., Liu, C. C., Yang, F., Zhao, J. and Sui, S. F.** (2015). Structural organization of an intact phycobilisome and its association with photosystem II. *Cell Res.* 25(6): 726-737.
- Chen, Z., Zhan, J., Chen, Y., Yang, M., He, C., Ge, F. and Wang, Q.** (2015). Effects of phosphorylation of beta subunits of phycocyanins on state transition in the model cyanobacterium *Synechocystis* sp. PCC 6803. *Plant Cell Physiol.* 56(10): 1997-2013.
- Collins, A. M., Liberton, M., Jones, H. D., Garcia, O. F., Pakrasi, H. B. and Timlin, J. A.** (2012). Photosynthetic pigment localization and thylakoid membrane morphology are altered in *Synechocystis* 6803 phycobilisome mutants. *Plant Physiol.* 158(4): 1600-1609.
- Cormann, K. U., Bartsch, M., Rogner, M. and Nowaczyk, M. M.** (2014). Localization of the CyanoP binding site on photosystem II by surface plasmon resonance spectroscopy. *Front. Plant Sci.* 5: 595.
- Danev, R., Buijsse, B., Khoshouei, M., Plitzko, J. M. and Baumeister, W.** (2014). Volta potential phase plate for in-focus phase contrast transmission electron microscopy. *Proc. Natl. Acad. Sci. USA* 111(44): 15635-15640.
- Daum, B., Nicastro, D., Austin, J., 2nd, McIntosh, J. R. and Kühlbrandt, W.** (2010). Arrangement of photosystem II and ATP synthase in chloroplast membranes of spinach and pea. *Plant Cell* 22(4): 1299-1312.
- de Broglie, L.** (1924). Recherches sur la théorie des Quanta, Migration - université en cours d'affectation.
- Dekker, J. P. and Boekema, E. J.** (2005). Supramolecular organization of thylakoid membrane proteins in green plants. *Biochim. Biophys. Acta* 1706(1-2): 12-39.
- Douce, R. and Joyard, R.** (1984). Chloroplast Biogenesis. Chapter 3: The regulatory role of the plastid envelope during development. *Elsevier Science.* 5: 71-132.
- Drews, G.** (2013). The intracytoplasmic membranes of purple bacteria - Assembly of energy-transducing complexes. *J. Mol. Microbiol.* 23(1-2): 35-47.
- Dubochet, J., Adrian, M., Chang, J. J., Homo, J. C., Lepault, J., McDowell, A. W. and Schultz, P.** (1988). Cryo-electron microscopy of vitrified specimens. *Q. Rev. Biophys.* 21(2): 129-228.

- Engel, B. D., Schaffer, M., Cuellar, L. K., Villa, E., Pnitzko, J. M. and Baumeister, W.** (2015). Native architecture of the *Chlamydomonas* chloroplast revealed by *in situ* cryo-electron tomography. *eLife* 4: e04889.
- Ferguson, S. J.** (2000). ATP synthase: What dictates the size of a ring? *Curr. Biol.* 10(21): R804-R808.
- Flori, S., Jouneau, P. H., Bailleul, B., Gallet, B., Estrozi, L. F., Moriscot, C., Bastien, O., Eicke, S., Schober, A., Bartulos, C. R., Marechal, E., Kroth, P. G., Petroustos, D., Zeeman, S., Breyton, C., Schoehn, G., Falconet, D. and Finazzi, G.** (2017). Plastid thylakoid architecture optimizes photosynthesis in diatoms. *Nat. Commun.* 8: 15885.
- Frank, J.** (2006). Three-dimensional electron microscopy of macromolecular assemblies: Visualization of biological molecules in their native state. *Oxford University Press*. ISSN: 9780195182187.
- Fristedt, R., Willig, A., Granath, P., Crevecoeur, M., Rochaix, J. D. and Vener, A. V.** (2009). Phosphorylation of photosystem II controls functional macroscopic folding of photosynthetic membranes in *Arabidopsis*. *Plant Cell* 21(12): 3950-3964.
- Fuhrmann, E., Bultema, J. B., Kahmann, U., Rupprecht, E., Boekema, E. J. and Schneider, D.** (2009). The vesicle-inducing protein 1 from *Synechocystis* sp. PCC 6803 organizes into diverse higher-ordered ring structures. *Mol. Biol. Cell* 20(21): 4620-4628.
- Gandini, C., Schmidt, S. B., Husted, S., Schneider, A. and Leister, D.** (2017). The transporter SynPAM71 is located in the plasma membrane and thylakoids, and mediates manganese tolerance in *Synechocystis* PCC6803. *New Phytol.*: n/a-n/a.
- Gao, H., Sage, T. L. and Osteryoung, K. W.** (2006). FZL, an FZO-like protein in plants, is a determinant of thylakoid and chloroplast morphology. *Proc. Natl. Acad. Sci. USA* 103(17): 6759-6764.
- Garcia, C., Khan, N. Z., Nannmark, U. and Aronsson, H.** (2010). The chloroplast protein CPSAR1, dually localized in the stroma and the inner envelope membrane, is involved in thylakoid biogenesis. *Plant J.* 63(1): 73-85.
- Gould, S. B., Waller, R. F. and McFadden, G. I.** (2008). Plastid evolution. *Annu. Rev. Plant Biol.* 59(1): 491-517.
- Gregor, J. and Klug, G.** (2002). Oxygen-regulated expression of genes for pigment binding proteins in *Rhodobacter capsulatus*. *J. Mol. Microbiol.* 4(3): 249-253.
- Gutu, A., Chang, F. and O'Shea, E. K.** (2018). Dynamical localization of a thylakoid membrane binding protein is required for acquisition of photosynthetic competency. *Mol. Microbiol.* 108(1): 16-31.
- Harris, D., Bar-Zvi, S., Lahav, A., Goldshmid, I. and Adir, N.** (2018). Membrane Protein Complexes: Structure and Function. The structural basis for the extraordinary energy-transfer capabilities of the phycobilisome. *Springer Singapore*. Subcellular Biochemistry 87: 57-82. ISSN: 978-981-10-7757-9.

- Hasan, S. S., Yamashita, E., Baniulis, D. and Cramer, W. A.** (2013). Quinone-dependent proton transfer pathways in the photosynthetic cytochrome *b6f* complex. *Proc. Natl. Acad. Sci. USA* 110(11): 4297-4302.
- Heidrich, J., Thurotte, A. and Schneider, D.** (2017). Specific interaction of IM30/Vipp1 with cyanobacterial and chloroplast membranes results in membrane remodeling and eventually in membrane fusion. *Biochim. Biophys. Acta*: doi: 10.1016/j.bbamem.2016.1009.1025.
- Heinz, S., Liauw, P., Nickelsen, J. and Nowaczyk, M.** (2016a). Analysis of photosystem II biogenesis in cyanobacteria. *Biochim. Biophys. Acta* 1857(3): 274-287.
- Heinz, S., Rast, A., Shao, L., Gutu, A., Gügel, I. L., Heyno, E., Labs, M., Rengstl, B., Viola, S., Nowaczyk, M. M., Leister, D. and Nickelsen, J.** (2016b). Thylakoid membrane architecture in *Synechocystis* depends on CurT, a homolog of the granal CURVATURE THYLAKOID1 proteins. *Plant Cell* 28: 2238–2260.
- Hennig, R., Heidrich, J., Saur, M., Schmäser, L., Roeters, S. J., Hellmann, N., Woutersen, S., Bonn, M., Weidner, T., Markl, J. and Schneider, D.** (2015). IM30 triggers membrane fusion in cyanobacteria and chloroplasts. *Nat. Commun.* 6: 7018.
- Hernandez-Prieto, M. A. and Futschik, M. E.** (2012). CyanoEXpress: A web database for exploration and visualisation of the integrated transcriptome of cyanobacterium *Synechocystis* sp. PCC6803. *Bioinformatics* 8(13): 634-638.
- Hernandez-Prieto, M. A., Semeniuk, T. A., Giner-Lamia, J. and Futschik, M. E.** (2016). The transcriptional landscape of the photosynthetic model cyanobacterium *Synechocystis* sp. PCC6803. *Sci. Rep.* 6: 22168.
- Hohmann-Marriott, M. F. and Blankenship, R. E.** (2011). Evolution of photosynthesis. *Annu. Rev. Plant Biol.* 62(1): 515-548.
- Huang, F., Fulda, S., Hagemann, M. and Norling, B.** (2006). Proteomic screening of salt-stress-induced changes in plasma membranes of *Synechocystis* sp. strain PCC 6803. *Proteomics* 6(3): 910-920.
- Inkson, B. J., Mulvihill, M. and Möbus, G.** (2001). 3D determination of grain shape in a FeAl-based nanocomposite by 3D FIB tomography. *Scripta Materialia* 45(7): 753-758.
- Jilly, R., Khan, N. Z., Aronsson, H. and Schneider, D.** (2018). Dynamin-Like Proteins Are Potentially Involved in Membrane Dynamics within Chloroplasts and Cyanobacteria. *Front. Plant Sci.* 9: 206.
- Jordan, P., Fromme, P., Witt, H. T., Klukas, O., Saenger, W. and Krauss, N.** (2001). Three-dimensional structure of cyanobacterial photosystem I at 2.5 Å resolution. *Nature* 411(6840): 909-917.
- Junglas, B. and Schneider, D.** (2018). What is Vipp1 good for? *Mol. Microbiol.* 108(1): 1–5.
- Karim, S., Alezzawi, M., Garcia-Petit, C., Solymosi, K., Khan, N. Z., Lindquist, E., Dahl, P., Hohmann, S. and Aronsson, H.** (2014). A novel chloroplast localized Rab GTPase

protein CPRabA5e is involved in stress, development, thylakoid biogenesis and vesicle transport in Arabidopsis. *Plant Mol. Biol.* 84(6): 675-692.

Karim, S. and Aronsson, H. (2014). The puzzle of chloroplast vesicle transport – involvement of GTPases. *Front. Plant Sci.* 5: 472.

Kim, E. and Archibald, J. M. (2008). The Chloroplast: Interactions with the Environment. Chapter 17: Diversity and evolution of plastids and their genomes. *Springer Berlin Heidelberg*. Plant Cell Monographs 13.

Kirchhoff, H. (2013). Architectural switches in plant thylakoid membranes. *Photosynth. Res.* 116(2-3): 481-487.

Kirchhoff, H., Hall, C., Wood, M., Herbstova, M., Tsabari, O., Nevo, R., Charuvi, D., Shimoni, E. and Reich, Z. (2011). Dynamic control of protein diffusion within the granal thylakoid lumen. *Proc. Natl. Acad. Sci. USA* 108(50): 20248-20253.

Kirchhoff, H., Li, M. and Puthiyaveetil, S. (2017). Sublocalization of cytochrome *b6f* complexes in photosynthetic membranes. *Trends Plant. Sci.* 22(7): 574-582.

Klinkert, B., Ossenbühl, F., Sikorski, M., Berry, S., Eichacker, L. and Nickelsen, J. (2004). PrtA, a periplasmic tetratricopeptide repeat protein involved in biogenesis of photosystem II in *Synechocystis* sp. PCC 6803. *J. Biol. Chem.* 279(43): 44639-44644.

Knoppová, J., Yu, J., Konik, P., Nixon, P. J. and Komenda, J. (2016). CyanoP is involved in the early steps of photosystem II assembly in the cyanobacterium *Synechocystis* sp. PCC 6803. *Plant Cell Physiol.* 57(9): 1921-1931.

Komenda, J., Knoppová, J., Kopečná, J., Sobotka, R., Halada, P., Yu, J., Nickelsen, J., Boehm, M. and Nixon, P. J. (2012a). The Psb27 assembly factor binds to the CP43 complex of photosystem II in the cyanobacterium *Synechocystis* sp. PCC 6803. *Plant Physiol.* 158(1): 476-486.

Komenda, J., Kuviková, S., Granvogl, B., Eichacker, L. A., Diner, B. A. and Nixon, P. J. (2007). Cleavage after residue Ala352 in the C-terminal extension is an early step in the maturation of the D1 subunit of photosystem II in *Synechocystis* PCC 6803. *Biochim. Biophys. Acta* 1767(6): 829-837.

Komenda, J., Nickelsen, J., Tichy, M., Prasil, O., Eichacker, L. A. and Nixon, P. J. (2008). The cyanobacterial homologue of HCF136/YCF48 is a component of an early photosystem II assembly complex and is important for both the efficient assembly and repair of photosystem II in *Synechocystis* sp. PCC 6803. *J. Biol. Chem.* 283(33): 22390-22399.

Komenda, J., Reisinger, V., Müller, B. C., Dobáková, M., Granvogl, B. and Eichacker, L. A. (2004). Accumulation of the D2 protein is a key regulatory step for assembly of the photosystem II reaction center complex in *Synechocystis* PCC 6803. *J. Biol. Chem.* 279(47): 48620-48629.

Komenda, J., Sobotka, R. and Nixon, P. J. (2012b). Assembling and maintaining the Photosystem II complex in chloroplasts and cyanobacteria. *Curr. Opin. Plant Biol.* 15(3): 245-251.

- Kroll, D., Meierhoff, K., Bechtold, N., Kinoshita, M., Westphal, S., Vothknecht, U. C., Soll, J. and Westhoff, P.** (2001). VIPP1, a nuclear gene of *Arabidopsis thaliana* essential for thylakoid membrane formation. *Proc. Natl. Acad. Sci. USA* 98(7): 4238-4242.
- Kubota, H., Sakurai, I., Katayama, K., Mizusawa, N., Ohashi, S., Kobayashi, M., Zhang, P., Aro, E. M. and Wada, H.** (2010). Purification and characterization of photosystem I complex from *Synechocystis* sp. PCC 6803 by expressing histidine-tagged subunits. *Biochim. Biophys. Acta* 1797(1): 98-105.
- Kühlbrandt, W.** (2014). The resolution revolution. *Science* 343(6178): 1443-1444.
- Kunkel, D. D.** (1982). Thylakoid centers: Structures associated with the cyanobacterial photosynthetic membrane system. *Arch. Microbiol.* 133(2): 97-99.
- Lamb, J. J. and Hohmann-Marriott, M. F.** (2017). Manganese acquisition is facilitated by PilA in the cyanobacterium *Synechocystis* sp. PCC 6803. *PLoS One* 12(10): e0184685.
- Lepetit, B., Goss, R., Jakob, T. and Wilhelm, C.** (2012). Molecular dynamics of the diatom thylakoid membrane under different light conditions. *Photosynth. Res.* 111(1): 245-257.
- Liang, C., Zhang, X., Chi, X., Guan, X., Li, Y., Qin, S. and Shao, H. B.** (2011). Serine/threonine protein kinase SpkG is a candidate for high salt resistance in the unicellular cyanobacterium *Synechocystis* sp. PCC 6803. *PLoS One* 6(5): e18718.
- Liberton, M., Howard Berg, R., Heuser, J., Roth, R. and Pakrasi, H. B.** (2006). Ultrastructure of the membrane systems in the unicellular cyanobacterium *Synechocystis* sp. strain PCC 6803. *Protoplasma* 227(2-4): 129-138.
- Liu, H., Zhang, H., Niedzwiedzki, D. M., Prado, M., He, G., Gross, M. L. and Blankenship, R. E.** (2013). Phycobilisomes supply excitations to both photosystems in a megacomplex in cyanobacteria. *Science* 342: 1104-1107.
- Liu, L.-N.** (2016). Distribution and dynamics of electron transport complexes in cyanobacterial thylakoid membranes. *Biochim. Biophys. Acta* 1857(3): 256-265.
- Low, H. H. and Lowe, J.** (2006). A bacterial dynamin-like protein. *Nature* 444(7120): 766-769.
- Low, H. H., Sachse, C., Amos, L. A. and Lowe, J.** (2009). Structure of a bacterial dynamin-like protein lipid tube provides a mechanism for assembly and membrane curving. *Cell* 139(7): 1342-1352.
- Mabbitt, P. D., Wilbanks, S. M. and Eaton-Rye, J. J.** (2014). Structure and function of the hydrophilic photosystem II assembly proteins: Psb27, Psb28 and Ycf48. *Plant Physiol. Biochem.* 81: 96-107.
- MacGregor-Chatwin, C., Sener, M., Barnett, S. F. H., Hitchcock, A., Barnhart-Dailey, M. C., Maghlaoui, K., Barber, J., Timlin, J. A., Schulten, K. and Hunter, C. N.** (2017). Lateral segregation of photosystem I in cyanobacterial thylakoids. *Plant Cell* 29(5): 1119-1136.

- McFadden, G. I.** (2014). Origin and evolution of plastids and photosynthesis in eukaryotes. *Cold Spring Harb. Perspect. Biol.* 6(4): a016105.
- McMullan, G., Faruqi, A. R., Clare, D. and Henderson, R.** (2014). Comparison of optimal performance at 300keV of three direct electron detectors for use in low dose electron microscopy. *Ultramicroscopy* 147: 156-163.
- Mereschkowsky, C.** (1905). Über Natur und Ursprung der Chromatophoren im Pflanzenreiche. *Biol. Centralbl.* 25: 593-604.
- Mullineaux, C. W.** (1994). Excitation energy transfer from phycobilisomes to photosystem I in a cyanobacterial mutant lacking photosystem II. *Biochim. Biophys. Acta* 1184(1): 71-77.
- Mullineaux, C. W.** (2008). The cyanobacteria. Molecular biology, genomics and evolution. Chapter 11: Biogenesis and dynamics of thylakoid membranes and the photosynthetic apparatus. *Caister Academic Press*: 289-303. ISSN: 978-1-904455-15-8.
- Mullineaux, C. W.** (2014). Co-existence of photosynthetic and respiratory activities in cyanobacterial thylakoid membranes. *Biochim. Biophys. Acta* 1837(4): 503-511.
- Nelson, N. and Junge, W.** (2015). Structure and energy transfer in photosystems of oxygenic photosynthesis. *Annu. Rev. Biochem.* 84(1): 659-683.
- Nevo, R., Charuvi, D., Shimoni, E., Schwarz, R., Kaplan, A., Ohad, I. and Reich, Z.** (2007). Thylakoid membrane perforations and connectivity enable intracellular traffic in cyanobacteria. *EMBO J.* 26(5): 1467-1473.
- Nickelsen, J. and Rengstl, B.** (2013). Photosystem II assembly: from cyanobacteria to plants. *Annu. Rev. Plant Biol.* 64: 609-635.
- Nierzwicki-Bauer, S. A., Balkwill, D. L. and Stevens, S. E.** (1983a). Three-dimensional ultrastructure of a unicellular cyanobacterium. *J. Cell Biol.* 97(3): 713-722.
- Nierzwicki-Bauer, S. A., Balkwill, D. L. and Stevens, S. E.** (1983b). Use of a computer-aided reconstruction system to examine the three-dimensional architecture of cyanobacteria. *J. Ultrastruct. Res.* 84(1): 73-82.
- Nowaczyk, M. M., Hebel, R., Schlodder, E., Meyer, H. E., Warscheid, B. and Rogner, M.** (2006). Psb27, a cyanobacterial lipoprotein, is involved in the repair cycle of photosystem II. *Plant Cell* 18(11): 3121-3131.
- Oelze, J. and Drews, G.** (1972). Membranes of photosynthetic bacteria. *Biochim. Biophys. Acta* 265(2): 209-239.
- Olive, J., Ajlani, G., Astier, C., Recouvreur, M. and Vernotte, C.** (1997). Ultrastructure and light adaptation of phycobilisome mutants of *Synechocystis* PCC 6803. *Biochim. Biophys. Acta* 1319(2): 275-282.
- Pesaresi, P., Pribil, M., Wunder, T. and Leister, D.** (2011). Dynamics of reversible protein phosphorylation in thylakoids of flowering plants: The roles of STN7, STN8 and TAP38. *Biochim. Biophys. Acta* 1807(8): 887-896.

- Pettersen, E. F., Goddard, T. D., Huang, C. C., Couch, G. S., Greenblatt, D. M., Meng, E. C. and Ferrin, T. E.** (2004). UCSF Chimera—A visualization system for exploratory research and analysis. *J. Comput. Chem.* 25(13): 1605-1612.
- Pogoryelov, D., Reichen, C., Klyszejko, A. L., Brunisholz, R., Muller, D. J., Dimroth, P. and Meier, T.** (2007). The oligomeric state of c rings from cyanobacterial F-ATP synthases varies from 13 to 15. *J. Bacteriol.* 189(16): 5895-5902.
- Praefcke, G. J. and McMahon, H. T.** (2004). The dynamin superfamily: universal membrane tubulation and fission molecules? *Nat. Rev. Mol. Cell Biol.* 5(2): 133-147.
- Pribil, M., Labs, M. and Leister, D.** (2014). Structure and dynamics of thylakoids in land plants. *J. Exp. Bot.* 65(8): 1955-1972.
- Pysznik, A. M. and Gibbs, S. P.** (1992). Immunocytochemical localization of photosystem I and the fucoxanthin-chlorophylla/c light-harvesting complex in the diatom *Phaeodactylum tricornutum*. *Protoplasma* 166(3): 208-217.
- Rast, A., Albert, S., Schaffer, M., Beck, F., Pfeffer, S., Nickelsen, J. and Engel, B. D.** *In situ* cryo-electron tomography of cyanobacterial thylakoid convergence zones reveals a biogenic membrane connecting thylakoids to the plasma membrane.
- Rast, A., Heinz, S. and Nickelsen, J.** (2015). Biogenesis of thylakoid membranes. *Biochim. Biophys. Acta* 1847(9): 821-830.
- Rast, A., Rengstl, B., Heinz, S., Klingl, A. and Nickelsen, J.** (2016). The role of Slr0151, a tetratricopeptide repeat protein from *Synechocystis* sp. PCC 6803, during photosystem II assembly and repair. *Front. Plant Sci.* 7: 605.
- Rengstl, B., Knoppova, J., Komenda, J. and Nickelsen, J.** (2013). Characterization of a *Synechocystis* double mutant lacking the photosystem II assembly factors YCF48 and Sll0933. *Planta* 237(2): 471-480.
- Rengstl, B., Oster, U., Stengel, A. and Nickelsen, J.** (2011). An intermediate membrane subfraction in cyanobacteria is involved in an assembly network for photosystem II biogenesis. *J. Biol. Chem.* 286(24): 21944-21951.
- Rexroth, S., Mullineaux, C. W., Ellinger, D., Sendtko, E., Rogner, M. and Koenig, F.** (2011). The plasma membrane of the cyanobacterium *Gloeobacter violaceus* contains segregated bioenergetic domains. *Plant Cell* 23(6): 2379-2390.
- Rigort, A., Bauerlein, F. J., Villa, E., Eibauer, M., Laugks, T., Baumeister, W. and Plitzko, J. M.** (2012). Focused ion beam micromachining of eukaryotic cells for cryoelectron tomography. *Proc. Natl. Acad. Sci. USA* 109(12): 4449-4454.
- Roose, J. L., Kashino, Y. and Pakrasi, H. B.** (2007). The PsbQ protein defines cyanobacterial photosystem II complexes with highest activity and stability. *Proc. Natl. Acad. Sci. USA* 104(7): 2548-2553.
- Ruska, E. and Knoll, M.** (1931). Die magnetische Sammelspule für schnelle Elektronenstrahlen. *Z. techn. Physik* 12: 389-400 und 448.

- Rütgers, M. and Schroda, M.** (2013). A role of VIPP1 as a dynamic structure within thylakoid centers as sites of photosystem biogenesis? *Plant Signal. Behav.* 8(11): e27037.
- Sacharz, J., Bryan, S. J., Yu, J., Burroughs, N. J., Spence, E. M., Nixon, P. J. and Mullineaux, C. W.** (2015). Sub-cellular location of FtsH proteases in the cyanobacterium *Synechocystis* sp. PCC 6803 suggests localised PSII repair zones in the thylakoid membranes. *Mol. Microbiol.* 96(3): 448-462.
- Sagan, L.** (1967). On the origin of mitosing cells. *J. Theor. Biol.* 14(3): 225-274.
- Sarcina, M., Tobin, M. J. and Mullineaux, C. W.** (2001). Diffusion of phycobilisomes on the thylakoid membranes of the cyanobacterium *Synechococcus* 7942. Effects of phycobilisome size, temperature, and membrane lipid composition. *J. Biol. Chem.* 276(50): 46830-46834.
- Saur, M., Hennig, R., Young, P., Rusitzka, K., Hellmann, N., Heidrich, J., Morgner, N., Markl, J. and Schneider, D.** (2017). A janus-faced IM30 ring involved in thylakoid membrane fusion is assembled from IM30 tetramers. *Structure* 25(9): 1380-1390.e1385.
- Sawant, P., Eissenberger, K., Karier, L., Mascher, T. and Bramkamp, M.** (2016). A dynamin-like protein involved in bacterial cell membrane surveillance under environmental stress. *Environ. Microbiol.* 18(8): 2705-2720.
- Schimper, A. F. W.** (1883). Über die Entwicklung der Chlorophyllkörner und Farbkörper. *Bot. Zeitung* 41: 105-162.
- Schottkowski, M., Gkalypoudis, S., Tzekova, N., Stelljes, C., Schünemann, D., Ankele, E. and Nickelsen, J.** (2009a). Interaction of the periplasmic PrtA factor and the PsbA (D1) protein during biogenesis of photosystem II in *Synechocystis* sp. PCC 6803. *J. Biol. Chem.* 284(3): 1813-1819.
- Schottkowski, M., Ratke, J., Oster, U., Nowaczyk, M. and Nickelsen, J.** (2009b). Pitt, a novel tetratricopeptide repeat protein involved in light-dependent chlorophyll biosynthesis and thylakoid membrane biogenesis in *Synechocystis* sp. PCC 6803. *Mol. Plant* 2(6): 1289-1297.
- Shen, J.-R.** (2015). The structure of photosystem II and the mechanism of water oxidation in photosynthesis. *Annu. Rev. Plant Biol.* 66(1): 23-48.
- Sherman, D. M., Troyan, T. A. and Sherman, L. A.** (1994). Localization of membrane proteins in the cyanobacterium *Synechococcus* sp. PCC7942 (Radial asymmetry in the photosynthetic complexes). *Plant Physiol.* 106(1): 251-262.
- Silva, P., Thompson, E., Bailey, S., Kruse, O., Mullineaux, C. W., Robinson, C., Mann, N. H. and Nixon, P. J.** (2003). FtsH is involved in the early stages of repair of photosystem II in *Synechocystis* sp PCC 6803. *Plant Cell* 15(9): 2152-2164.
- Sobti, M., Smits, C., Wong, A. S. W., Ishmukhametov, R., Stock, D., Sandin, S. and Stewart, A. G.** (2016). Cryo-EM structures of the autoinhibited *E. coli* ATP synthase in three rotational states. *eLife* 5: e21598.

- Spät, P., Maček, B. and Forchhammer, K.** (2015). Phosphoproteome of the cyanobacterium *Synechocystis* sp. PCC 6803 and its dynamics during nitrogen starvation. *Front. Microbiol.* 6: 248.
- Stengel, A., Gügel, I. L., Hilger, D., Rengstl, B., Jung, H. and Nickelsen, J.** (2012). Initial steps of photosystem II de novo assembly and preloading with manganese take place in biogenesis centers in *Synechocystis*. *Plant Cell* 24(2): 660-675.
- Stingaciu, L.-R., O'Neill, H., Liberton, M., Urban, V. S., Pakrasi, H. B. and Ohl, M.** (2016). Revealing the dynamics of thylakoid membranes in living cyanobacterial cells. *Sci. Rep.* 6: 19627.
- Su, X., Fraenkel, P. G. and Bogorad, L.** (1992). Excitation energy transfer from phycocyanin to chlorophyll in an *apcA*-defective mutant of *Synechocystis* sp. PCC 6803. *J. Biol. Chem.* 267(32): 22944-22950.
- Tang, K., Ding, W.-L., Höppner, A., Zhao, C., Zhang, L., Hontani, Y., Kennis, J. T. M., Gärtner, W., Scheer, H., Zhou, M. and Zhao, K.-H.** (2015). The terminal phycobilisome emitter, LCM: A light-harvesting pigment with a phytochrome chromophore. *Proc. Natl. Acad. Sci. USA* 112(52): 15880-15885.
- Tauschel, H. D. and Drews, G.** (1967). Thylakoidmorphogenese bei *Rhodospseudomonas palustris*. *Arch. Mikrobiol.* 59(4): 381-404.
- Tomitani, A., Knoll, A. H., Cavanaugh, C. M. and Ohno, T.** (2006). The evolutionary diversification of cyanobacteria: molecular-phylogenetic and paleontological perspectives. *Proc. Natl. Acad. Sci. USA* 103(14): 5442-5447.
- Tóth, T. N., Chukhutsina, V., Domonkos, I., Knoppová, J., Komenda, J., Kis, M., Lénárt, Z., Garab, G., Kovács, L., Gombos, Z. and van Amerongen, H.** (2015). Carotenoids are essential for the assembly of cyanobacterial photosynthetic complexes. *Biochim. Biophys. Acta* 1847(10): 1153-1165.
- Tottey, S., Waldron, K. J., Firbank, S. J., Reale, B., Bessant, C., Sato, K., Cheek, T. R., Gray, J., Banfield, M. J., Dennison, C. and Robinson, N. J.** (2008). Protein-folding location can regulate manganese-binding versus copper- or zinc-binding. *Nature* 455(7216): 1138-1142.
- Tyystjärvi, T., Aro, E.-M., Jansson, C. and Mäenpää, P.** (1994). Changes of amino acid sequence in PEST-like area and QEEET motif affect degradation rate of D1 polypeptide in photosystem II. *Plant Mol. Biol.* 25(3): 517-526.
- Umena, Y., Kawakami, K., Shen, J. R. and Kamiya, N.** (2011). Crystal structure of oxygen-evolving photosystem II at a resolution of 1.9 Å. *Nature* 473(7345): 55-60.
- van de Meene, A. M., Hohmann-Marriott, M. F., Vermaas, W. F. and Roberson, R. W.** (2006). The three-dimensional structure of the cyanobacterium *Synechocystis* sp. PCC 6803. *Arch. Microbiol.* 184(5): 259-270.
- van de Meene, A. M., Sharp, W. P., McDaniel, J. H., Friedrich, H., Vermaas, W. F. and Roberson, R. W.** (2012). Gross morphological changes in thylakoid membrane structure

- are associated with photosystem I deletion in *Synechocystis* sp. PCC 6803. *Biochim. Biophys. Acta* 1818(5): 1427-1434.
- van Thor, J. J., Mullineaux, C. W., Matthijs, H. C. P. and Hellingwerf, K. J.** (1998). Light harvesting and state transitions in cyanobacteria. *Bot. Acta* 111(6): 430-443.
- Vermaas, W. F., Timlin, J. A., Jones, H. D., Sinclair, M. B., Nieman, L. T., Hamad, S. W., Melgaard, D. K. and Haaland, D. M.** (2008). *In vivo* hyperspectral confocal fluorescence imaging to determine pigment localization and distribution in cyanobacterial cells. *Proc. Natl. Acad. Sci. USA* 105(10): 4050-4055.
- Wang, Q., Sullivan, R. W., Kight, A., Henry, R. L., Huang, J., Jones, A. M. and Korth, K. L.** (2004). Deletion of the chloroplast-localized Thylakoid formation1 gene product in *Arabidopsis* leads to deficient thylakoid formation and variegated leaves. *Plant Physiol.* 136(3): 3594-3604.
- Wegener, K. M., Welsh, E. A., Thornton, L. E., Keren, N., Jacobs, J. M., Hixson, K. K., Monroe, M. E., Camp, D. G., Smith, R. D. and Pakrasi, H. B.** (2008). High sensitivity proteomics assisted discovery of a novel operon involved in the assembly of photosystem II, a membrane protein complex. *J. Biol. Chem.* 283(41): 27829-27837.
- Westermann, M., Neuschaefter-Rube, O., Morschel, E. and Wehrmeyer, W.** (1999). Trimeric photosystem I complexes exist *in vivo* in thylakoid membranes of the *Synechocystis* strain B09201 and differ in absorption characteristics from monomeric photosystem I complexes. *J. Plant Physiol.* 155(1): 24-33.
- Westphal, S., Heins, L., Soll, J. and Vothknecht, U. C.** (2001). VIPP1 deletion mutant of *Synechocystis*: A connection between bacterial phage shock and thylakoid biogenesis? *Proc. Natl. Acad. Sci. USA* 98(7): 4243-4248.
- Wilde, A., Lunser, K., Ossenbühl, F., Nickelsen, J. and Borner, T.** (2001). Characterization of the cyanobacterial *ycf37*: mutation decreases the photosystem I content. *Biochem. J.* 357(Pt 1): 211-216.
- Wu, J. and Bauer, C. E.** (2010). RegB kinase activity is controlled in part by monitoring the ratio of oxidized to reduced ubiquinones in the ubiquinone pool. *MBio* 1(5).
- Yang, H., Liao, L., Bo, T., Zhao, L., Sun, X., Lu, X., Norling, B. and Huang, F.** (2014). Slr0151 in *Synechocystis* sp. PCC 6803 is required for efficient repair of photosystem II under high-light condition. *J. Integr. Plant Biol.* 56(12): 1136-1150.
- Yang, H., Liu, J., Wen, X. and Lu, C.** (2015). Molecular mechanism of photosystem I assembly in oxygenic organisms. *Biochim. Biophys. Acta* 1847(9): 838-848.
- Yokoyama, R., Yamamoto, H., Kondo, M., Takeda, S., Ifuku, K., Fukao, Y., Kamei, Y., Nishimura, M. and Shikanai, T.** (2016). Grana-localized proteins, RIQ1 and RIQ2, affect the organization of light-harvesting complex II and grana stacking in *Arabidopsis*. *Plant Cell* 28(9): 2261-2275.

- Yoshioka-Nishimura, M. and Yamamoto, Y.** (2014). Quality control of photosystem II: The molecular basis for the action of FtsH protease and the dynamics of the thylakoid membranes. *J. Photochem. Photobiol. B: Biol.* 137: 100-106.
- Zak, E., Norling, B., Maitra, R., Huang, F., Andersson, B. and Pakrasi, H. B.** (2001). The initial steps of biogenesis of cyanobacterial photosystems occur in plasma membranes. *Proc. Natl. Acad. Sci. USA* 98(23): 13443-13448.
- Zhan, J., Zhu, X., Zhou, W., Chen, H., He, C. and Wang, Q.** (2016). Thf1 interacts with PS I and stabilizes the PS I complex in *Synechococcus* sp. PCC7942. *Mol. Microbiol.* 102(4): 738-751.
- Zhang, J., Ma, J., Liu, D., Qin, S., Sun, S., Zhao, J. and Sui, S. F.** (2017). Structure of phycobilisome from the red alga *Griffithsia pacifica*. *Nature* 551(7678): 57-63.
- Zhang, L., Paakkari, V., van Wijk, K. J. and Aro, E. M.** (1999). Co-translational assembly of the D1 protein into photosystem II. *J. Biol. Chem.* 274(23): 16062-16067.
- Zhang, L. and Sakamoto, W.** (2015). Possible function of VIPP1 in maintaining chloroplast membranes. *Biochim. Biophys. Acta* 1847(9): 831-837.
- Zhang, Y. Z., Chen, X. L., Wang, L. S., Zhou, B. C., He, J. A., Shi, D. X. and Pang, S. J.** (2002). *In vitro* assembly of R-phycoerythrin from marine red alga *Polysiphonia urceolata*. *Acta Biochim. Biophys. Sinica* 34(1): 99-103.

6 APPENDIX

The following section contains one peer-reviewed review article published in an international journal as well as the peer-reviewed supplemental data of the studies Rast *et al.* (2016, section 3.1) and Heinz *et al.* (2016b, section 3.2). Moreover, supporting material for the manuscript from section 3.3 is included. The main findings and conclusions are shortly summarized in the beginning of each chapter.

6.1 Biogenesis of thylakoid membranes

Rast, A., Heinz, S. and Nickelsen, J. (2015). *Biochim. Biophys. Acta* 1847:821-30

Photosynthesis takes place in the specialized membrane network called thylakoids. Although many details are known about the molecular structure and function of the photosynthetic complexes, we are just starting to illuminate the formation and assembly of those complexes and the thylakoid membrane itself. Several assembly factors assist in the complex mechanisms of building the photosynthetic machinery including the insertions of pigments and metal ions. One of the best studied assembly processes is the formation of PSII. In chloroplasts as well as in cyanobacteria, several steps during PSII assembly require the same assembly factors whereas others are assisted by plant or cyanobacterial specific factors.

<https://doi.org/10.1016/j.bbabbio.2015.01.007>

6.2 Supplementary Material - The role of Slr0151, a tetratricopeptide repeat protein from *Synechocystis* sp. PCC 6803, during photosystem II assembly and repair

Rast, A., Rengstl, B., Heinz, S., Klingl, A. and Nickelsen, J. (2016). *Front. Plant Sci.* 7: 605.

The supplemental material of the study described in chapter 3.1 (Rast *et al.*, 2016) provides additional controls for the main data. Shown are the *slr0151*⁻ mutant generation and the protein levels in the *slr0151*⁻ mutant as well as of the Slr0151 protein in different PSII mutants.

<https://doi.org/10.3389/fpls.2016.00605>

6.3 Supplemental data - Thylakoid membrane architecture in *Synechocystis* depends on CurT, a homolog of the granal CURVATURE THYLAKOID1 proteins

Heinz, S., Rast, A., Shao, L., Gutu, A., Gügel, I.L., Heyno, E., Labs, M., Rengstl, B., Viola, S., Nowaczyk, M.M., Leister, D. and Nickelsen, J. (2016). *Plant Cell* 28: 2238-2260

The supplemental data of the study described in chapter 3.2 (Heinz *et al.*, 2016b) provide additional controls for the main results. Shown are the *curT*⁻ mutant generation, the growth phenotype at different conditions, the pigment analysis, and the absorbance spectra of the *curT* mutant and the wild-type. The expression level of the upstream gene *slr0482* was analyzed in the presence and absence of CurT. Moreover, co-expression of the *curT* gene was bioinformatically the CyanoEXpress 2.2 database and are shown (Hernandez-Prieto and Futschik, 2012; Hernandez-Prieto *et al.*, 2016). The tagged CurT-CFP protein expressed in the *curT*-CFP strain was shown to function and accumulate as the wild-type CurT protein. Controls for fluorescence microscopy and immunogold labeling electron microscopy are depicted. In addition, the ultrastructure of the mutant lacking the D1 protein is shown, in which biogenesis centers are still formed. Furthermore, three supplemental movies are available online (<http://www.plantcell.org/content/suppl/2016/08/19/tpc.16.00491.DC1>).

<https://doi.org/10.1105/tpc.16.00491>

6.4 Supporting material - *In situ* cryo-electron tomography of cyanobacterial thylakoid convergence zones reveals a biogenic membrane connecting thylakoids to the plasma membrane.

Rast, A., Albert, S., Schaffer, M., Beck, F., Pfeffer, S., Nickelsen, J. and Engel, B.D.

Electron dense material was observed in the contact area of the thylapse that might correspond to probably unknown proteins, which are responsible for the closely appressed convergence and plasma membrane. Exemplary membranograms with corresponding segmented membrane surfaces are shown for a better understanding. The tomogram volume of a *Synechocystis* cell depends on the lamella thickness. Therefore, the calculation of the visible volume of a 100 nm thick lamella is exemplarily shown.

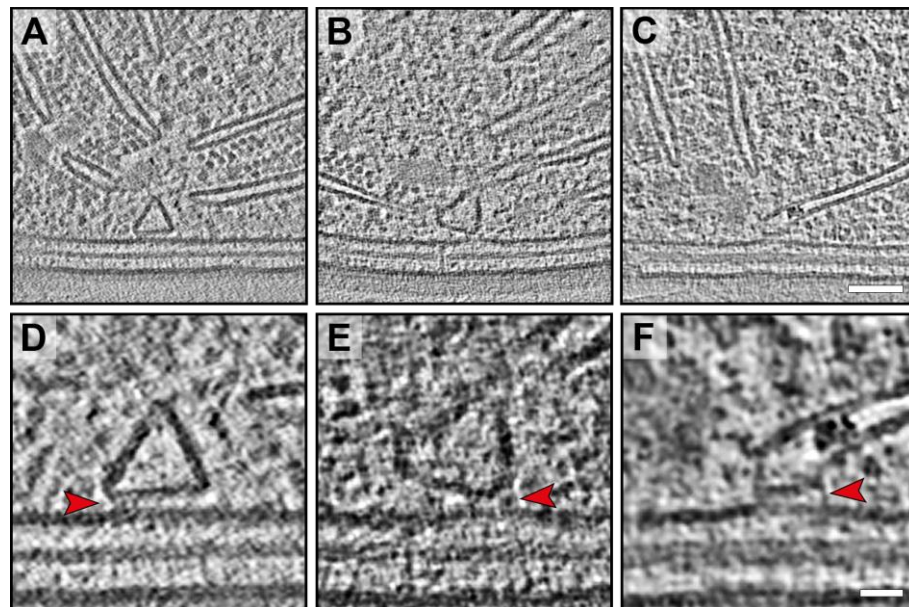


Figure S1. Electron dense material in the 2.5-nm-gap between convergence and plasma membrane. A-C) Tomographic slices containing a thylapse and (D-F) corresponding close-ups. Red arrowheads highlight the electron dense material in the gap between the convergence and plasma membranes. Scale bars: A-C) 50 nm and D-F) 20 nm.

Membranogram representation  Segmented membrane surface

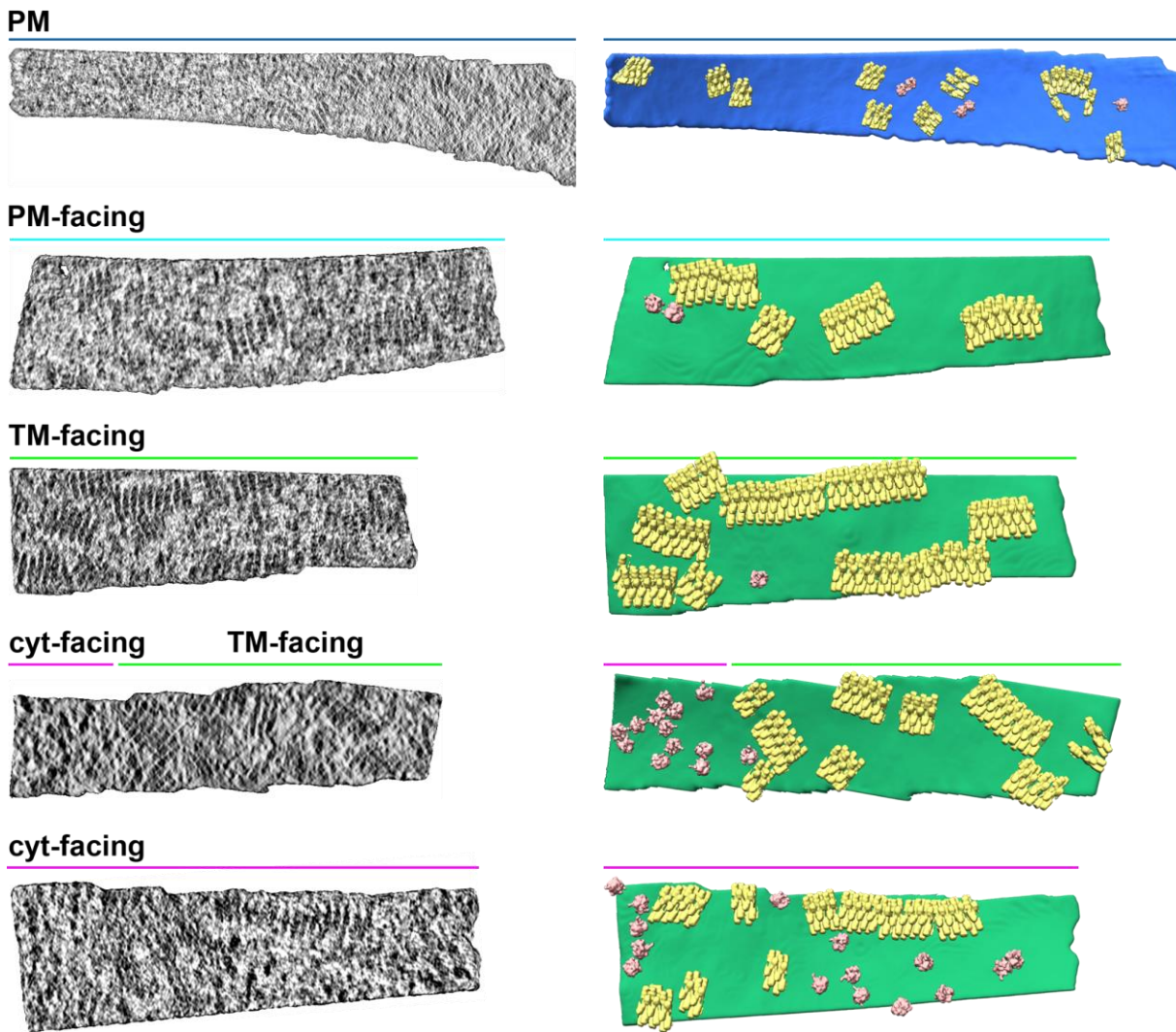


Figure S2. Five exemplary membranograms showing the different membrane regions. Left panel shows the membranogram representation and the right panel shows the respective segmented membrane surface with phycobilisomes (yellow) and 70S ribosomes (red).

Lamella volume**Cell volume**

<p> $x = 928 \text{ pixel}$ $y = 928 \text{ pixel}$ $\text{pixel size} = 13.68 \text{ \AA}$ $z = 100 \text{ nm}$ </p> <p> $V_{\text{Lamella}} = (x * \text{pixel size}) * (y * \text{pixel size}) * z;$ </p> <p> $V_{\text{Lamella}} = (928 * 13.68 \text{ \AA})^2 * 0.1 \text{ \mu m} = 0.159 \text{ \mu m}^3$ </p>	<p> $r_{\text{Synechocystis cell}} = 1 \text{ \mu m}$ $\pi = 3.1415$ </p> <p> $V_{\text{Cell}} = \frac{4}{3} * \pi * r^3;$ </p> <p> $V_{\text{Cell}} = \frac{4}{3} * \pi * 1 \text{ \mu m}^3 = 4.188 \text{ \mu m}^3$ </p>
---	---

Visible cell's volume in tomogram

$$\frac{V_{\text{Lamella}}}{V_{\text{Cell}}} = \frac{0.159 \text{ \mu m}^3}{4.188 \text{ \mu m}^3} = 4 \%$$

Figure S1. Visible cell's volume in tomogram. X and Y dimensions are the full dimensions of a twice-binned tomogram. The Z dimension is given by the lamella thickness. The pixel size is 13.68 Å for a twice-binned tomogram. The volume V of *Synechocystis* cell depends on its radius r and circle constant π .

LIST OF PUBLICATIONS

Peer-reviewed publications:

Rast, A., Rengstl, B., Heinz, S., Klingl, A., and Nickelsen, J. (2016). The role of Slr0151, a tetratricopeptide repeat protein from *Synechocystis* during Photosystem II assembly and repair. *Front. Plant Sci.* 7: 605.

Heinz, S., **Rast, A.**, Shao, L., Gutu, A., Gügel, I.L., Heyno, E., Labs, M., Rengstl, B., Viola, S., Nowaczyk, M.M., Leister, D., and Nickelsen, J. (2016b). Thylakoid membrane architecture in *Synechocystis* depends on CurT, a homolog of the granal CURVATURE THYLAKOID1 proteins. *Plant Cell* 28: 2238-2260.

Rast, A., Heinz, S., Nickelsen, J. (2015). Biogenesis of thylakoid membranes. *Biochim. Biophys. Acta* 1847:821-830.

Manuscripts:

Rast, A., Albert, S., Schaffer, M., Beck, F., Pfeffer, S., Nickelsen, J., and Engel, B.D. *In situ* cryo-electron tomography of cyanobacterial thylakoid convergence zones reveals a biogenic membrane connecting thylakoids to the plasma membrane.

Heinz, S., Hamm, J., Rengstl, B., Stengel, A., **Rast, A.**, Funk, C., Nickelsen, J. The pilus-related PilQ protein and the protease HhoA form a complex with the assembly factor PrtA during manganese delivery to cyanobacterial photosystem II.

Hoffmann, K., **Rast, A.**, Oworah-Nkruma, R., Geimer, S., Rexroth, S. Thylakoid biogenesis induced in *Synechocystis* sp. PCC 6803 by recovery from nitrogen-deficiency induced chlorosis.

LIST OF ABBREVIATIONS

Å	angstrom
ATP	adenosine triphosphate
BDLP	bacterial dynamin-like protein
c-terminal	carboxy terminal
CCD	charge coupled device
CFP	cyan fluorescent protein
CM	convergence membrane
CPRapA5e	chloroplast localized RapA5e
CPSAR1	chloroplast Sar1
cryo-ET	cryo-electron tomography
CtpA	c-terminal processing protease
CURT/ CurT	CURVATURE THYLAKOIDS
EDX	energy dispersive x-ray
EELS	electron energy loss spectroscopy
EM	electron microscopy
FIB	focused ion beam
FZL	fuzzy onion-like protein in plants
GFP	green fluorescent protein
IsiA	iron stress induced protein
kDa	kilo Dalton
L	thylakoid lumen
mRNA	messenger RNA
NADPH	reduced form of nicotine adenine dinucleotide phosphate
OM	outer membrane
P680	special pair chlorophylls of PSII
P700	special pair chlorophylls of PSI
pD1	precursor of D1 protein
PDB	protein data bank
PDM	PratA-defined membrane
Pitt	POR interacting TPR
PM	plasma membrane
POR	protochlorophyllide oxidoreductase
PratA	processing-associated TPR protein
PsaA	reaction center subunit of PSI
PSI	photosystem I
PSII	photosystem II
RC47	reaction center complex lacking CP47
Riq	reduced induction of non-photochemical quenching
RNA	ribonucleic acid
SpkG	serine/ threonine protein kinase G
T	threonine

LIST OF ABBREVIATIONS

TEM	transmission electron microscopy
THF1	THYLAKOID FORMATION1
TM	thylakoid membrane
TPR	tetratricopeptide repeat
tRNA	transfer RNA
VIPP1	vesicle inducing protein in plastids

*Daß ich nicht mehr mit saurem Schweiß
Zu sagen brauche, was ich nicht weiß;
Daß ich erkenne, was die Welt
Im Innersten zusammenhält*

Faust. Der Tragödie erster Teil. Johann Wolfgang von Goethe

Für Isolde und Kurt

DANKSAGUNG

Prof. Nickelsen möchte ich für das großartige Thema, die vielen konstruktiven wissenschaftlichen Gespräche und seine permanente Betreuung und Unterstützung danken.

Bei Prof. Klingl und Prof. Bramkamp möchte ich mich für die Unterstützung bei der Elektronen- und Lichtmikroskopie, sowie für die vielen wissenschaftlichen Gespräche über Membranen in Bakterien bedanken.

Ein riesiges Dankeschön an Steffen Heinz für kritische Gespräche nicht nur über unsere Daten, sondern auch über vieles mehr. Music and Prokaryote World Domination!

Ein großes Dankeschön geht natürlich auch an die Arbeitsgruppe Nickelsen. Es war eine großartige Zeit und toll mit euch zusammen zu arbeiten. Herzlichen Dank an Laura, die immer eine zündende Idee hatte, wenn irgendwo der Wurm drin war. Zudem möchte ich mich bei Julia und Matthias bedanken, die beide Teile meines Themas geerbt haben. Ein weiterer Dank geht an Karin, die unermüdlich Ordnung in den Laboralltag bringt. Zudem möchte ich mich noch bei allen Hiwis und Studenten bedanken.

Juri, Giacomo and Helge, I am very grateful for your support with the delta vision and for the excursion to the Elyra.

I would like to thank the colleagues at the Max-Planck Institute, especially Benjamin Engel and Miroslava Schaffer for their interest in a green topic, the opportunity to analyze *Synechocystis* in that detail and their constant support. Furthermore, I would like to thank Ben for critical reading of the manuscript. Moreover, big thanks to Sahradha Albert for teaching me the art of subtomogram averaging, to Florian Beck for helping me with Matlab and PyTom problems and Stefan Pfeffer for support with the ribosomes.

Ich möchte allen Co-Autoren für die konstruktiven Gespräche und die gute Zusammenarbeit herzlich danken.

DANKSAGUNG

Großen Dank möchte ich nochmal an alle Mitglieder der Forschergruppe FOR2092 aussprechen, insbesondere den Doktoranden. Unsere Diskussionen über spannende Daten, experimentelle Fehlschläge und seltsame Ergebnisse waren immer sehr fruchtbar und hilfreich.

Ein großer Dank geht an Steffen, Sahradha, Nina und Axel für das konstruktive und hilfreiche Korrekturlesen dieser Arbeit.

Zu guter Letzt, möchte ich mich bei meiner Familie und Großfamilie bedanken, für die stetige Unterstützung und den Rückhalt den sie mir immer gegeben hat. Insbesondere möchte ich mich bei Susanne und meinen Eltern bedanken, die mir noch einige Formulierungstipps gegeben haben.

PERMISSIONS AND COPYRIGHTS

Figure I in section 1.2 Thylakoid structure was taken from:

Rast, A., Heinz, S. and Nickelsen, J. (2015). Biogenesis of thylakoid membranes. *Biochim. Biophys. Acta* 1847:821-30

Copyright © 2015 Elsevier B.V. All rights reserved.

Please note that, as the author of this Elsevier article, you retain the right to include it in a thesis or dissertation, provided it is not published commercially. Permission is not required, but please that you reference the journal as the original source. For more information on this and on your retained rights, please visit:

<https://www.elsevier.com/about/our-business/policies/copyright#Authorrights>

Figure II in subsection 1.2.2 Thylakoid structure in cyanobacteria was adapted from:

Kunkel, D. D. (1982). Thylakoid centers: Structures associated with the cyanobacterial photosynthetic membrane system. *Arch. Microbiol.* 133(2): 97-99.

Nierzwicki-Bauer, S. A., Balkwill, D. L. and Stevens, S. E. (1983a). Three-dimensional ultrastructure of a unicellular cyanobacterium. *J. Cell Biol.* 97(3): 713-722.

van de Meene, A. M., Hohmann-Marriott, M. F., Vermaas, W. F. and Roberson, R. W. (2006). The three-dimensional structure of the cyanobacterium *Synechocystis* sp. PCC 6803. *Arch. Microbiol.* 184(5): 259-270.

Figure V in section 1.6 Cryo-electron tomography was adapted from:

Asano, S., Engel, B. D. and Baumeister, W. (2016). In situ cryo-electron tomography: a post-reductionist approach to structural biology. *J. Mol. Biol.* 428(2 Pt A): 332-343.

All permissions obtained via the Copyright Clearance Center for usage in my dissertation are attached below.

SPRINGER NATURE LICENSE TERMS AND CONDITIONS

Mar 29, 2018

This Agreement between Ludwig-Maximilians -- Anna Rast ("You") and Springer Nature ("Springer Nature") consists of your license details and the terms and conditions provided by Springer Nature and Copyright Clearance Center.

License Number	4318161202028
License date	Mar 29, 2018
Licensed Content Publisher	Springer Nature
Licensed Content Publication	Archives of Microbiology
Licensed Content Title	Thylakoid centers: Structures associated with the cyanobacterial photosynthetic membrane system
Licensed Content Author	Dennis D. Kunkel
Licensed Content Date	Jan 1, 1982
Licensed Content Volume	133
Licensed Content Issue	2
Type of Use	Thesis/Dissertation
Requestor type	academic/university or research institute
Format	print and electronic
Portion	figures/tables/illustrations
Number of figures/tables /illustrations	2
Will you be translating?	no
Circulation/distribution	<501
Author of this Springer Nature content	no
Title	Thylakoid membrane architecture in cyanobacteria
Instructor name	Prof. Dr. Jörg Nickelsen
Institution name	Ludwig-Maximilians-Universität München
Expected presentation date	Apr 2018
Portions	I would like to use: Figure 1 on page 98 and Figure 8 on page 98.
Requestor Location	Ludwig-Maximilians-Universität München Großhaderner Str. 2-4 Planegg-Martinsried, Bavaria 82152 Germany Attn: Ludwig-Maximilians-Universität München
Billing Type	Invoice
Billing Address	Ludwig-Maximilians-Universität München Großhaderner Str. 2-4
Total	Planegg-Martinsried, Germany 82152 Attn: Ludwig-Maximilians-Universität München 0.00 EUR

Welcome To RightsLink

Apr 20, 2018

This is a License Agreement between Ludwig-Maximilians -- Anna Rast ("You") and Rockefeller University Press ("Rockefeller University Press") provided by Copyright Clearance Center ("CCC"). The license consists of your order details, the terms and conditions provided by Rockefeller University Press, and the payment terms and conditions.

All payments must be made in full to CCC. For payment instructions, please see information listed at the bottom of this form.

License Number	4318160874019
License date	Mar 29, 2018
Licensed Content Publisher	Rockefeller University Press
Licensed Content Title	The journal of cell biology
Licensed Content Date	Dec 31, 1969
I would like to...	Thesis/Dissertation
Requestor type	Academic institution
Format	Print, Electronic
Portion	image/photo
Number of images/photos requested	2
The requesting person/organization is:	Anna Rast
Title or numeric reference of the portion(s)	I would like to use: Figure 5 from page 716 and Figure 7 from page 716
Title of the article or chapter the portion is from	Three-dimensional ultrastructure of a unicellular cyanobacterium.
Editor of portion(s)	N/A
Author of portion(s)	Nierzwicki-Bauer SA, Balkwill DL, Stevens SE Jr.
Volume of serial or monograph.	97
Issue, if republishing an article from a serial	3
Page range of the portion	713-722
Publication date of portion	September 1, 1983
Rights for	Main product
Duration of use	Life of current edition
Creation of copies for the disabled	yes
With minor editing privileges	no
For distribution to	Worldwide
In the following language(s)	Original language of publication
With incidental promotional use	no
The lifetime unit quantity of new product	Up to 499
Title	Thylakoid membrane architecture in cyanobacteria
Instructor name	Prof. Dr. Jörg Nickelsen
Institution name	Ludwig-Maximilians-Universität München
Expected presentation date	Apr 2018
Billing Type	Invoice
Billing Address	Ludwig-Maximilians-Universität München Großhaderner Str. 2-4

Planegg-Martinsried, Germany 82152
Attn: Ludwig-Maximilians-Universität München

Total (may include CCC user fee) 0.00 USD

SPRINGER NATURE LICENSE TERMS AND CONDITIONS

Mar 29, 2018

This Agreement between Ludwig-Maximilians -- Anna Rast ("You") and Springer Nature ("Springer Nature") consists of your license details and the terms and conditions provided by Springer Nature and Copyright Clearance Center.

License Number	4318151116162
License date	Mar 29, 2018
Licensed Content Publisher	Springer Nature
Licensed Content Publication	Archives of Microbiology
Licensed Content Title	The three-dimensional structure of the cyanobacterium Synechocystis sp. PCC 6803
Licensed Content Author	Allison M.L. van de Meene, Martin F. Hohmann-Marriott, Wim F.J. Vermaas et al
Licensed Content Date	Jan 1, 2005
Licensed Content Volume	184
Licensed Content Issue	5
Type of Use	Thesis/Dissertation
Requestor type	academic/university or research institute
Format	print and electronic
Portion	figures/tables/illustrations
Number of figures/tables /illustrations	2
Will you be translating?	no
Circulation/distribution	<501
Author of this Springer Nature content	no
Title	Thylakoid membrane architecture in cyanobacteria
Instructor name	Prof. Dr. Jörg Nickelsen
Institution name	Ludwig-Maximilians-Universität München
Expected presentation date	Apr 2018
Portions	I would like to use: Figure 2A,B from page 263 Figure 5L from page 266
Requestor Location	Ludwig-Maximilians-Universität München Großhaderner Str. 2-4 Planegg-Martinsried, Bavaria 82152 Germany Attn: Ludwig-Maximilians-Universität München
Billing Type	Invoice
Billing Address	Ludwig-Maximilians-Universität München Großhaderner Str. 2-4 Planegg-Martinsried, Germany 82152 Attn: Ludwig-Maximilians-Universität München
Total	0.00 EUR

**ELSEVIER LICENSE
TERMS AND CONDITIONS**

Apr 20, 2018

This Agreement between Ludwig-Maximilians -- Anna Rast ("You") and Elsevier ("Elsevier") consists of your license details and the terms and conditions provided by Elsevier and Copyright Clearance Center.

License Number	4332871197278
License date	Apr 20, 2018
Licensed Content Publisher	Elsevier
Licensed Content Publication	Journal of Molecular Biology
Licensed Content Title	In Situ Cryo-Electron Tomography: A Post-Reductionist Approach to Structural Biology
Licensed Content Author	Shoh Asano,Benjamin D. Engel,Wolfgang Baumeister
Licensed Content Date	Jan 29, 2016
Licensed Content Volume	428
Licensed Content Issue	2
Licensed Content Pages	12
Start Page	332
End Page	343
Type of Use	reuse in a thesis/dissertation
Intended publisher of new work	other
Portion	figures/tables/illustrations
Number of figures/tables /illustrations	1
Format	both print and electronic
Are you the author of this Elsevier article?	No
Will you be translating?	No
Original figure numbers	I would like to use Figure 1 from page 333 in my thesis.
Title of your thesis/dissertation	Thylakoid membrane architecture in cyanobacteria
Publisher of new work	Ludwig-Maximilians-Universität München
Author of new work	Prof. Dr. Jörg Nickelsen
Expected completion date	Apr 2018
Estimated size (number of pages)	1
Requestor Location	Ludwig-Maximilians-Universität München Großhaderner Str. 2-4 Planegg-Martinsried, Bavaria 82152 Germany Attn: Ludwig-Maximilians-Universität München
Publisher Tax ID	GB 494 6272 12
Total	0.00 EUR

EIDESSTATTLICHE VERSICHERUNG UND ERKLÄRUNG

Eidesstattliche Versicherung

Ich versichere hiermit an Eides statt, dass die vorgelegte Dissertation von mir selbständig und ohne unerlaubte Hilfe angefertigt ist.

München, 03.05.2018

Anna Rast

Erklärung

Hiermit erkläre ich, dass die Dissertation nicht ganz oder in wesentlichen Teilen einer anderen Prüfungskommission vorgelegt worden ist. Des Weiteren habe ich mich **nicht** anderweitig einer Doktorprüfung ohne Erfolg unterzogen.

München, 03.05.2018

Anna Rast